Mechanical Conditioning of Cell Layers for Tissue Engineering

by

ELAINE LINDA LEE

Submitted in partial fulfillment of the requirements

For the degree of Doctor of Philosophy

Dissertation Advisor: Horst von Recum, PhD

Department of Biomedical Engineering

CASE WESTERN RESERVE UNIVERSITY

JANUARY 20, 2012

CASE WESTERN RESERVE UNIVERSITY

SCHOOL OF GRADUATE STUDIES

We hereby approve the thesis/dissertation of

Elaine Linda Lee

candidate for the PhD degree *.

(signed) Horst A. von Recum, PhD

(chair of the committee)

Christopher J. Hernandez, PhD

Marc S. Penn, MD, PhD, FACC

Xin Yu, ScD

(date) _____

*We also certify that written approval has been obtained for any proprietary material contained therein.

Table of Contents

List of Tables

List of Figures

Acknowledgements

I would like to thank my advisor, Dr. Horst von Recum, for his enthusiastic encouragement and continued support. During my time at Case Western Reserve University, his guidance and mentorship encouraged me to grow as a scientist, researcher, and engineer. I especially want to thank him for his unwavering patience with me during some of the most turbulent times in my life. In both my professional and personal lives, I would have perished in the darkest shadows without his persistence in steering me back toward the sunny side of the street.

I also would like to thank my committee members, Dr. Chris Hernandez, Dr. Marc Penn, and Dr. Xin Yu, for their invaluable guidance and insight.

To past and present members of the von Recum lab, I want to thank them for their expertise and comradeship. I would like to thank Sage, who taught me everything she knew when I was a first-year student and who I continue to rely on with her infinite wisdom. To Nick, I would like to say thank you for buoying my sinking spirits through times of frustration and disappointment. Thanks to Edgardo, Sonia, and Andrew for the laughter and for cheering me on. Thanks to Reddy for help with the NIPAAm chemistry. Thanks to Seth for teaching me how to do RT-PCR and Westerns, and to Kelli, who performed endless numbers of Westerns for me.

Lastly, I want to thank my family and friends. To my roommates, Jaime, Laura, and Grayden, and my friends, Megan and Mary, I could not have lasted the long slumps of despair and hopelessness without their unshakable friendship. And most importantly, I want to thank my parents and my brothers for their endless love and encouragement.

Mechanical Conditioning of Cell Layers for Tissue Engineering

Abstract

by

ELAINE LINDA LEE

Approximately every minute, someone will die of a coronary event. Myocardial infarction patients experience the loss of cardiomyocytes, which cannot regenerate. The goal of cell therapy then becomes to regenerate this tissue. Although there has been limited success using intracoronary injections, cardiac patches made of cellular sheets of cardiomyocytes and other cells offer advantages, such as a targeted delivery. However, although current cardiac patches do improve heart function, the fibers in the patch are misaligned, which may lead to maladaptive remodeling. We can increase the integrity of the cardiac patch by mechanically conditioning individual cellular sheets of cardiomyocytes, thereby increasing the biochemical secretion of cardiac proteins and extracellular matrix (ECM). Additionally, we can induce cellular alignment to increase electrical pacing.

Current technology will allow for stretching or nondamaging detachment of cellular sheets, but not both. We have modified a silicone membrane with poly (N-isopropylacrylamide-co-acrylic acid) (P(NIPAAm-co-AAc)) copolymers to create a bioreactor that can mechanically condition cells and subsequently detach those cells with cell-cell and cell-matrix junctions intact. P(NIPAAm-co-AAc) is a copolymer that allows for cell attachment at 37°C, and spontaneous cell detachment at room

temperature, thereby bypassing the need for enzymatic treatments that would damage the synthesized ECM. Using this bioreactor, we have been able to condition sheets of cardiomyocytes and other cells (e.g., NIH3T3 cells) at the native conditions to induce secretion of cardiac proteins and ECM so that we can influence the cellular sheets to have the natural mechanical properties of heart tissue. We also demonstrate that we can detach those sheets without damage so that they can be layered to form a cellular patch for regenerating tissue following myocardial infarction.

Chapter I: Mechanical Conditioning

Elaine L. Lee and Horst A. von Recum

Case Western Reserve University, Cleveland, OH 44106

* This has been submitted as a book chapter in *CRC's Biomedical Engineering Handbook*, 4th ed.

Why do we need mechanical conditioning

The body's tissues and organs are subjected to multiple types of forces: gravitational, static, dynamic, and cyclical. All of the body is affected by the pull of Earth's gravity (or lack thereof in space), which in turn applies hydrostatic pressure to all organs and tissues. Under a static force of constant magnitude, organs such as the liver are able to maintain tone. Conversely, other parts of the body are made to withstand gradual or sudden changes in force, like the bones do when different stresses are applied in the act of walking compared to running. Still yet, the function of other organs is to repeatedly resist against stress, such as the beating of the heart.

Just as a new paper clip and one bent to the point before fracture will have different stiffnesses to hold sheets of paper together, the rupture of the extracellular matrix (ECM) and the cells when a tissue or organ is injured causes a change in the mechanical forces at the site of injury (Ingber 2008a, Sims et al. 1992). The body must remodel to compensate for the unbalanced mechanical function and to eventually restore normal function to an unstressed state. However, in some cases, the organ may

never fully remodel or may even propagate improper stresses and cause greater injury, such as hypertrophy of the heart from hypertension. Consequently, the inquisitive scientist can use a mechanical cell stimulator to manipulate stresses that deviate from normal conditions in a controlled environment to determine the subsequent trajectory of a tissue from a healthy to diseased state. Similarly, to the innovative biomedical engineer, the goal becomes to engineer functionally viable replacement or regenerative tissues using stress parameters that mimic the native environment to induce the desired ECM remodeling and to reduce recovery time.

Cellular response to mechanical stimuli vs. the living cell as a mechanical structure

The living cell is an adaptive mechanical structure that both receives and responds to biochemical, biomechanical, and bioelectrical signals; and its responsiveness on the cellular level influences the mechanical function on the tissue and organ level (Chiquet et al. 2007, Sarasa-Renedo and Chiquet 2005, Chiquet et al. 1996). By the same token, physical forces acting at the level of the organ can influence the function on the cellular level. In other words, form follows function: The cell increases transcription and assembly of proteins into architecture such that the function of the tissue or organ is optimal (Russell et al. 2000). For example, when the work load exceeds the preexisting capacity of the muscle fiber, such as during a workout exercise, the stretched muscle cell will undergo hypertrophy (i.e., an increase in mass and cross-sectional area) by increasing production of contractile proteins actin and myosin (van Wamel et al. 2000, Russell et al. 2000). As a result, the muscle cell has an increased

potential for force production that is directly proportional to the amount of hypertrophy. In the absence of such a stimulus, the muscle will atrophy.

Mechanical stimulation of cells results in cell-generated responses for a variety of cell processes (Figure 1.1) (Trepat et al. 2007):

1. Directing cell lineage, such as directing bone marrow-derived stromal cells to regenerate bone, cartilage, or ligaments (Potier et al. 2010, Guilak et al. 2009).
2. Increasing cell proliferation, such as the proliferation of fibroblasts in forming scar tissue following an injury (Palatinus et al. 2010).
3. Increasing ECM production, such as the longitudinal growth of long bones where chondrocytes synthesize cartilage (composed of Type II collagen, proteoglycans, and elastin) before ossification (Villemure and Stokes 2009).
4. Inducing cellular alignment, such as cyclic stretching of cardiomyocytes to induce alignment perpendicular to the direction of strain (Shimko and Claycomb 2008, Ingber 2010).
5. Inducing cell migration, such as inhibition of vascular smooth muscle cell migration under laminar shear stress (Wang et al. 2006a).
6. Influencing cell adhesion, such as the upregulaton of α-actin for cell-cell and cell-matrix adhesion (Wang et al. 2010).
7. Increasing cell signaling, such as the mechanical deformation of a sensory neuron's plasma membrane that can cause stretch-activated ion channels to be opened to ion flow (Martinac 2004, Fan and Walsh 1999, Nishimura et al. 2008).

8. Influencing cell morphology, such as when the membrane is perturbed, causing actin filaments in the cytoskeleton to reorganize and reinforce the area of perturbation (Nishimura et al. 2008).

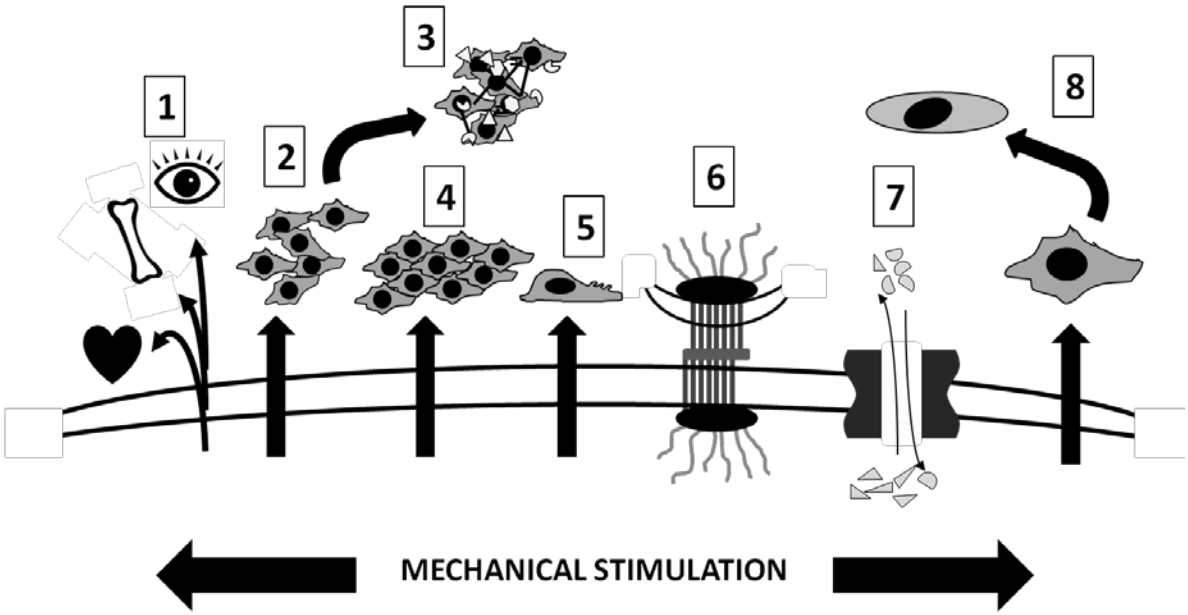

Figure 1.1. Mechanical stimulation can affect a variety of cell responses: (1) differentiation, (2) proliferation, (3) extracellular matrix production, (4) alignment, (5) migration, (6) adhesion, (7) signaling, and (8) morphology.

In relation to Newton's third law (i.e., every action has an equal and opposite reaction), the cell shape is controlled by the cytoskeleton, which counterbalances the forces exerted by neighboring cells and the environment, such as the rigidity of the adhesion substrate (Sims et al. 1992, Fletcher and Mullins 2010). Ingber modeled the cell as an architecture that is constantly under tension to stabilize its shape, known as

the “tensegrity” model (Figure 1.2A) (Ingber 2008b, Ingber 2010). The actin cytoskeleton within the cell acts as rods attached to the cell membrane that are under constant tension. When these internal struts are unanchored to a culture substrate or another cell structure, the cell has a rounded shape maintained only by the resistance of the struts against the membrane, such as when cells are trypsinized. When these struts are anchored to a rigid substrate, the cell model flattens and spreads, much like the adherence of a cell to a substrate. Indeed, disruption of actin polymerization by pharmacological treatment with cytochalasin D will lead to disruption of the membrane’s potential response to stretching via stretch-activated channels, thus preventing changes in cell morphology (Nishimura et al. 2008). Conversely, microtubules have been shown to bear compression, and resist the forces generated by the contracting actin cytoskeleton. Brangwynne et al. (2006) demonstrated this phenomenon using cardiomyocytes transfected with GFP-tubulin, where the microtubules buckle in unison with each contraction and straighten when the cells relax. Similarly, several groups have shown that excessive microtubule proliferation in hypertrophied hearts leads to passive stiffening and contractile dysfunction, which can be restored using colchicine to disrupt the microtubules (Tagawa et al. 1998, Nishimura et al. 2006, Zile et al. 1999, Ishibashi et al. 1996, Tsutsui et al. 1993).

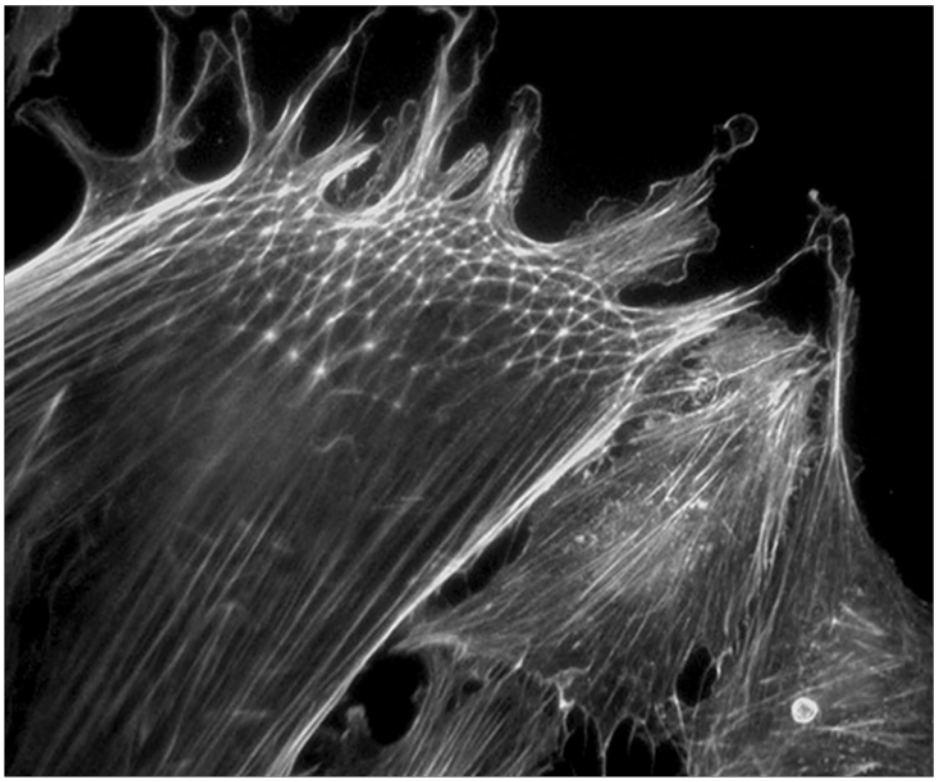

from http://www.subtletechnologies.com/2006/symposium/Ingber.html

Figure 1.2A

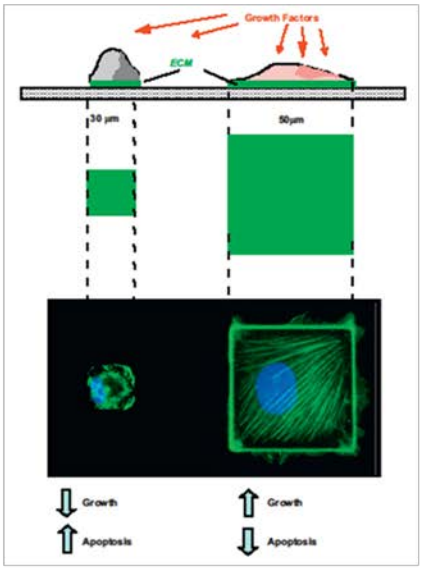

from Ingber DE. Tensegrity-based mechanosensing from macro to micro. Prog Biophys Mol Biol 2008;97:163-79.

Figure 1.2B

Figure 1.2. (A) Internal structs composed of cytoskeletal actin filaments in Ingber's tensegrity model are extended under constant tension when the cell is adhered to a substrate. (B) The cell's growth and function are dictated by its interactions with the extracellular matrix. The cell cycle can be modulated by the membrane's tension. Adhered cells spread over a large area will experience high tension, signaling cell growth; conversely, cells that are prevented from spreading will experience low tension and become apoptotic. Reprinted with the permissions of Donald E. Ingber.

The tensegrity model and the micromechanical cell response to physical distortion have been elegantly demonstrated using several different cell types by Ingber's group (Huang et al. 1998, Parker et al. 2002, Chen et al. 1997, Singhvi et al. 1994, Ingber 2008b, Ingber 2008a, Huang and Ingber 2000). An elastomeric stamp was used to micropattern a gold substrate with defined shapes of different sizes to allow uniform absorption of ECM and resist absorption of proteins elsewhere (Figure 1.2B). Cells that typically demonstrate spread lamellipodia under standard culture substrates (e.g., hepatocytes, capillary endothelial cells, fibroblasts, smooth muscle cells) attached preferentially to the adhesive domains and conformed to the specific shapes. Cells spread over larger surface areas exhibited the highest rates of cell growth, while cells on intermediate-sized domains became quiescent and differentiated, and cells prevented from spreading underwent apoptosis under the same conditions (Chen et al. 1997). Thus, the degree of mechanical distention can control the cell growth and death. In addition, cells spread over angular polygon domains reoriented the cytoskeletons and

focal adhesions to concentrate tractional forces on the corners (Parker et al. 2002). When cell tension was released, the lamellipodia extended first from the corners, whereas cells on circular domains had no preferential direction of spreading, indicating that the direction of cell movement is influenced directly by the interaction between the cell and ECM, which is critical in embryonic and tissue development. Similar studies also demonstrated that contractility (e.g., heart cells) can also be altered as a result of changes to the matrix (Polte et al. 2004).

How does the cell "sense" these changes in physical force? Transmembrane cell surface receptors (i.e., integrins) physically link the load-responsive cytoskeleton to the ECM and are theorized to be capable of mediating mechanosensing (Gov 2009, Yeung et al. 2005, Ingber 2010, Fletcher and Mullins 2010, Guilak et al. 2009). Through the integrins, the cell transfers mechanical signals from the macroscale to the nanoscale. The conversion of external mechanical signals to changes in intracellular biochemical signals and gene expression is known as mechanotransduction. Thus, if the external mechanical signal transmitted to the cell can be controlled in vitro, we can steer cell development to express proteins and matrix desirable to functional tissues.

Mechanotransduction and mechanical conditioning terminology

Cells can be mechanically stimulated by tensile, compressive, or shear forces. *Force* (*F*) is a vector with magnitude (mass times acceleration or $F = ma$) and direction. *Tension* is an applied force (or stress) external to the cell that pulls and causes it to elongate, and can also cause an increase in volume. Conversely, *compression* decreases

the length of the cell. To apply compression, pressure is usually applied. *Pressure* (*P*) is a three-dimensional, isotropic, compressive stress that describes the force per unit area:

$$P = \frac{F_n}{A}$$

Isotropy describes a material property in which the values are the same when measured along axes in all directions; *anisotropy* describes a material property in which the values along axes are different. An example of anisotropy is the induced alignment of cells with repeated applications of stress in one direction.

Stress (σ) is the measure of average normal force per unit area, assumed to be uniformly distributed within a deformable body:

$$\sigma_{avg} = \frac{F_n}{A}$$

Thus, pressure is a type of stress. The SI unit for stress is *pascal* (Pa), which is equivalent to one Newton-force per square meter (1 N/m^2). A normal force or stress is considered to be *tensile* if it is stretched perpendicularly out of the plane or *compressive* if it is acting inward. Tensile stresses are usually denoted by a positive sign convention, and compressive stresses are negative. For example, the vertical cables supporting a suspension bridge are under tension, being pulled downward by the weight of the

bridge. The concrete pillars supporting a bridge from underneath experience compressive stress.

Forces acting on the transverse plane are *shear forces*, which can be normalized over the unit area to obtain the *shear stress* (τ):

$$\tau_{avg} = \frac{F_s}{A}$$

Shear stress is usually described by a "sliding" motion, such as when blocks from the game Jenga® are pulled from the tower or a log is pulled longitudinally out of a stack of firewood.

Strain is a dimensionless quantity defined as elongation per unit length:

$$\varepsilon = \frac{\delta}{L} \qquad \text{or} \qquad e = \frac{\Delta L}{L} = \frac{\ell - L}{L}$$

where ε is the true strain and e is the engineering strain. δ is defined as the total elongation and L is the total length. Similarly, imagine a fiber being pulled. To measure e, the original length of the fiber L and the final length ℓ need to be measured. As with tensile and compressive stresses, strains can also be tensile or compressive and follow the same sign convention. A *linearly elastic* material will assume that for infinitesimally small strains or deformations, the relationship between stress and strain is linear.

Stiffness (k) describes how much a material can resist deformation:

$$k = \frac{AE}{L}$$

where *A* is the cross-sectional area, *E* is the elastic or Young's modulus, and *L* is the length. *Young's modulus* (*E*) describes the ratio of uniaxial stress to uniaxial strain for an isotropic material:

$$E = \frac{tensile\ stress}{tensile\ strain} = \frac{\sigma}{\varepsilon} = \frac{F/A_0}{\Delta L/L_0}$$

where A_0 and L_0 are the original cross-sectional area and length, respectively, to which the force is applied. Conversely, *compliance* is the inverse of stiffness.

The relationship between stress and strain of a material can be graphically represented on a *stress-strain curve* (Figure 1.3). Along the first portion of the curve, the relationship is linear, indicating the linearly elastic region or the Young's modulus. Imagine eating ice cream with a stainless steel spoon: The spoon may deform slightly as it scoops more ice cream from the bowl, but ultimately it returns to its original configuration. When the material reaches its *yield strength*, the material will no longer return to its original shape when the applied force is removed and thus permanently deforms. *Strength* refers to the stress at which the material permanently deforms or fractures. Imagine that more ice cream is desired, but scooping the ice cream directly from the carton fresh out of the freezer causes the spoon to reach its *yield strength* and bend permanently. Materials usually *strain harden* (i.e., material strengthens as it

plastically deforms) until reaching their *ultimate strength*, which is the maximum amount of stress the material can withstand. Beyond this point, a *neck* forms, where the cross-sectional area quickly decreases before reaching the *breaking strength*, where the material ruptures. Continuing to scoop the frozen ice cream will cause the shaft of the spoon to become harder until the stainless steel ultimately breaks.

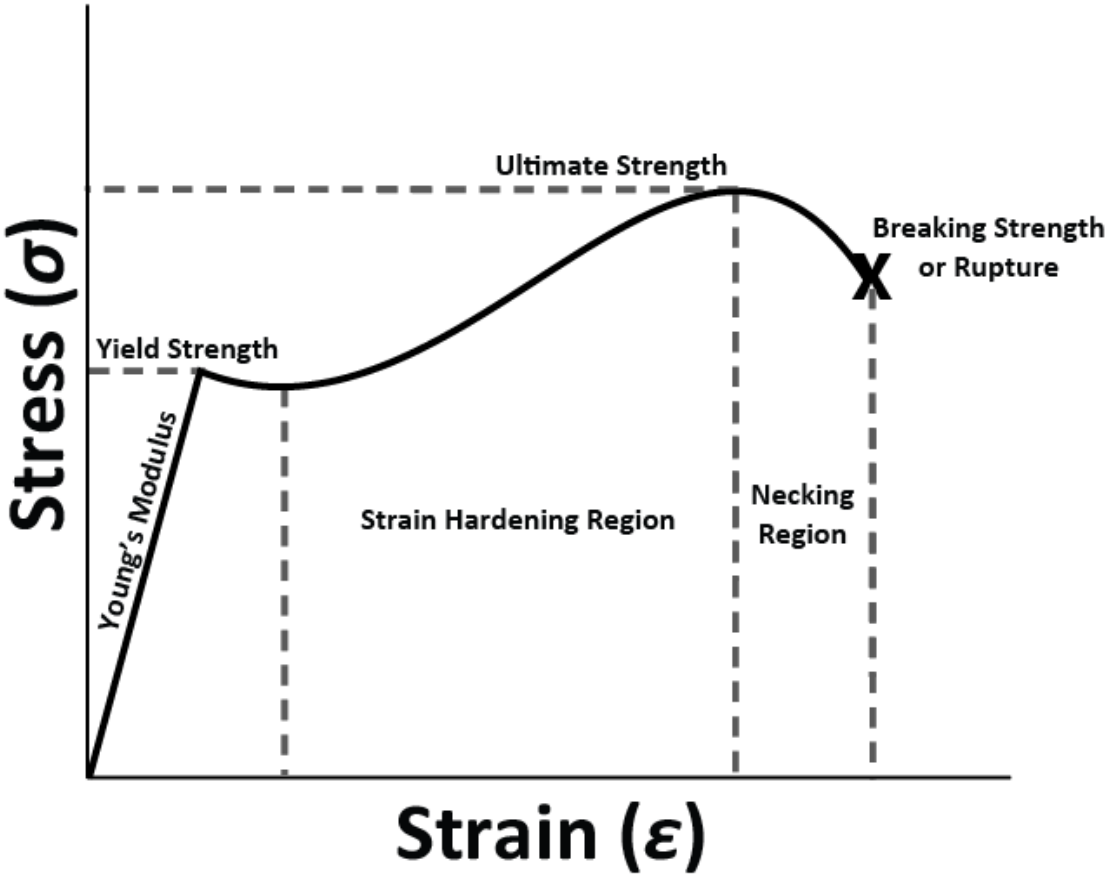

Figure 1.3. A material's relationship between stress and strain can be represented graphically.

Uniaxial or *axial force* is a load directed along one principal axis of an object, and *biaxial force* is a load directed perpendicularly to two principal axes in the same plane.

Equibiaxial refers to equal loads directed along all axes in all directions (i.e., isotropy). *Static* refers to loads in equilibrium, whereas *dynamic* refers to loads in motion. For example, a gymnast in perfect balance on a beam will have a static load on her bones, compared to when her bones will be dynamically loading when she tumbles to dismount off the beam.

Current technologies — Advantages and disadvantages

Brown (2000) presents an excellent review of the types of mechanical stimulation systems. More detail can also be found in Gooch and Tennant (1997). A summary of the devices and methods used to study the effects of physical forces on cells in culture can be found in Table 1.1.

Table 1.1. Summary of devices used to study effects of physical forces on cells in culture (Adapted from Gooch & Tennant 1997).

Name of device/method of developing force	Primary force	Stress profile	Comments
Parallel-plate flow chamber	Shear	• Parabolic velocity profile[1] • Greatest at plate surfaces • Wall stress:[2] $\tau_w = \frac{6\mu Q}{bh^2}$ • Homogeneous • Not a function of position • Linear decrease of pressure as a function of position, usually negligible	• Possible presence of not fully developed laminar flow where fluid enters device[3] • Requires significant number of cells at start of experiment[4] • Simple hardware • Easy to visualize

	Radial flow chamber	Shear	• Linearly decreasing velocity profile • Greatest near center, minimum at outer edge • Wall stress:[5] $$\tau_w = \frac{3\mu Q}{\pi r h^2}$$ • Varies as a function of position	• Possible presence of not fully developed laminar flow where fluid enters device[3] • Requires significant number of cells at start of experiment • Simple hardware • Easy to visualize

	Cone-and-plate viscometer[6]	Shear	• Flow determined by Reynolds number:[6]
			$$R = \frac{r^2\omega\alpha^2}{12\nu} = \frac{r^2\omega\alpha^2\rho}{12\mu}$$
			• For R << 1:
			  ○ Laminar flow
			  ○ Linearly proportional gradient velocity to α
			  ○ Spatially homogeneous flow
				• Possible presence of secondary flows
				• Simple hardware
				• Difficult to visualize

- Wall stress: [6]

$$\tau_w = \mu \frac{\partial U}{\partial y}\Big|_{y=0} = \frac{\mu\omega}{\alpha}$$

- Ideal stress not a function of position

Rotary orbital shaker[7,8]	Shear	• Average stress dependent on rotary speed:[8]
		  ○ 25 rpm: 0.67±0.23 dyn/cm^2
		  ○ 40 rpm: 1.68±0.14 dyn/cm^2
		  ○ 55 rpm: 2.54±0.31 dyn/cm^2
		• Laminar flow
		• Uniform hydrodynamic environment
			• Spatial embryoid body distribution dependent on rotary speed
			• EB size dependent on rotary speed (decreases as rotary speed increases)
			• Simple hardware
			• Easy to visualize

Longitudinal stretch[1]	Tension	• Dynamic or static load • Anisotropic • Peak strain typically ranges from 1–10% • Greatest at the center of the device	• Creates corresponding compressive stress in perpendicular direction • Boundary condition created at grips • May also generate shear stress due to

		• Four-point bending systems deliver low, homogeneous strains	motion of cells relative to fluid • Complicated hardware • Difficult to visualize
Out-of-plane circular substrate stretch[1]	Tension	• Usually dynamic load • Heterogeneous radial strain unless membrane is very thin[9,10] • Greatest at the center of the device	• May be subjected to other stresses depending on signal input, media movement, or pre-existing system tension • Simple hardware • Difficult to visualize

In-plane substrate stretch[1]	Tension	• Isotropic
		• Homogeneous equibiaxial strain
			• Plate approach
			  ○ Simple hardware
			  ○ Easy visualization
			• Biaxial grip approach[11]
			  ○ Complicated hardware

			○ Difficult to visualize
Matrix-contracting gel system[1]	Tension	• Dependent on cell contractile response[12-14]	• Can embed a strain gauge
Compression of gas/liquid phase	Compression	• Static or dynamic load • Spatially homogeneous[1,15]	• Cells do not need to be adhered • Change in concentration of dissolved gas due to increase in oxygen and carbon dioxide partial pressures or osmotic balance[16] • May require different media composition to accommodate pressure changes[17] • Proper humidification required[18] • Simple hardware

Direct compression of specimen phase	Compression	• Static or dynamic load • Spatially homogeneous	• Accommodates explanted tissue specimens[19-22] or polymeric carriers[1] • May cause anisotropic strain deformation from flat plate abutment • Simple hardware

1. Brown TD. J Biomech 2000;33:3-14.
2. Bacabac RG et al. J Biomech 2005;38:159-67.
3. Gooch KJ, Tennant CJ. Mechanical Forces: Their Effects on Cells and Tissues. New York: Springer; 1997.
4. Brown D, Larson R. BMC Immunol 2001;2:9.
5. Kandlikar SG et al. Heat transfer and fluid flow in minichannels and microchannels. Kidlington, Oxford: Elsevier; 2005.
6. Einav S et al. Experiments in Fluids 1994;16:196-202.
7. Carpenedo RL et al. Stem Cells 2007;25:2224-34.
8. Sargent CY et al. Biotechnol Bioeng 2010;105:611-26.
9. Brown TD et al. Am J Med Sci 1998;316:162-8.
10. Brown TD et al. Comput Methods Biomech Biomed Engin 2000;3:65-78.

11. Eastwood M et al. Biochim Biophys Acta 1994;1201(2):186-92.

12. Dahlmann-Noor AH et al. Exp Cell Res 2007;313:4158-69.

13. Lambert CA et al. Lab Invest 1992;66:444-51.

14. Chamson A et al. Arch Dermatol Res 1997;289:596-9.

15. Myers KA et al. Biochem Cell Biol 2007;85:543-51.

16. Ozawa H et al. J Cell Physiol 1990;142:177-85.

17. Tanck E et al. J Biomech 1999;32:153-61.

18. Maul TM et al. J Biomech Eng 2007;129:110-6.

19. Aufderheide AC, Athanasiou KA. Ann Biomed Eng 2006;34:1463-74.

20. Guilak F et al. Osteoarthritis Cartilage 1994;2:91-101.

21. Burton-Wurster N et al. J Orthop Res 1993;11:717-29.

22. Torzilli PA et al. J Biomech 1997;30:1-9.

Fluid Shear Systems

Fluid shear influences a number of cellular phenomena, including but not limited to vasoconstriction via vascular smooth muscle cells, mechanoreception via plasma membrane receptors or ion channels, and nitric oxide release via endothelial cells. Two main types of systems dominate the application of fluid shear stress: parallel plate and cone-and-plate systems. These systems are most useful for studying cell adhesion and engineering vasculature under physiologic flow conditions; however, the main challenge of these systems is keeping a homogeneous fluid flow to produce uniform shear stress.

The parallel plate system is a flow chamber that applies laminar shear flow with an incompressible fluid (i.e., homogeneous and has constant density throughout) by a pressure differential (Figure 1.4A), where the wall shear stress (τ_w) is given by (Bacabac et al. 2005):

$$\tau_w = \frac{6\mu Q}{bh^2}$$

where μ is the fluid viscosity, Q is the volumetric flow rate, b is the width of the chamber, and h is the distance between the plates for rectangular flow chambers. The parabolic velocity profile will generate a shear stress profile that has the maximum magnitude at the plate surfaces, with >85% exposed to homogeneous shear wall stress for b/h>20. For radial parallel plate systems, τ_w is given as a function of radial position r by (Figure 1.4B) (Kandlikar et al. 2006):

$$\tau_w = \frac{3\mu Q}{\pi r h^2}$$

Radial parallel plate systems have a flow inlet from the center of the plate that flows radially outward, covering a larger surface area and having a linearly decreasing velocity profile as it flows from the inner to the outer region. Thus, the highest shear stress is near the center, and the minimum shear stress is at the outer edge. This shear stress profile is most useful for examining a range of stress values with a single experiment, as opposed to several different experiments at different flow rates.

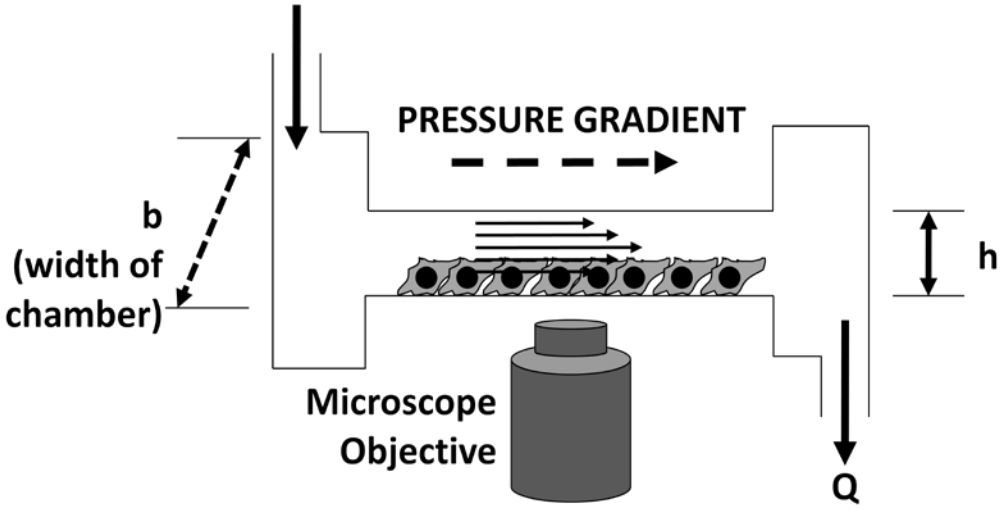

Figure 1.4A.

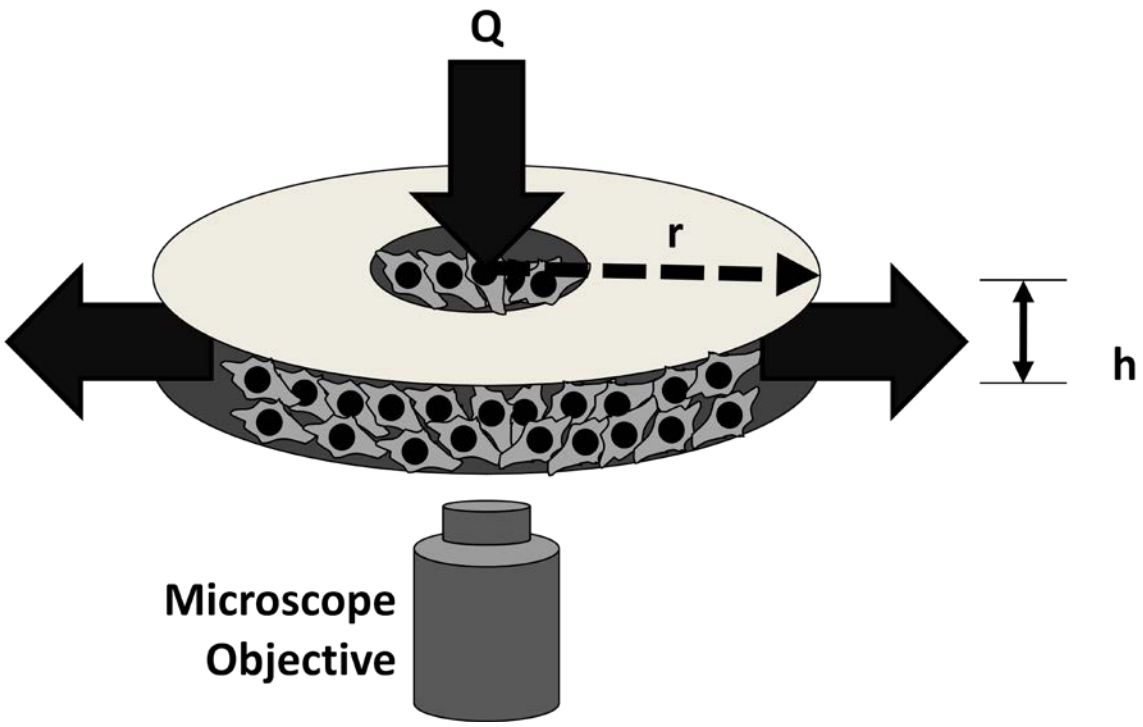

Figure 1.4B.

Figure 1.4. (A) Parallel-plate flow chamber systems apply homogeneous laminar shear stress. (B) Radial parallel plate flow chamber systems apply the highest shear stress near the center and minimum shear stress at the outer edge.

Two slits are formed at opposite ends of a rectangular or radial chamber, between which the pressure difference is created where the lowest speed will occur where the pressure is highest (i.e., the chamber is most narrow) (Brown 2000). Fluid flow can be created by a gravity pressure head (i.e., steady shear stress) or an active pump (i.e., transient shear stress). The parallel plate system requires minimal equipment (fluid flow chamber, tubing, pump if required) and requires a minimal amount of media, which can easily be accessed for changing media. If desired, the

media can also be recirculated. The chamber construction is made to allow easy visualization under a microscope. The system should produce homogeneous fluid flow in the absence of bubbles in the tubing, which can cause cells to be stripped from the substrate. Also, depending on the substrate, the initial adhesion of cells may be low and thus require a significant number of cells (approximately $10^6 – 10^7$ cells), which can be problematic when studying rare cell populations (Brown and Larson 2001). In addition, for inhibition studies, chambers that do not recirculate media may require large quantities of expensive inhibitors.

The second most common system to study shear stress is the cone-and-plate fluid shear system, which places a cone's axis perpendicular to a flat plate to rotate the cone (Figure 1.5) (Brown 2000, Einav et al. 1994). By controlling the angular velocity of the cone rotation, a spatially homogeneous fluid shear stress can be achieved over the plate on which the cone rotates. To determine laminar flow, the Reynolds number (*Re*) can be obtained by:

$$Re = \frac{r^2 \omega \alpha^2}{12\nu} = \frac{r^2 \omega \alpha^2 \rho}{12\mu}$$

where r is the radial distance from the cone's surface, ω is the angular velocity of the cone, α is the angle between the cone and the plate in radians, ν is the kinematic viscosity, μ is the dynamic viscosity, and ρ is density. For values of $Re \ll 1$, the centrifugal force is small, the fluid velocity is a linearly proportional gradient to α, and the fluid shear stress is constant over the entire plate. As *Re* increases, centrifugal force

increases, creating flow in the radial direction near the rotating cone, but the corresponding centripetal flow close to the stationary plate negates it. The shear stress thus changes in magnitude and direction; for *Re* > 4, flow becomes turbulent, which can be achieved via the conic taper and the imposed angular velocity. For *Re* << 1, the fluid wall stress (τ_w) is constant over the flat plate and is given by:

$$\tau_w = \mu \frac{\partial U}{\partial y}\bigg|_{y=0} = \frac{\mu\omega}{\alpha}$$

where *U* is the fluid velocity parallel to the wall and *y* is the distance to the wall. Although the hardware for the system is simple, it also makes modulating a constant shear stress for sustained periods of time difficult since the flow field will often develop transient peaks in shear stresses. In addition, microscopic visualization can be challenging.

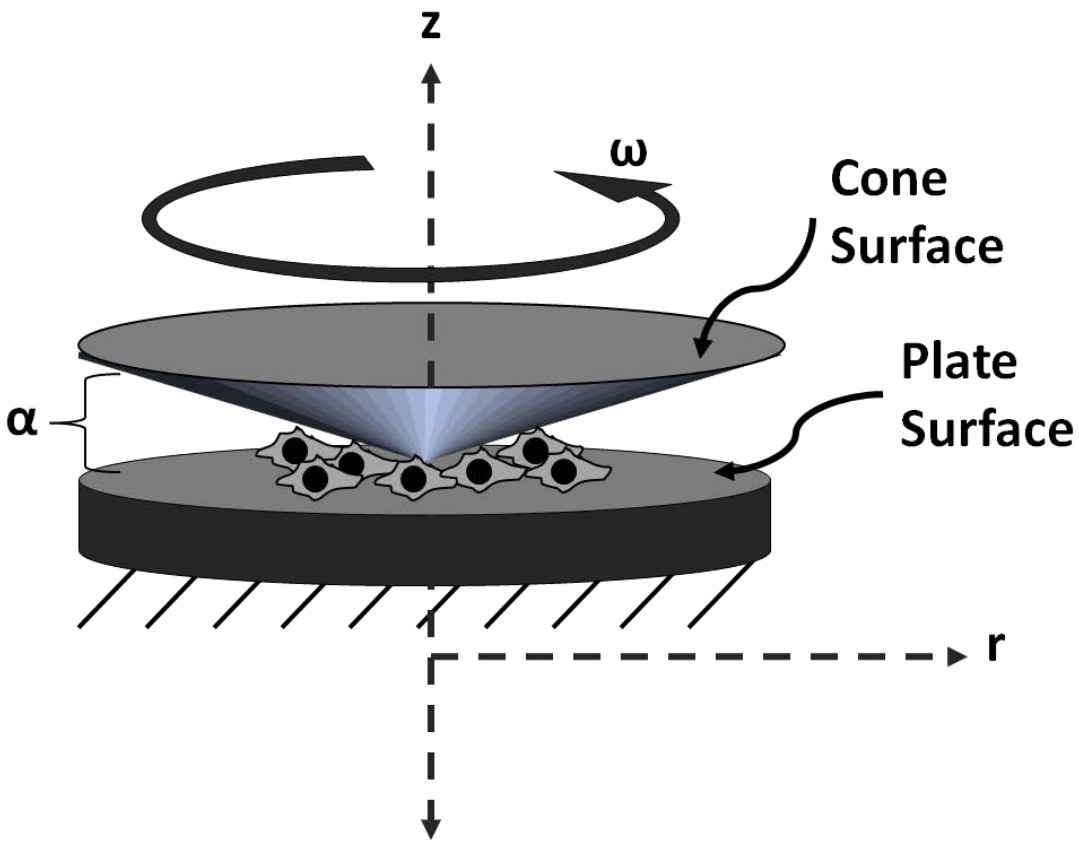

Figure 1.5. Cone-and-plate systems apply homogenous laminar shear stress.

More recently, several groups have used fluid shear via rotary suspension culture bioreactors to induce embryonic stem cell aggregation into embryoid bodies (EBs) and differentiation on a large scale (Kim and von Recum 2009, Kim and von Recum 2010, Cormier et al. 2006, Sargent et al. 2010, Carpenedo et al. 2007). EBs recapitulate the path of cellular morphogenic events of embryos as in the native development environment, from embryo to the formation of the three germ layers (ectoderm, endoderm, and mesoderm) (Coucouvanis and Martin 1995, Keller 1995). Other methods of EB formation are problematic: (A) Hanging drop formation is tedious, has low yield,

and is not easily scalable (Maltsev et al. 1994); (B) Centrifugation into 96-well plates also has the same issues as hanging drop formation (Ng et al. 2005); and (C) Static suspension cultures produce heterogeneous-sized EBs, which lead to heterogeneous differentiation and thus lower yield (Dang et al. 2002). Many groups have turned to large rotary suspension culture bioreactors and spinner flask methods to increase EB production with excellent results (Chen et al. 2006, Dang et al. 2002, Gerecht-Nir et al. 2004, Wang et al. 2006b, Zandstra et al. 2003). However, as a consequence of space constraints, a few groups have reduced the scale to simply that of a 10-cm Petri dish, achieving suspension through a rotary orbital shaker (Kim and von Recum 2009, Kim and von Recum 2010, Carpenedo et al. 2007, Sargent et al. 2010). Carpenedo et al. (2007) reported the first successful large-scale, size-controllable production of EBs using this method, and Kim and von Recum (2009, 2010) demonstrated successful differentiation of early, middle, and late progenitors for endothelial cells, illustrating the effects of shear mechanical stimulation on endothelial differentiation. Sargent et al. (2010) later characterized the hydrodynamic conditions necessary for EB formation with optimal and uniform distribution for rotary orbital shaker suspension cultures. EBs decreased in size but increased in yield as the speed increased (20–25 rpm gives 500 µm diameter EBs; 40–50 rpm, 225 µm; 55–60 rpm, 140 µm). More importantly, the rotary orbital conditions did not hinder the normal progression of differentiation, and differentiation markers for all three germ layers increased. Thus, compared to static culture conditions, hydrodynamic forces significantly influence gene expression and impact the internal organization of cells within EBs.

Tensile Loading Systems

The most common biologic stressor studied is tensile stress (see terminology section for definitions and equations), and examples of biologic phenomena are numerous. Microscopic tears in tendon fibrils may disrupt homeostatic tension, and the subsequent stress absence may induce apoptosis to tendon cells (Egerbacher et al. 2008). Ventricular myocytes undergoing tensile deformations can stimulate mechanosensitive currents that lead to spontaneous contraction (Bett and Sachs 2000). When the skin is stretched, mRNA for collagen synthesis and other ECM proteins increases, indicating upregulation at a pretranslational level (Lambert et al. 1992).

Tensile loading systems can be categorized into four different groups: longitudinal stretch, out-of-plane circular substrate distention, in-plane substrate distention, and contracting systems (Brown 2000). Longitudinal stretch systems apply uniaxial or anisotropic deformations, while out-of-plane circular substrate systems apply radial distention. In-plane substrate systems allow for biaxial or equibiaxial stretching. The last system involves matrix contraction to study cell responsive behavior.

Longitudinal stretch systems generally employ gripped substrates that are run by a stimulating driver (Figure 1.6A) (see Table 1.2 for descriptions) (Brown 2000). Most mechanical conditioning systems are designed to deliver peak strains in the range of 1–10% (Brown 2000). Tensile loading systems have advanced from simple static stretch to complex systems that can allow control of parameters such as duty cycle, stress magnitude, frequency, and waveform. However, these loading systems still have

limitations. The tensile stress of the substrate causes a corresponding compressive stress in the perpendicular direction. Additionally, because the substrates must be gripped, a boundary condition is created.

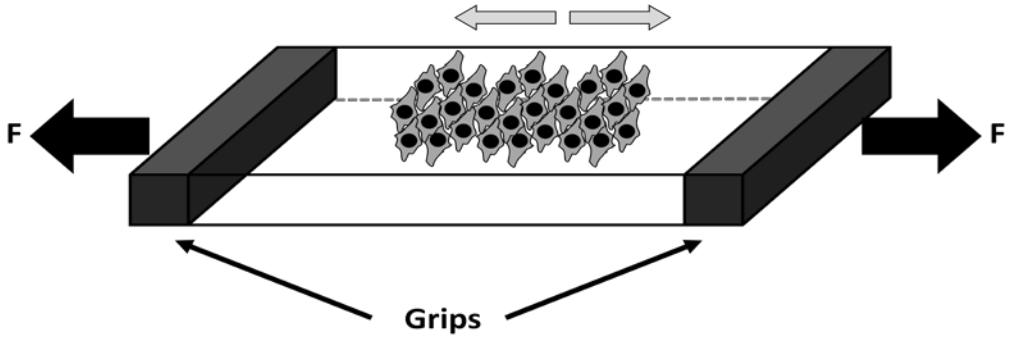

Figure 1.6A.

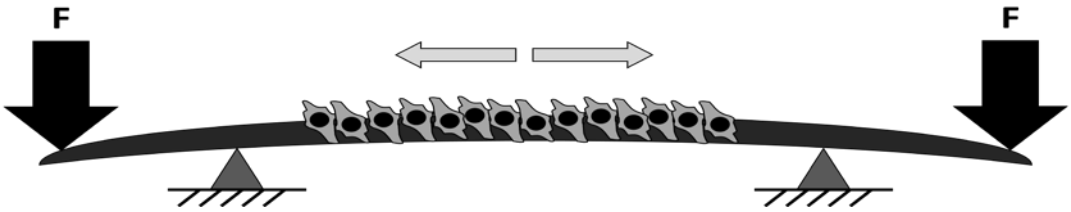

Figure 1.6B.

Figure 1.6. Longitudinal tensile loading systems apply uniaxial stress by (A) gripping and pulling on a substrate or (B) bending a substrate.

Table 1.2. Methods to apply tension.

Method	Description	Select References
Longitudinal Strain (Uniaxial Strain)		
Immobilized specimens	• Frame supports stretched specimen • Static stretch applied	• Weiser et al. 1995 • Somjen et al. 1980 • Meikle et al. 1979
Thumbscrew-driven stretch frame	• Frame with thumbscrews supports substrate • Strain increases with each turn of the screw • Quasi-static stretch applied	• Komuro et al. 1990
Cam systems	• Eccentric disks rotated axially by a motor • Translates rotary motion into oscillatory linear motion • Dynamic stretch applied	• Gupta et al. 2008 • Eastwood et al. 1994 • Ives et al. 1986 • De Witt et al. 1984

		• Leung et al. 1977
Linear actuators	• Applies cyclic force in controlled, linear manner • Based on principle of inclined plane turned into a screw thread • Dynamic stretch applied	• Alexander et al. 1999 • Ozerdem and Tözeren 1995
Solenoid-driven and electromagnetically-driven metal bars	• Coil of wire through which current passes to generate energy via a magnetic field • Magnetic field attracts metal bars embedded within substrate • Dynamic stretch applied	• Forth and Layne 2008 • Smalt et al. 1997 • Xu et al. 1996 • Alexander 1976
Pneumatic pistons	• Convert potential energy of compressed air into kinetic energy • Transfers energy to piston to impart force • Dynamic stretch applied	• Chokalingam et al. 2009 • Gustafson et al. 2006 • Sotoudeh et al. 1998
Mounted substrate-substrate bending	• Cells seeded on rectangular substrate • Substrates mounted to a base substrate attached to outrigger arm	• Neidlinger-Wilke et al. 2009 • Neidlinger-Wilke et al. 1994 • Murray and Rushton 1990

	• Powered by stepper motor, which allows waveforms to be varied easily • Dynamic stretch applied	• Vandenburgh and Karlisch 1989
Four-point bending systems	• Do not need grips for substrate (no boundary condition) • Deliver low, homogeneous strains • Maneuvers substrate using shielded electromagnetic actuators or seed plastic strip as substrate • Can also embed strain gauges	• Li et al. 2010 • Carpenter et al. 2006 • Jessop et al. 2002 • Robling et al. 2001 • Bottlang et al. 1997 • Pitsillides et al. 1995 • Jones et al. 1991
Out-of-Plane Circular Substrate (Radial Strain)		
Template displacement	• Convex template prong pressed vertically against underside of substrate for displacement • Static or dynamic load	• Rana et al. 2008 • Felix et al. 1996 • Matsuo et al. 1996

		• Williams et al. 1992 • Vandenburgh and Karlisch 1989 • Hasegawa et al. 1985
Flexible bottom substrate using vacuum	• Vacuum applied underneath membrane • Distends below origin position • Imparts strain to cells seeded on top of membrane • Controllable parameters include percent strain (vacuum magnitude), waveform, frequency, and duty cycle • Uniform strain only for very thin membrane	• Banes et al. 1985
Positive pressure displacement (fluid) on flexible substrate	• Flexible sheets clamped down into a circular shape • Pressure from fluid causes upward displacement from origin position • Can be driven by pneumatic cylinders or solenoid-based devices	• Ellis et al. 1995 • Brighton et al. 1991 • Winston et al. 1989

In-Plane Distention (Equibiaxial Strain)

Flat plate upward displacement Flat plate with applied vacuum	• Flat plate is frictionless (e.g., lubricated) • Plate driven upward (e.g., piston) • Modification of in out-of-plane, flexible bottom system using vacuum • Insert a frictionless flat plate and apply vacuum for periphery downward displacement	• Hung and Williams 1994 • Schaffer et al. 1994 • Gilbert et al. 1994
Multiaxial tension loading system	• Applies stretch on two axes perpendicular to each other • Cells seeded in intersection of two membranes	• Gupta et al. 2008 • Norton et al. 1995 • Eastwood et al. 1994
Matrix contracting systems		
Acid-soluble gel matrices	• Metabolite secretion causes gel dissolution • Cell tension will cause contractile response • Gel contracts as a result of cellular contraction	• Dahlmann-Noor et al. 2007 • Chamson et al. 1997 • Lambert et al. 1992 • Tomasek et al. 1992

Alternatively, to circumvent the boundary problem, some groups have designed four-point bending systems (Figure 1.6B) that typically deliver low, homogeneous strains (Robling et al. 2001, Jessop et al. 2002, Li et al. 2010), which may not load in the physiological range (such as with osteoclasts entombed in mineralized matrices). Groups have driven substrate stretch using a number of options, such as shielded electromagnetic actuators (Bottlang et al. 1997) and cell-seeded plastic strips (Pitsillides et al. 1995). The substrates in four-point bending systems often engage strain gauges to quantify the amount of strain (Jones et al. 1991).

Out-of-plane circular substrate systems typically create deformations proportionate with respect to the radius, with the maximum strain occurring at the center and zero strain at the periphery. The substrate is flexible and displaced from its originating position via template displacement (Figure 1.7A), vacuum of substrate (Figure 1.7B), or positive fluid displacement of substrate (Figure 1.7C) (see Table 1.2 for descriptions) (Brown 2000).

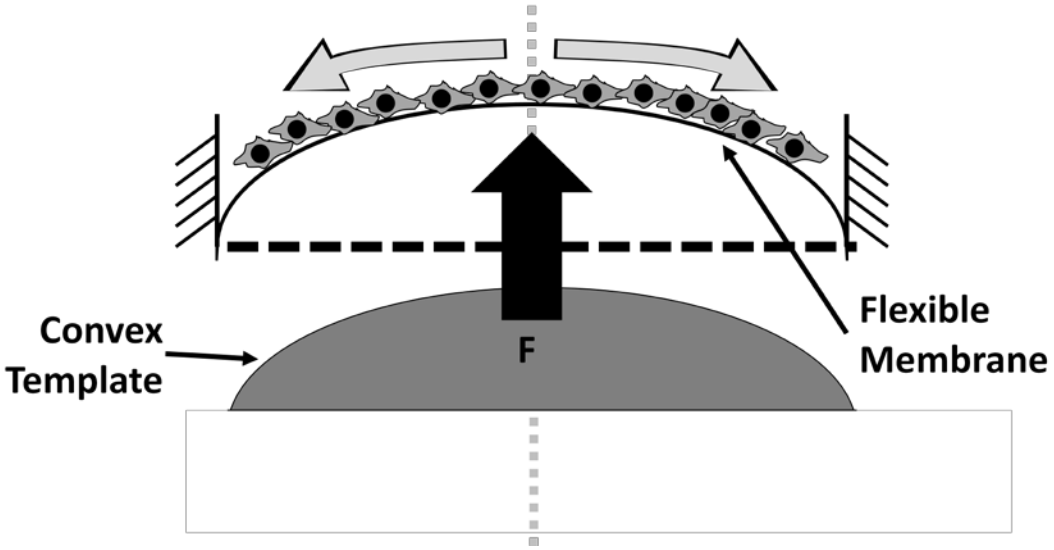

Figure 1.7A.

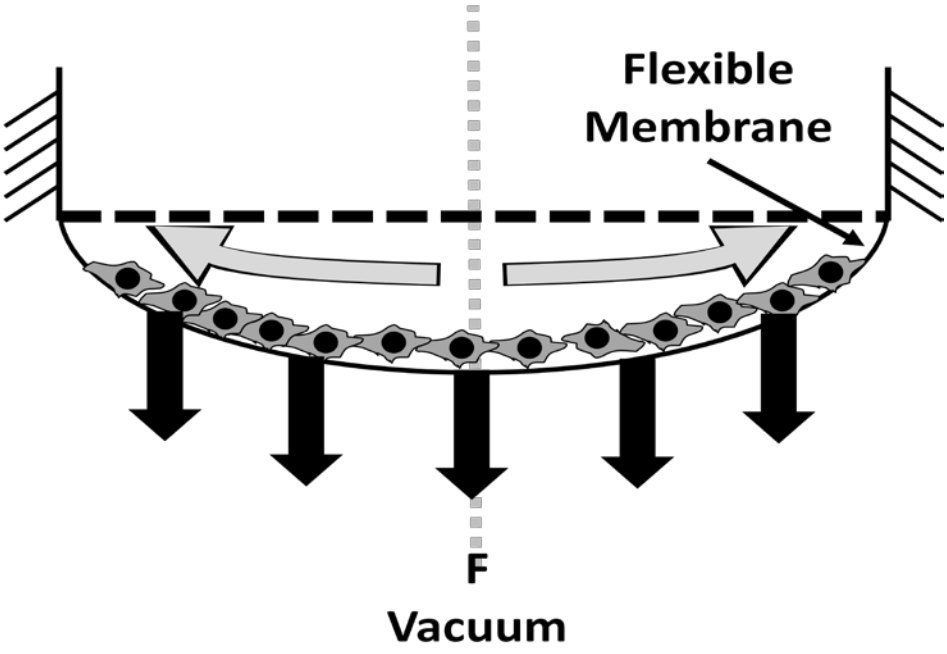

Figure 1.7B.

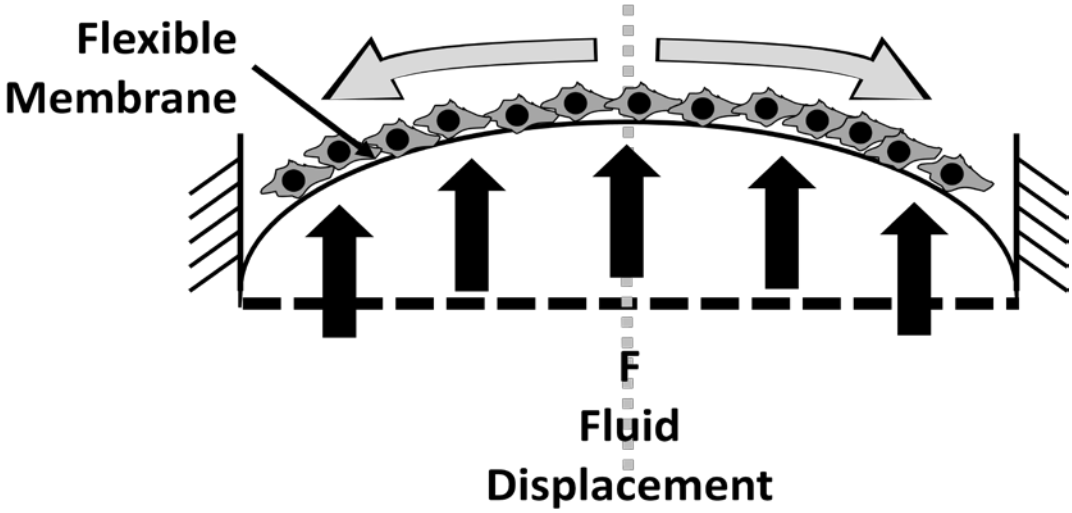

Figure 1.7C.

Figure 1.7. Out-of-plane circular substrate distention systems apply radial strain (linearly decreasing with respect to the center) by (A) physical displacement with a solid template, (B) downward displacement with applied vacuum, or (C) upward displacement with positive pressure fluid flow.

The first to report using a template to displace a substrate, Hasegawa et al. (1985) claimed that the curvature of convex templates governed distention in the membrane, and therefore the input strain. However, although the group claimed their template produced uniform strain, they did not provide any means (calculated or measured) to verify the specific template used, and Williams et al. (1992) disputed Hasegawa et al.'s claim through analytical solutions that demonstrate surface strains due to bending are not negligible. Nevertheless, the design inspired several subsequent modifications, such as changing the substrate area (Felix et al. 1996), applying static stretch via thumbscrew-driven stretch frame (Rana et al. 2008), or using pulsating rounded prongs (Vandenburgh and Karlisch 1989) or flat-ended circular pistons (Matsuo et al. 1996).

Banes et al. (1985) first introduced the concept of applying a vacuum to a flexible bottom substrate. The device became one of the most requested mechanostimulus devices and is now marketed as the Flexcell Tension System (Flexcell International Corporation, Hillsborough, NC). Its popularity with the scientific community outpaced thorough analysis by the engineering community, who later determined the substrate had inhomogeneous radial strain (Gilbert et al. 1994, Gilbert et al. 1990, Brown et al. 2000). Redesigned in 1995, the current iteration is a very thin substrate that closely resembles ideal membrane behavior and has radial strain homogeneity (Brown et al. 2000, Brown et al. 1998). Converse to vacuum application, positive pressure displacement can be done using flowing fluid (Winston et al. 1989, Brighton et al. 1991),

Several factors may influence the cells in these systems to be subjected to stresses other than tension. For example, cells on diaphragmatic substrates subjected to pressure differentials may also be exposed to shear stresses due to media movement relative to the cells. Other factors may include the input signal magnitude, frequency, and waveform; the depth and viscosity of the nutrient media; and any pre-existing tension in the system (Brown 2000). The constant movement in these systems also makes cellular observation under microscopy difficult.

Alternative solutions to work around strain heterogeneity in out-of-plane circular deformation systems feature in-plane distention to achieve homogeneous biaxial or equibiaxial strain. A few groups physically limit cell adhesion to a specific spot by spot-plating or masking to achieve uniform deformation; however, the more common method is to change the area impacted by deformation while keeping the culture plane level. One approach axially upwardly punctuates a large area of the substrate from underneath using a frictionless plate (e.g., lubricated) (Figure 1.8A) (Hung and Williams 1994, Schaffer et al. 1994); the other approach modifies the Flexcell, using a large area frictionless plate and applying vacuum from underneath along the periphery (Figure 1.8B). Cells centered over the plate are stretched in an outwardly radial direction when the deforming component causes the overlying substrate to slide over plate edges with negligible friction, and both methods allow easy access for visualization. In an entirely different approach, some groups grip a membrane or substrate (e.g., collagen) and pull in two perpendicular directions, where the cells seeded in the intersection of both membranes are exposed to isotropic stretch (Figure 1.8C,D) (Eastwood et al. 1994,

Gupta et al. 2007, Gupta et al. 2008, Norton et al. 1995). Although friction is negligible, the hardware necessary to implement this approach is challenging and does not allow easy access for microscopy.

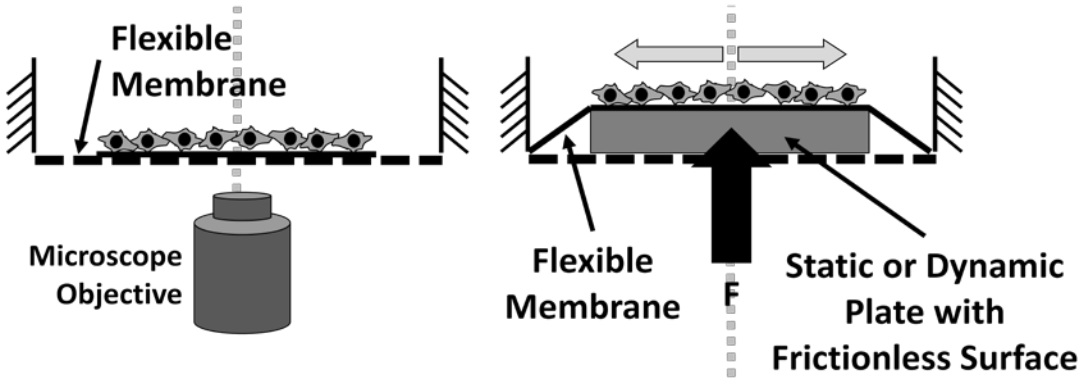

Figure 1.8A.

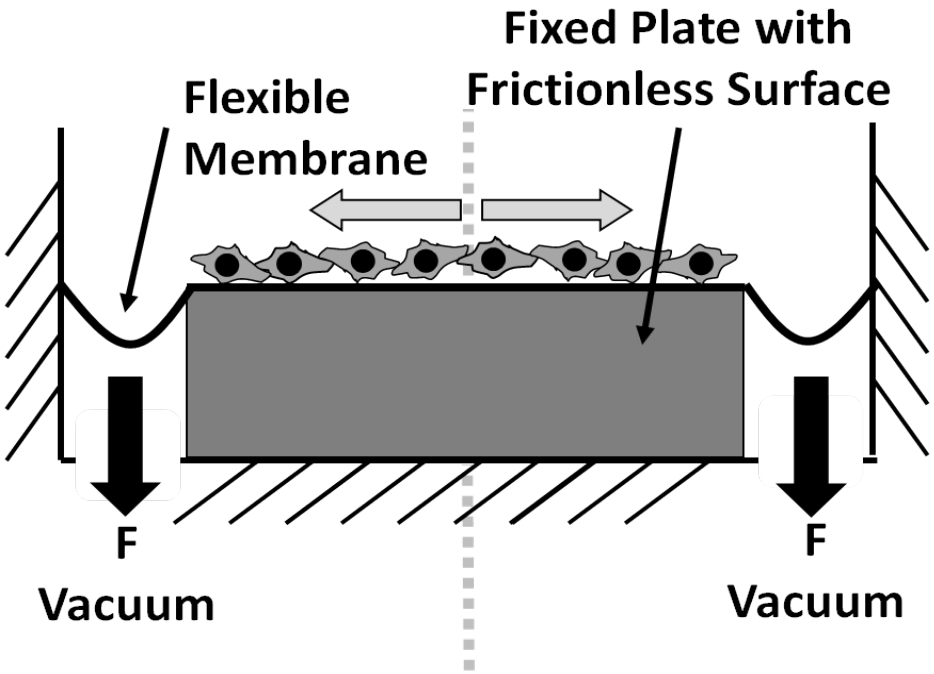

Figure 1.8B.

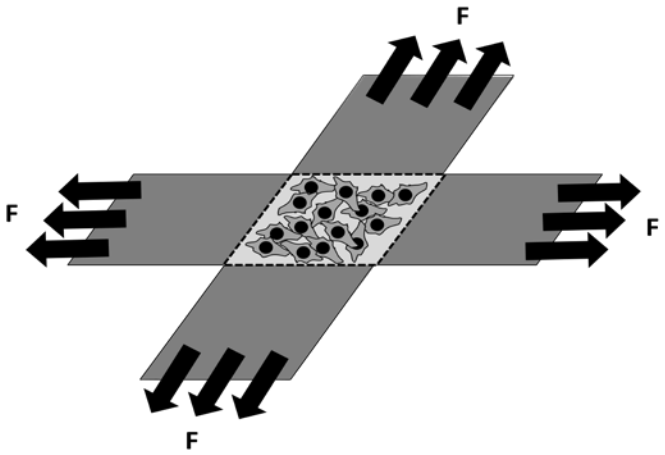

Figure 1.8C.

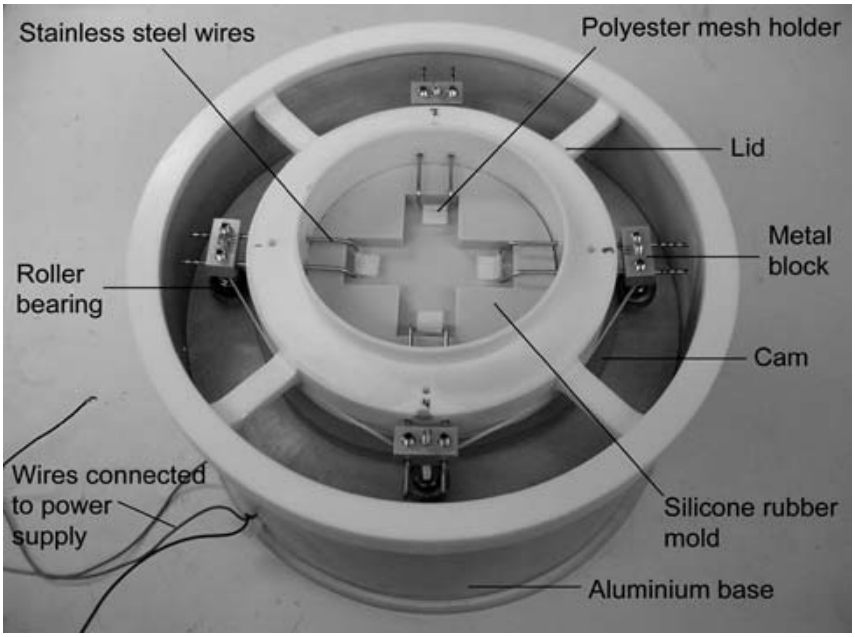

Figure 1.8D.

Figure 1.8. In-plane displacement systems apply homogeneous equibiaxial strain to flexible membranes by (A) upward plate displacement or (B) downward vacuum displacement. Alternatively, (C) isotropic strain may be applied with two axes of stretch, situated perpendicular to each other. (D) gives an example of such a system. Reprinted with the permission of K. Jane Grande-Allen.

Finally, matrix contracting systems use acid-soluble gel matrices seeded with cells as a way to study cellular response to tension. The secretion of metabolites will cause gel dissolution (Lambert et al. 1992, Dahlmann-Noor et al. 2007, Tomasek et al. 1992, Chamson et al. 1997, Brown 2000), and the subsequent residual stress from the adherent cell results in spontaneous cellular contraction and thus gel contraction. The gel may also be embedded with a strain gauge as a way to quantify the contractile response.

Compressive Loading Systems

Chondrocytes that decrease aggrecan expression in articular cartilage (Lammi et al. 1994), osteocytes that signal a decrease in bone resorption by inhibiting osteoclast formation (Lau et al. 2010), and irritant receptors lining the inside of the epithelium of the airways that are activated by sustained inflation of the lungs (Kappagoda and Ravi 2006) are all examples of biologic phenomena response to compressive stresses (see terminology section for definitions and equations). To study cell behavior to compression in a variety of tissues (e.g., cartilage, bone, airways, vasculature), scientists frequently use positive or negative hydrostatic pressure (i.e., the pressure exerted by a fluid at equilibrium due to the force of gravity) to apply mechanical stress to the tissue or cell culture (Myers et al. 2007, Brown 2000).

Hydrostatic pressure systems have relatively simple equipment setup in comparison to tensile loading systems: A flat plate is used to press down on the contained culture (Figure 1.9A). The system may or may not also have an incubator gas

phase pressurized on top of the media. The simplicity in equipment allows replicate experiments to be run simultaneously using a manifold design (Brown 2000). The load application may be static or transient and is spatially homogeneous. Unlike fluid shear and tensile loading systems, cells in compressive loading systems do not need to be adhered to a substrate to be subject to hydrostatic pressure. In addition, hydrostatic pressure systems generally do not require direct contact with the flat plate, which guarantees that the specimen is not impacted by the plate and that metabolite transfer between cells and media is not impeded physically. On the other hand, incubator partial pressures of oxygen and carbon dioxide must increase to reach physiologic stress levels under normal culture conditions (Ozawa et al. 1990). Consequential to the increase in gas pressures, different media composition or alterations to the physical chemistry may be required unless the load is low in magnitude or high in frequency (Tanck et al. 1999). In cyclic pressure systems, the constant movement of air can cause a change in osmotic balance as water from culture media evaporates, leading to disruption in cell processes and even cell death (Maul et al. 2007). In conjunction with this problem, proper humidification of the chamber is difficult to preserve for long-term experiments (>2 days). Finally, compressive loading systems are limited in use for engineering tissues since very few tissues experience purely hydrostatic pressures.

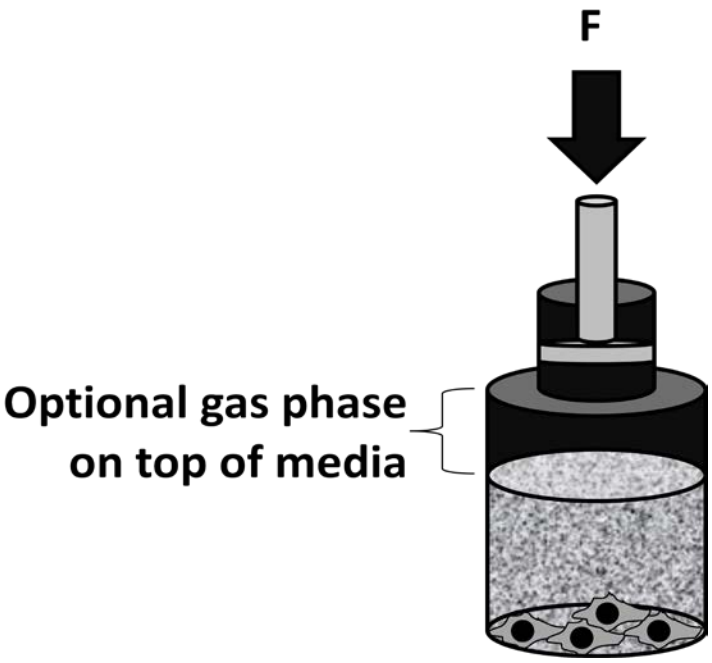

Figure 1.9A.

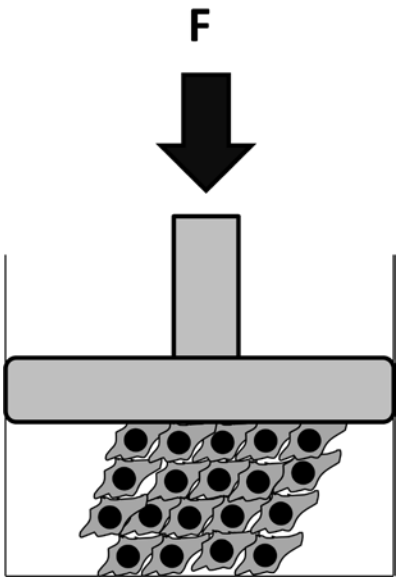

Figure 1.9B.

Figure 1.9. Compressive loading systems use a plate to apply pressure (A) directly to the liquid phase or on top of a buffering gaseous phase. (B) Specimens can also be loaded by directly abutting the plate to the sample.

Alternatively, some approaches have placed the specimens directly against a hydraulically-operated flat plate, such as with cartilage, which mimics direct contact in vivo loading (Figure 1.9B) (Brown 2000, Aufderheide and Athanasiou 2006, Guilak et al. 1994, Burton-Wurster et al. 1993, Torzilli et al. 1997). This method accommodates a variety of three-dimensional specimens, such as tissue explants or cells seeded within a matrix or polymeric carrier, a distinct advantage over non-contact pressure application since interactions between cells and a carrier can be studied (Brown 2000). Again, the hardware required is simple, although the plate's direct abutment to the specimen may cause strain deformations as a result of friction, not uniaxial compression. The specimens may be unconfined or confined during compression; the latter conditions more closely mimic physiologic conditions but may impede diffusion of nutrients and metabolites. In addition, because the uniaxial loading application induces an anisotropic strain field (as opposed to isotropic in non-contact compression), competing cellular or molecular response mechanisms may be activated.

Only a few novel systems have been custom-designed (Hasel et al. 2002, Nagatomi et al. 2002, Pugin et al. 1998, Sumpio et al. 1994, Parkkinen et al. 1995, Maul et al. 2007, Shaikh et al. 2010), since pressure application is conceptually different from tensile systems. Hydrostatic pressure is generally non-directional in its application (except for gravity), and the actual compressibility of fluid-filled cellular structures is orders of magnitude smaller than tensile deformations (Myers et al. 2007). For example, an erythrocyte experiencing a 10 MPa load (the upper limit of loads experienced in vivo) will only result in a roughly 0.4% volume change due to compression. Despite its small

magnitude stress contribution in comparison to shear and tensile stresses, cyclic hydrostatic pressure is thought to be an important stimulus in determining cell phenotype (Myers et al. 2007).

Upcoming Technologies

The mechanical stimulation systems described previously have been used to distinguish the effects of the applied stress independent from other stress parameters. The next level of complexity in mechanical stimulation systems combines these technologies with independent control to understand interactions between simultaneous stresses and to provide tools to the tissue engineer. Novel systems for application of both fluid shear and longitudinal distention have been used to study stretch-activated membrane ion channels in chondrocytes (Wright et al. 1996), understand the response of tendon cells to cyclic loading (Lavagnino et al. 2008), and to engineer heart valve tissue (Engelmayr Jr. et al. 2008). Other groups have grown cells on the insides of distensible tubular constructions and applied fluid shear to study vasculature responses to wall strain (Ayajiki et al. 1996, Moore et al. 1994, Benbrahim et al. 1994). With the constant, dynamic loading undertaken, bone and cartilage have been studied for the interaction between compressive and shear forces (Heiner and Martin 2004, Orr and Burg 2008). In addition, these groups designed their devices with the forethought to become culture systems for tissue engineering.

Translation is limited until we can recover mechanically conditioned cells without damage. For example, by modifying the surface of the silicone substrate with an *N*-

isopropylacrylamide (NIPAAm)-based polymer, Lee and von Recum (2010) introduced a nondamaging cellular detachment component to the existing baseplate substrate for a commercially available mechanical culture tension system. NIPAAm-based polymers have advantageous properties to tissue engineers. Above 32°C (e.g., body temperature), cells preferentially and viably attach and grow on these materials. Below 32°C, the polymer resumes hydrophilic behavior, and swells to allow spontaneous cellular detachment, thus avoiding enzymatic (e.g., trypsinization) or mechanical (e.g., scraping) damage to the cells and ECM. Thus, cells may be mechanically stimulated on NIPAAm-modified substrates at parameters specific to the engineered regenerative or replacement tissue to induce synthesis of ECM that can withstand native stresses. The resulting cellular sheet with synthesized matrix can then be detached intact with cells and subsequently layered with other sheets to create a three-dimensional tissue. Current engineered tissues will reach diffusion limits for oxygen and nutrient delivery without a blood supply nearby. The cell sheet layering method is promising since it can circumvent the diffusion limiting problem (Okano et al. 1993, Shimizu et al. 2006): Layers of vasculature or layers of cells with high angiogenic potential can be placed between sheets of the target tissue.

Conclusion

The human body has an amazing capacity to regenerate after an injury. But sometimes, the remodeling environment presents unnatural mechanical stimuli that may promote maladaptation instead of healing. Understanding how cells respond to

mechanical stimuli is a critical step in learning how to direct cells in vitro to produce regenerative tissues. Additionally, current and future mechanical conditioning technologies that reconstruct the fluid shear, tensile, and compressive forces of the in vivo environment can enable tissue engineers in improving patient recovery.

Chapter II: Cell Culture Platform with Mechanical Conditioning and Non-damaging Cellular Detachment

Elaine L. Lee and Horst A. von Recum

Case Western Reserve University, Cleveland, OH 44106

*This article has been reprinted with permission and modifications from *J Biomater Mater Res A* 2010;93(2):411-8 and was awarded the Student Award in the Master's Degree Category for the Society of Biomaterials.

Abstract

Cells implanted following injury may remodel undesirably with improper mechanical stimulation from surrounding tissue. Proper conditioning of tissue engineered constructs before implantation can lead to suitable tissue architectures, along with an extracellular matrix (ECM) environment that more closely mimics native tissue. Additionally, cell implantation without bulky polymeric scaffolding is often desirable. Previous researchers have created devices capable of applying mechanical forces to cells (e.g. stretch) but cellular removal from these devices, such as by trypsin, often results in irreversible damage. Conversely, devices are available that can detach intact cells, but these are inelastic, non-stretchable substrates. We have created a cell culture platform that allows for mechanical conditioning and then subsequent non-damaging detachment of those cells. We have modified silicone culture surfaces, to incorporate thermally responsive polymers of N-isopropylacrylamide (NIPAAm) to create an elastic substrate that can also change surface properties with temperature

change. A copolymer of NIPAAm and 10% w/w acrylic acid (AAc) was conjugated to an amine-bonded silicone surface through carbodiimide chemistry. Cells were able to attach to the resulting surfaces at 37°C and showed detachment by rounded morphology at 25°C. Following mechanical stretching, cells were still able to spontaneously detach from these modified silicone surfaces with temperature change.

Introduction

Advances in cell therapy have demonstrated remarkable potential for therapeutic management of diseases and for improving function to damaged tissue.[1-8] However, cells implanted following injury may remodel undesirably with improper mechanical stimulation from surrounding tissue. Proper conditioning of tissue engineered constructs before implantation can lead to suitable tissue architectures, as well as extracellular matrix (ECM) growth that more closely mimics native tissue. Additionally, polymeric implant materials may elicit undesired responses, such as inflammation, even with degradable materials. A strategy that can deliver cells in prefabricated natural extracellular matrix (ECM) scaffolding without implanting extraneous bulky polymers is highly desirable.[2,6,8]

ECM allows cells to adhere, grow, migrate, and differentiate, as well as functionally sustains mechanical forces such as stress, tension, compression, and shear to allow cells to maintain shape.[9] Since both stem cells and transplanted cells are highly sensitive to surrounding environmental stimuli, the load demands at an injury site may heavily influence a random alignment of cells, and may even lead to undesired

remodeling or cell death.[9-18] As demonstrated in stem cells,[19,20] smooth muscle cells,[21] endothelial cells,[22] and various cardiovascular tissues,[23,24] mechanical conditioning before implantation may provide such cellular orientation and ECM growth stimulus.[25]

Cells subjected to cyclic deformations, such as cardiomyocytes, will elongate and orient perpendicularly to the axis of deformation.[25-28] The kinds and magnitudes of mechanical stresses acting on the tissue can influence the growth of the ECM. By manipulating the types and magnitudes of stresses applied, researchers can manage the gene expression, which effects cell differentiation and ECM protein secretion, influencing the overall mechanical properties and success rate of engineered tissue.[29]

However, while present mechanical conditioning methods use flexible substrates such as collagen and silicone, these devices cannot detach cells without damage.[25,30-33] Instead, removal of cells requires either enzymatic digestion (e.g., trypsin) or physical scraping, which can lead to irreversible damage to cells and the developed ECM.[34] A device built to allow mechanical conditioning using a flexible membrane with spontaneous cell detachment under more mild conditions, such as temperature change, is favored.

Many researchers have demonstrated previously that non-damaging cell detachment from traditional tissue culture surfaces is possible using thermally responsive polymers such as poly(N-isopropylacrylamide) (P(NIPAAm)).[35-38] P(NIPAAm) forms a dense, hydrophobic film suitable for cell attachment at 37°C, but has a conformation change that allows it to become a loose, hydrated network that can cause spontaneous cell detachment below 32°C. As a result, cells can be detached as

continuous 2D sheets while simultaneously maintaining cell-to-cell and cell-to-matrix interactions.[39] However, the existing thermally responsive cell culture detachment substrates have only been used in conjunction with hard, inelastic materials such as polystyrene, which are unsuitable for cyclic mechanical conditioning of cells. In addition, thermally responsive surfaces initially made by Okano and associates used a high-energy electron beam to graft P(NIPAAm) onto the surface of a tissue-culture polystyrene dish.[40] Such methods of P(NIPAAm) grafting are highly damaging to the flexible membranes, and the low mechanical strength of P(NIPAAm) alone makes it unsuitable for mechanical conditioning.

A few researchers have applied thermally responsive coatings to other surfaces, including silicone. Polydimethylsiloxane (PDMS or silicone) is a transparent biomaterial with good compatibility and high mechanical strength and elasticity.[41] Although studies have demonstrated the feasibility of a thermally responsive coating on flexible membranes, their end use was intended for applications other than cell culture, more specifically for drug delivery. Liu and Sheardown created an ophthalmic biomaterial with an interpenetrating network of P(NIPAAm) and silicone to increase the permeability and delivery of oxygen and glucose to the eye.[41] Reddy and associates created a flexible wound dressing with P(NIPAAm) and polyurethane that was loaded with a cell attractant.[42] Although Ma and colleagues have recently demonstrated cell detachment from P(NIPAAm) grafted onto silicone (>1 mm thick) using benzophenone photopolymerization, their application concentrates on applying this technology to

microchips and microchannels for fluid manipulation, rather than using a thin silicone membrane for cell conditioning.[43]

We have fabricated a device that combines elastic properties required for cyclic mechanical conditioning and thermally reversible cellular detachment properties required for non-damaging removal of cells (Figure 2.1). We have chemically modified silicone membrane surfaces with P(NIPAAm) copolymers for use as a bioreactor to mechanically stimulate controlled ECM growth. Our initial study successfully demonstrates our device's ability to attach and detach cells from our modified flexible silicone membranes. Future studies will evaluate how these materials translate to the detachment of continuous cell sheets.

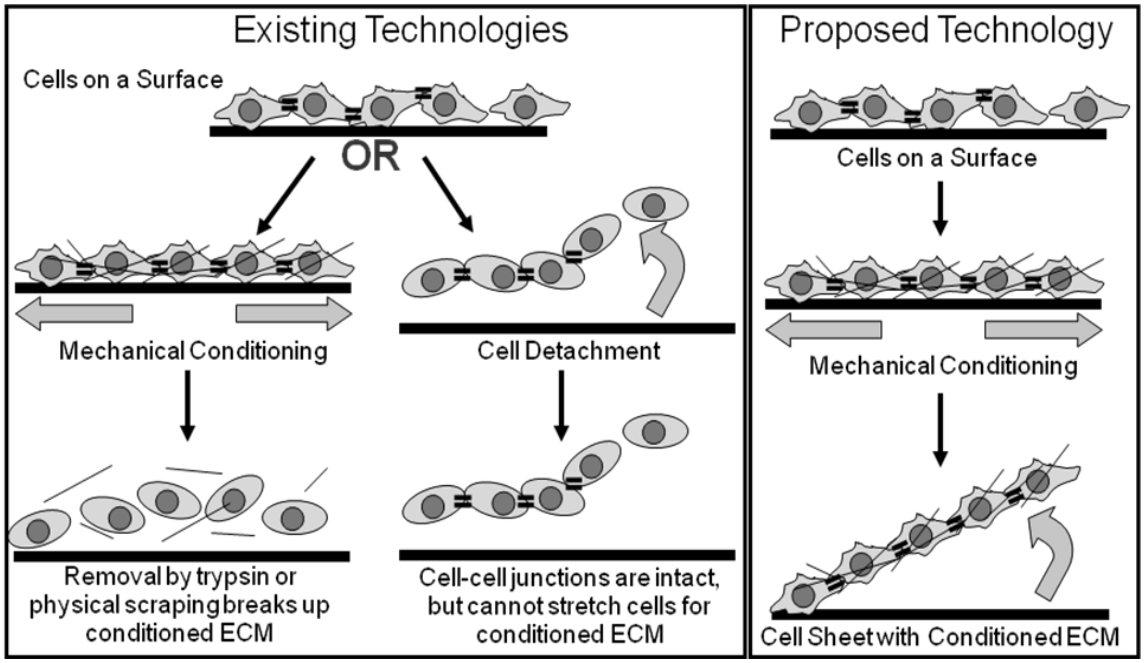

Figure 2.1. Schematic representing existing technologies (Left) where stem cells can either be mechanically conditioned for improved function (e.g., ECM (—)) or be detached from the substrate without use of degrading enzymes (e.g., maintain cell-cell junctions (=)), but not both. The proposed technology (Right) allows cells to be conditioned as needed, and then allows for detachment of the conditioned sheet of cells while maintaining ECM and cell-cell junctions.

Experimental

Materials

Commercial materials used in the polymer synthesis were obtained as follows: *N*-isopropylacrylamide (NIPAAm monomer) from Acros Organics (Pittsburgh, PA); 2,2'-azobisisobutyronitrile (AIBN) from Sigma-Aldrich (St. Louis, MO); acrylic acid (AAc) from Acros; and tetrahydrofuran (THF) from Acros. All other chemicals were obtained from

Fisher Scientific (Worcester, MA) in the highest grade available and used as is. NIPAAm monomer was purified by recrystallizing in 70:30 v/v hexanes : toluene at 40°C; AIBN was purified by recrystallizing in ethanol at 40°C. Acrylic acid was purified by solvent distillation.

Commercial materials used in the surface modification of silicone were obtained as follows: *N*,*N*'-dicyclohexylcarbodiimide (DCC) from Acros and BioFlex Culture Plate-Amino from Flexcell International (Hillsborough, NC). The BioFlex Culture Plate-Amino features a low density of amines bonded to the surface of a silicone membrane, encased in a 6-well dish frame (9.62 cm^2/well, 0.508 mm membrane thickness). Culture dishes with UpCell surface from Thermo Scientific Nunc (Waltham, MA) are commercially available dishes with P(NIPAAm) electron beam-grafted onto a polystyrene dish and were used as a positive control for cell detachment.

Materials used in the cell culture studies were as follows: Dulbecco's Modified Eagle's Medium (DMEM) from Thermo Scientific HyClone (Logan, UT); fetal bovine serum (FBS) from HyClone; penicillin-streptomycin from Hyclone; phosphate buffered saline solution (PBS) from HyClone; and tissue-culture polystyrene dishes from Starstedt (Newton, NC).

*Poly(*N*-isopropylacrylamide-co-acrylic acid) synthesis and analysis*

Poly(*N*-isopropylacrylamide-co-acrylic acid) (P(NIPAAm-co-AAc)) was made with 3 g NIPAAm monomer, 300 mg AAc, and 30 mg AIBN as an initiator in 60 ml THF (Figure 2.2, Top). The reaction was oxygen-purged twice under freeze/thaw cycles under

vacuum and then allowed to react overnight at 70°C. The resulting polymer was purified by redissolving in 30 ml acetone, and dropwise precipitated in 15 vol diethyl ether. The resulting polymer was then filtered and stored desiccated at 4°C.

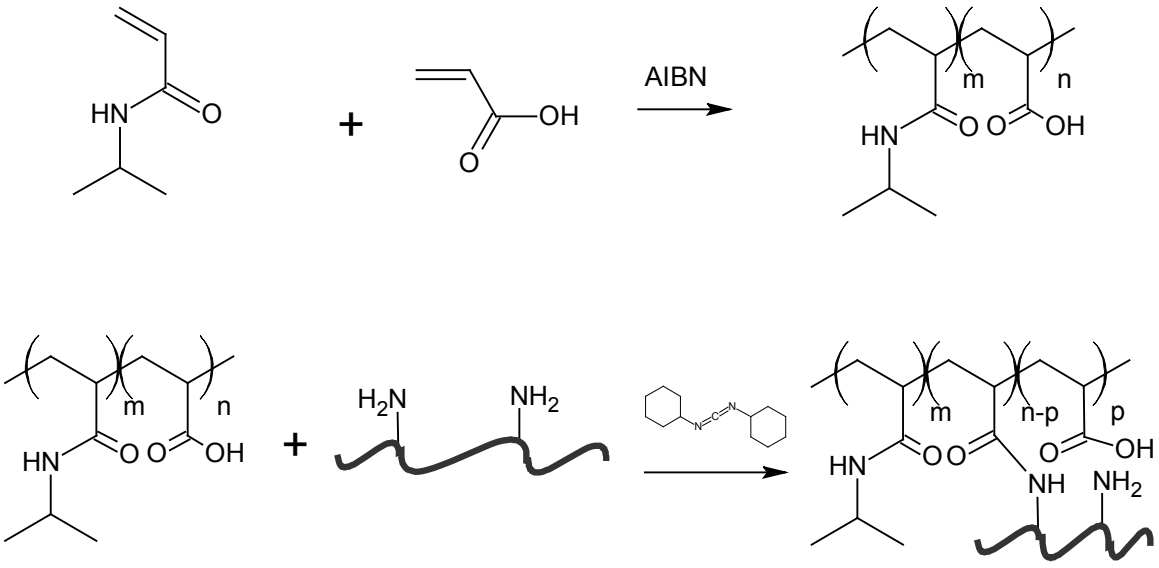

Figure 2.2. Chemistry of copolymerization of N-isopropylacrylamide and acrylic acid to form P(NIPAAm-co-AAc) (Top). Chemistry of conjugation of P(NIPAAm-co-AAc) to amine-bonded silicone membrane (Bottom).

The amount of free acid available was determined by acid titration against potassium hydroxide, which was used to determine the number of reactive carboxyl groups.

The lower critical solution temperature (LCST) was determined by the OptiMelt MPA-100 (Stanford Research Systems, Inc., Sunnyvale, CA). Above the LCST, the soluble polymer precipitates out of deionized water as it becomes more hydrophobic, causing

the solution to become cloudy. The temperature was ramped from 25°C to 70°C at 1°C/min in deionized water.

Surface modification of Flexcell BioFlex Culture Plates

The silicone membrane in the BioFlex Culture Plate-Amino was first swollen to equilibrium with 1 ml tert-butanol per well for 40 min. P(NIPAAm-co-AAc) polymer was dissolved in tert-butanol (10 mg/ml), to which 20 mg/ml DCC was dissolved in the solution to act as the crosslinking agent (Figure 2.2, Bottom). 1 ml P(NIPAAm-co-AAc) and DCC in tert-butanol solution was added to each well, and the dish was sealed with a capture cover (Genetra Systems; Minneapolis, MN) to prevent evaporation. The reaction was allowed to react for 24 hours at room temperature. Simultaneously, several controls were dissolved in tert-butanol (10 mg/ml) and cast as films onto membranes to demonstrate successful conjugation of P(NIPAAm-co-AAc) to the amine-bonded silicone surface: (a) P(NIPAAm), (b) P(NIPAAm) with DCC, and (c) P(NIPAAm-co-AAc) without DCC. At the end of the reaction, the remaining tert-butanol was decanted and the membranes were dried under a vacuum flow hood.

To remove excess reagents following prewash testing, the entire dish was washed in excess tert-butanol at 30°C for 20–40 minutes, then rinsed in excess room temperature water. The washing process was repeated 2 more times to ensure complete removal of excess reagents.

Chemical analysis of surface modification

A 1-cm by 2-cm strip was cut from each well or from the polystyrene culture dish with UpCell surface. All samples were analyzed by attenuated total reflection Fourier transform infrared spectroscopy (ATR-FTIR) using a flat plate germanium crystal (Pike Technologies; Madison, WI) for a Bio-Rad Excalibur FTS 3000MX system (Bio-Rad Laboratories; Philadelphia, PA). The ratios of the peaks at 1650 nm^{-1} (C=O peak) and 3300 nm^{-1} (NH peak) for P(NIPAAm) were compared to the peak at 2970 nm^{-1} (CH_3 anti-symmetric stretching peak) for silicone. A calibration curve was established to quantify the density of polymer coating by dissolving known amounts of P(NIPAAm-co-AAc) in water and casting films (0.01, 0.02, 0.05, 0.1, 0.5, 1 mg/cm^2), as previously described.[35,37] The polymer density on the modified silicone membranes was estimated from this calibration curve.

The surfaces of the modified silicone membrane and the polystyrene culture dish with UpCell surface were also analyzed for elemental composition by electron spectroscopy for chemical analysis (ESCA) using a PHI VersaProbe XPS (Physical Electronics; Chanhassen, MN). The ratios of the elements of carbon, nitrogen, oxygen, and silicon were analyzed.

Contact angle

The FTA200 (First Ten Angstroms; Portsmouth, VA) was used to measure contact angles of modified silicone membranes and positive control polystyrene with UpCell surface before and after washing (as described above), as well as at 25°C and 37°C to

show thermal reversibility in comparison to tissue culture polystyrene. The temperature was maintained by a syringe heater and an external chamber (First Ten Angstroms) that was controlled by a Benchtop RTD/Thermocouple PID Temperature Controller (Cole-Parmer; Vernon Hills, IL).

Cell detachment

The modified silicone membranes were tested in cell culture for attachment and detachment of cells in comparison to tissue culture polystyrene dishes (both nontreated and treated with UpCell surface) controls. Cell culture tests were performed with NIH 3T3 fibroblasts cultured in DMEM with 10% FBS, 100 U/ml penicillin, and 100 µg/ml streptomycin.

3T3 cells (100,000 cells/9.62 cm^2, the area of one well in a 6-well Flexcell dish) were seeded overnight on washed, modified silicone membrane samples and polystyrene controls. The cultures were allowed to detach as the media was brought to room temperature over the course of 1 hr. The images were captured by light microscopy on a Nikon Eclipse TE300 epi-inverted fluorescence microscope (Nikon Instruments, Inc.; Melville, NY) using a Q Imaging Retiga-SRV Fast 1394 camera (Q Imaging; Surrey, British Columbia) and Image-Pro Plus, V. 6.2 (MediaCybernetics; Bethesda, MD).

Cell stretching and fluorescence immunostaining

3T3 cells (200,000 cells/well) were seeded on unmodified and modified silicone membranes and mechanically conditioned on the Flexcell® FX-4000™ Tension System (Flexcell International Corporation; Hillsborough, NC) at 5% elongation strain, 1 Hz for 24 hrs. Cell detachment following cell stretching was demonstrated as described above.

Following cell stretching, cells were stained to discern the differences in cell morphology between unmodified and modified membranes. Cells were fixed for 20 minutes in 3.7% paraformaldehyde in PBS and permeabilized with 0.1% TritonX-100 in PBS for 5 minutes. Following three washes in PBS for 5 minutes each, nonspecific proteins were blocked in 1% bovine serum albumin (BSA) in PBS for 5 minutes. Alexa Fluor 488 Phalloidin (Invitrogen) was then incubated for 20 minutes at room temperature at 0.165 µM with 0.5% BSA in PBS. Following primary antibody, cells were washed two times with PBS for 5 minutes each. Cells were then counterstained and mounted on glass slides using VECTASHIELD Mounting Medium with DAPI (Vector Labs; Burlingame, CA). Cell morphology and phalloidin staining was observed under fluorescence microscopy using the Nikon Eclipse TE300 microscope, Q Imaging Retiga-SRV Fast 1394, and Image-Pro Plus, V. 6.2. Images were compiled using ImageJ 1.421 (National Institutes of Health; Bethesda, MD).

Results and Discussion

Thermally reversible culture substrate

AAc content polymerized in P(NIPAAm-co-AAc) was 10% as determined by acid titration analysis, which confirms available carboxyls capable of conjugating with the amine groups present on the commercially available silicone membrane. The LCST of P(NIPAAm-co-AAc) was approximately 34°C, which matches literature values for this copolymer[38] and falls within the necessary range for cell culture at 37°C, and for spontaneous cell detachment at room temperature.

Surface analysis by ATR-FTIR showed that the ratio of the P(NIPAAm) peak (1650 nm^{-1}, 3300nm^{-1}) to the silicone peak (1000–1100 nm^{-1}) is greater for the modified silicone membrane in comparison to the unmodified silicone membrane and polystyrene controls (Figure 2.3). The higher peak ratio (1.1 times greater) of the unwashed modified silicone membrane to the washed membrane is expected, and indicates the presence of excess P(NIPAAm-co-AAc) that remains unconjugated. In addition, following washing, the modified silicone surface has a peak ratio of a slightly greater intensity than the polystyrene commercially grafted with P(NIPAAm), indicating that enough P(NIPAAm-co-AAc) is present on the silicone surface as that of the commercial product to allow for thermally reversible cell detachment (data not shown). In addition, all cast film controls have P(NIPAAm) peaks before washing, but these peaks disappear following the wash step. The absence of the P(NIPAAm) peaks following washing in the cast film controls demonstrates that the thermally reversible nature of the substrate is only from the successful conjugation of P(NIPAAm-co-AAc) to the

amine-bonded silicone membrane. Comparing the silicone modified with P(NIPAAm-co-AAc) to the cast film standards gives a polymer density range between 0.05–0.07 mg/cm².

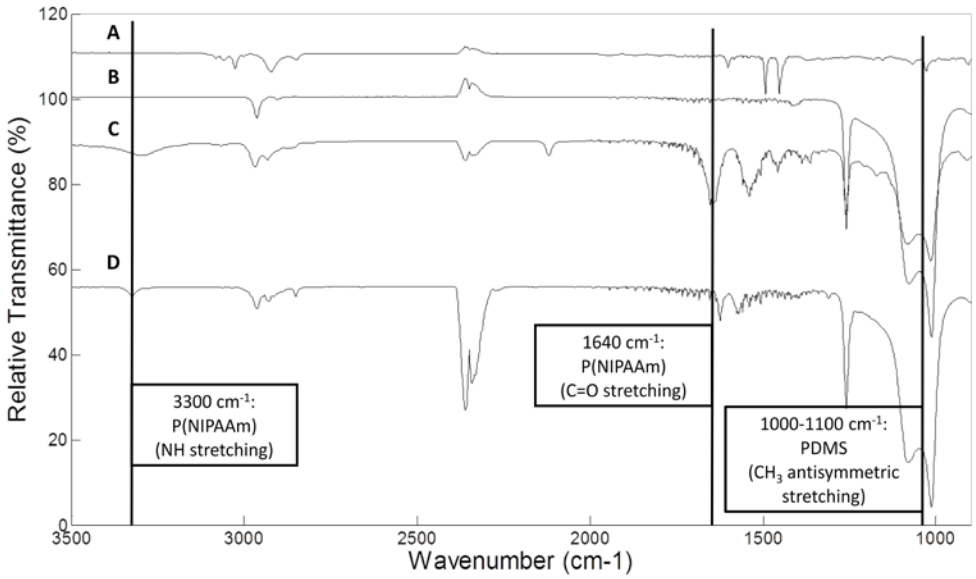

Figure 2.3. FTIR for (A) tissue-culture polystyrene, (B) unmodified silicone, (C) silicone modified with P(NIPAAm-co-AAc) before washing and (D) after washing. NIPAAm peak at 3300 cm^{-1} (NH stretching) is present before and after washing for P(NIPAAm-co-AAc) as compared to negative controls tissue-culture polystyrene and silicone, demonstrating covalent attachment.

Analysis by ESCA of the modified silicone membrane surfaces following the wash steps showed an increased atomic percentage of nitrogen in comparison to the commercial amine-bonded silicone membrane alone, indicating successful conjugation of P(NIPAAm-co-AAc) to the silicone surface (Table 2.1). The atomic ratio of nitrogen in the modified silicone surface is three times greater than that of the polystyrene control

and unmodified silicone membranes (see Table 2.1). Additionally, when the atomic ratios are normalized to that of nitrogen in the unmodified amine-bonded silicone membrane, the atomic ratio of silicone from the unmodified amine-bonded silicone to P(NIPAAm-co-AAc)-modified silicone remains about the same with a concomitant increase in carbon and decrease in oxygen, indicating the reaction of the hydroxyl groups in the amide bond formation with carbodiimide chemistry.

Table 2.1. Atomic Ratios of Thermally Reversible Culture Substrates

Polymer	Carbon	Oxygen	Nitrogen	Silicon
TCPS	71.6	20.7	0.0	7.7
Unmodified silicone membrane	46.4	30.0	0.0	23.5
Unmodified amine-bonded silicone membrane	44.2 ± 0.9	32.0 ± 0.9	0.5 ± 0.1	23.3 ± 0.7
Amine-bonded silicone membrane modified with P(NIPAAm-co-AAc)	49.0 ± 0.6	28.3 ± 0.6	1.5 ± 0.4	21.2 ± 0.9

Atomic ratio values are means of 6 measurements ± standard deviation.

Contact angle of the modified silicone membrane surfaces before and after washing were measured below the LCST (25°C) and above the LCST (37°C) and compared to polystyrene controls, unmodified membranes, and P(NIPAAm) solvent-cast as a film onto a silicone membrane (Table 2.2). As expected, no contact angle change was observed for either the unmodified silicone membranes or the polystyrene surface, indicating that P(NIPAAm) is not present. Before washing, P(NIPAAm) solvent-cast as a film onto the silicone membrane exhibited more hydrophilic contact angle at 25°C compared to 37°C, which was not present after washing, as expected for P(NIPAAm) not conjugated to the silicone surface. For P(NIPAAm-co-AAc) conjugated to the silicone membrane, no statistically significant change in contact angle with temperature was shown before washing, but was present following washing. We surmise that the presence of the methyl groups in tert-butanol may have been shielding the hydrophilic groups in P(NIPAAm) before the samples were washed, but the hydrophilic groups may have become exposed following washing. The change in contact angle following washing of the modified silicone samples further confirms the presence of temperature responsive polymer.

Table 2.2. Contact Angle of Thermally Reversible Culture Substrates

	Prewashed		Washed	
Polymer	25°C	37°C	25°C	37°C
Tissue culture-treated polystyrene (TCPS)	65.91 ± 1.4	65.86 ± 2.0	---	---
Unmodified amine-bonded silicone membrane	72.35 ± 2.1	74.13 ± 3.3	---	---
P(NIPAAm) on amine-silicone	35.04 ± 5.2	61.13 ± 1.8	71.29 ± 2.5	70.43 ± 2.3
Amine-bonded silicone membrane modified with P(NIPAAm-co-AAc)	61.87 ± 4.1	62.08 ± 1.6	33.45 ± 15.8	66.21 ± 2.8

Contact angle values are means of 3 measurements ± standard deviation. Single-factor analysis of variance (ANOVA) performed on data resulted in $P < 0.05$ comparisons between temperatures for highlighted samples.

Cell culture on reversible surfaces

3T3 fibroblasts were cultured on polystyrene controls, unmodified silicone membranes, and modified silicone membranes. Cells demonstrated an attached morphology, with focal adhesions to all surfaces at 37°C. As expected, the control unmodified amine-bonded silicone membrane did not show a discernible change in cell

shape with a temperature change, as expected. Although some observable cell shrinkage occurred along with the silicone as it cooled to room temperature, the focal adhesions and elongated shape on the majority of the cells remained.

By contrast and as expected, the commercial polystyrene with electron beam-grafted P(NIPAAm) UpCell surface demonstrated that cells transitioned from an elongated to a round morphology as focal adhesions were released from the surface as the temperature changed from 37°C to 25°C (Figure 2.4). By 20 min, all cells exhibited a rounded morphology on the polystyrene control with electron beam-grafted P(NIPAAm), indicating detachment from the dish. Our silicone membrane modified with P(NIPAAm-co-AAc) also demonstrated that cells changed from an elongated to a rounded morphology as the temperature transitioned from 37°C to 25°C. At 1 hr, nearly all cells exhibited release of focal adhesions and rounded cell morphology after temperature transition on the silicone membrane modified with P(NIPAAm-co-AAc), demonstrating our modified substrate is successful at spontaneous detachment of cells without enzymatic or harmful physical means.

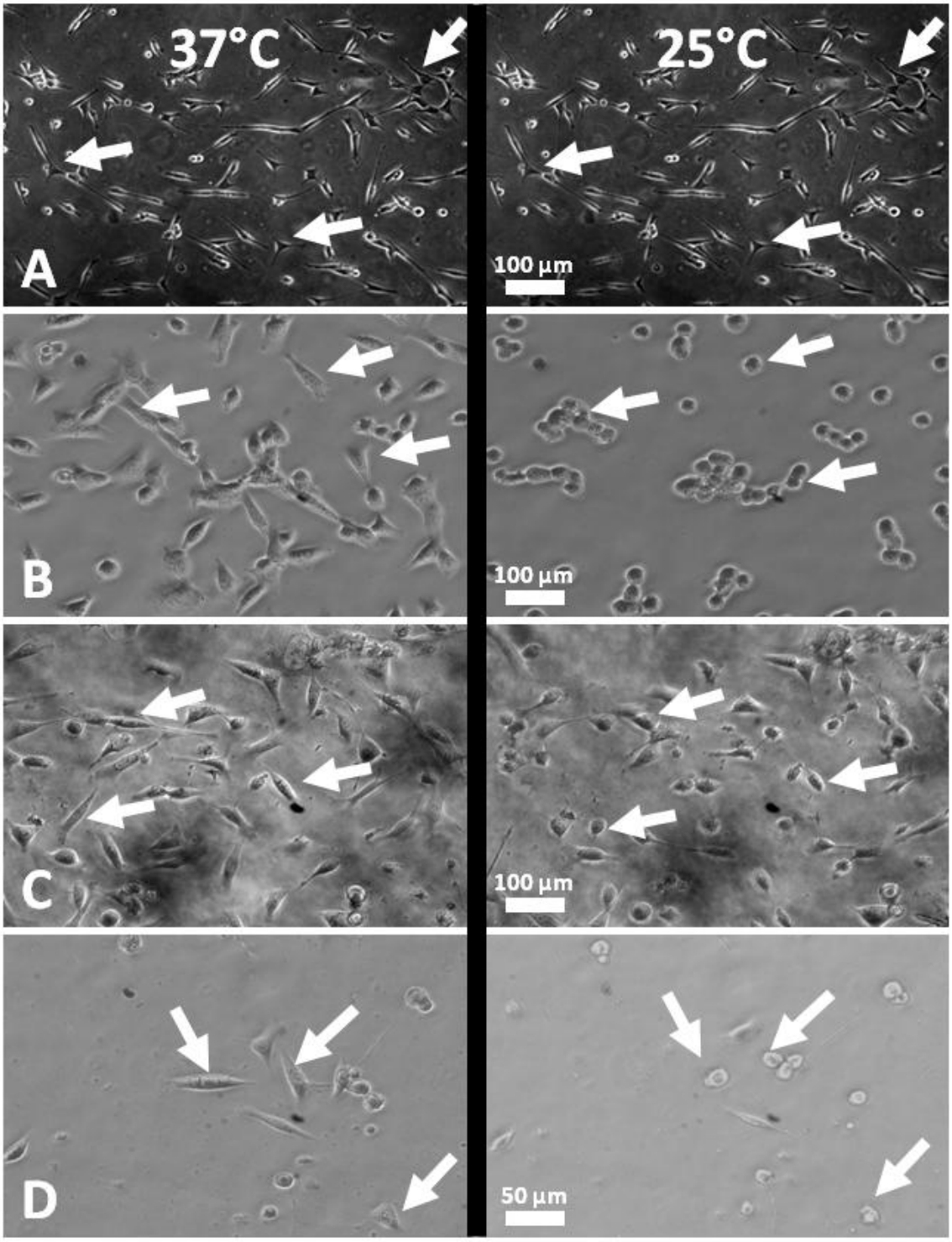

Figure 2.4. Cells grown on (A) negative control unmodified silicone, (B) positive control P(NIPAAm) electron-beam grafted onto polystyrene (UpCell), and (C) silicone modified with P(NIPAAm-co-AAc) before stretching, and (D) silicone modified with P(NIPAAm-co-

AAc) following mechanical stretching were compared at 37°C at time 0 min (Left) and again at 25°C after 1 hr (Right). Cells were attached to all membranes at 37°C, and detached only for the P(NIPAAm-co-AAc)-modified surfaces with a change in temperature. Cells were still able to detach with a change in temperature following mechanical stretching (D). Arrows indicate correlating cells at different temperatures.

Following cell stretching, cells exhibited an elongated and attached morphology that became more rounded at the end of 1 hr as the media temperature transitioned from 37°C to 25°C.

Cell stretching

A comparison of immunostained cells on unmodified and modified silicone membranes showed no discernible differences in cell morphology, demonstrating cell growth on unmodified silicone is comparable to cells grown on temperature responsive modified silicone surface (Figure 2.5). Qualitative comparisons of stretched cells show alignment on both unmodified and modified silicone membranes. A quantitative comparison of the differences in elongation and alignment between unstretched and stretched cells will be compared using CellProfiler in future studies.[44]

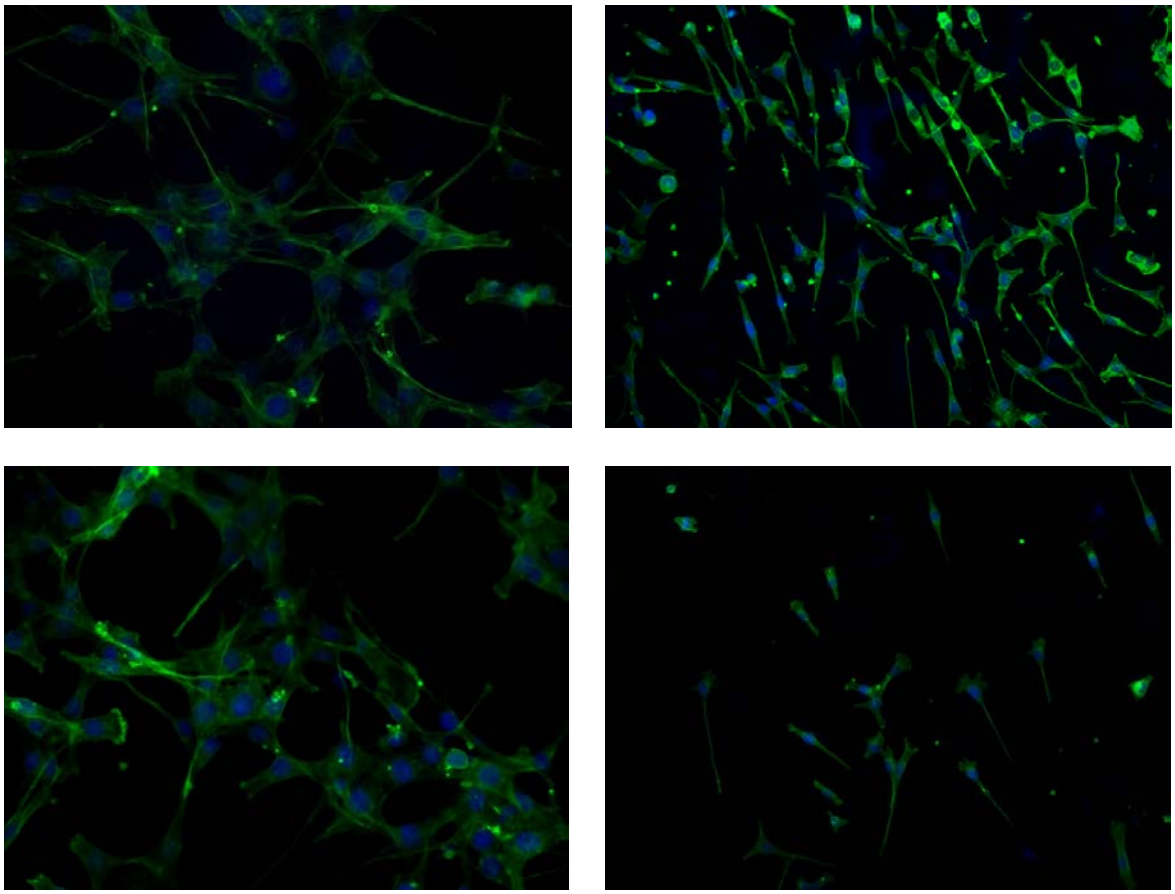

Figure 2.5. Cells were grown on unmodified (Top) and modified (Bottom) silicone membranes, both before (Left) and after (Right) mechanical stretching. On both membranes, comparable cell morphology is maintained, and cells are able to align with stretching.

Conclusion

We were able to modify silicone surfaces with P(NIPAAm-co-AAc) to allow cell detachment with a change in temperature. Following mechanical conditioning, the modified membranes were able to retain the ability to detach cells. This has implications for future tissue engineering constructs for implantation: We can use many different cell

types, such as differentiated embryonic stem cells, to recreate the ECM in vitro to better mimic the structural integrity of the native tissue with hopes for increasing the chances for successful integration. We are currently investigating cell detachment of cellular sheets.

Acknowledgements

This work was supported by an award from the American Heart Association and a pilot award from the Center for Stem Cell and Regenerative Medicine and the State of Ohio.

Chapter III: Functional Comparison of Cell Culture Platform with Mechanical Conditioning and Nondamaging Cell Detachment to Unmodified Bioreactor

Elaine L. Lee and Horst A. von Recum

Case Western Reserve University, Cleveland, OH 44106

Abstract

The treatment of atherosclerotic vascular disease and the future of vascular tissue engineering rely on the ability to manipulate the differentiation of endothelial and smooth muscle cells. Lining the inner lumen of blood vessels, endothelial cells are subjected to cyclic strain due to wall distension and shear stress due to frictional force by blood flow. When exposed to cyclic strain, many studies have shown that vascular smooth muscle cells exhibit a more contractile, mature smooth muscle phenotype. Cevallos and associates demonstrated that human umbilical vein endothelial cells (HUVECs) can be induced to express smooth muscle cell markers by applying cyclic strain. However, although mechanical forces can be used advantageously to fabricate a small diameter graft with natural scaffolding, conditioned cells must be recovered without damage to the fabricated extracellular matrix. Our bioreactor allows for cyclic strain to be applied to cell cultures, and then subsequently allows the conditioned monolayer culture to be detached without damage. The detached monolayers' pattern formation can be kept with precise control and can then be rolled up to form a vascular graft. In this study, we replicate the experiments performed by Cevallos and collaborators to demonstrate that our modified cell culture bioreactor can perform

comparably to the unmodified bioreactor while also allowing complete cellular recovery without damage.

Introduction

Mechanical stimulation can affect cell morphology, proliferation, migration, and differentiation.[1-6] It can influence the up- and downregulation of mRNA and proteins, as well as define the extracellular matrix (ECM).[2,3] The pulsatile forces subjected on the cardiovascular system by the beating heart regulate vascular development, wound healing, atherosclerotic lesion formation, cell alignment, differentiation, migration, survival or apoptosis, vascular remodeling, and autocrine and paracrine functions.[7] Understanding the effects of the mechanical forces on the vascular system can have great potential in creating cellular replacement therapies for vascular tissue engineering.[8]

Endothelial cells line the inner lumen of blood vessels, which are subjected to two hemodynamic forces: cyclic strain due to wall distension and shear stress due to frictional force by blood flow.[1] The treatment of atherosclerotic vascular disease and the future of vascular tissue engineering rely on the ability to manipulate the differentiation of vascular (endothelial and smooth muscle) cells.[8] As the most numerous cell type in the natural vessel wall and a key physiological component, novel bioartificial vascular grafts should keep vascular smooth muscle cells in a quiescent mature contractile phenotype.[9] Huang and Niklason have developed a pulsatile bioreactor to regenerate vessels with a chemo-mechanical environment that mimics native vessels.[10] Using

smooth muscle cells seeded on a tubular polyglycolic acid (PGA) mesh, they created vessels that could allow endothelial cells to coat the luminal side of vessels 1–3 mm in diameter. Sharifpoor and colleagues use 10 wt% polyethylene glycol (PEG) and 65 wt% salt in the scaffold fabrication of elastomeric degradable/polar/hydrophobic/ionic (D-PHI) polyurethane, resulting in a scaffold with mechanical properties that maintained the physiologically relevant mechanical strain experienced by vascular smooth muscle cells in vivo.[11]

When exposed to cyclic strain, many studies have shown that vascular smooth muscle cells exhibit a more contractile, mature smooth muscle phenotype,[12-15] and it has been demonstrated that smooth muscle cells are pivotal in maintaining vascular homeostasis, in which the contractile capability helps to maintain hemodynamics.[16] In the case of vascular cell differentiation, the role of hemodynamic forces is just beginning to be elucidated. Shimizu and associates show that cyclic strain can induce mouse embryonic stem cell differentiation into vascular smooth muscle cells;[17] similarly, Riha and coworkers demonstrated that cyclic strain can affect murine embryonic mesenchymal progenitor cells, inducing vascular smooth muscle differentiation.[18] Additionally, Cevallos and associates demonstrated that human umbilical vein endothelial cells (HUVECs) can be induced to express smooth muscle cell markers by applying cyclic strain;[19] conversely, Wang and colleagues demonstrated that shear stress induces transdifferentiation of smooth muscle cells to endothelial cells.[20]

The influence of mechanical forces upon gene expression and signaling is well documented,[1-6] and can be used advantageously to fabricate the native ECM and natural

scaffolding necessary to engineer a small diameter graft,[8] removing the necessity for polymeric scaffolding that can be subject to inflammatory responses.[21] For example, PGA can cause adverse host reactions and may cause remnants to be discharged for an extended period of time.[22,23] Residual polymer fragments can also disrupt the organization of the vascular wall.[24] However, engineering a fully implantable small diameter graft without polymeric scaffolding is dependent on cellular recovery without damage to the fabricated ECM. As such, our device allows for cyclic strain to be applied to cell cultures, and then subsequently allows the conditioned monolayer culture to be detached without damage.[21] The detached monolayers' pattern formation can be kept with precise control and can then be rolled up to form a vascular graft.

We have modified a commercial product of the Flexcell Tension System (Flexcell International Corp), which applies negative vacuum pressure to a plate with flexible substrate bottoms to apply axial or equibiaxial strain to cultured cells.[21] We have chemically modified the silicone surface of these commercially available BioFlex plates with poly N-(isopropylacrylamide-co-acrylic acid) (P(NIPAAm-co-AAc)) copolymers such that we have created a modified cell culture platform that can apply cyclic strain to cell monolayers, then subsequently detach the monolayer as a continuous cell sheet while simultaneously maintaining cell-to-cell and cell-to-matrix interactions. P(NIPAAm-co-AAc) is a copolymer that allows for cell attachment at 37°C and spontaneous, nondamaging cell detachment with a decrease in temperature below 34°C. Not only are cell-to-cell and cell-to-ECM adhesions maintained, but cell viability and proliferation capability are also maintained. As a result, we have fabricated a bioreactor that can be

used to apply cyclic strain to mechanically stimulate controlled ECM growth while allowing intact retrieval of the secreted ECM without damage.

In this paper, we replicate the experiments performed by Cevallos and collaborators[19] to demonstrate that our modified cell culture bioreactor can perform comparably to the unmodified bioreactor by inducing transdifferentiation of endothelial cells to smooth muscle cells while also allowing complete cellular recovery without damage.

Materials and Methods

Materials

HUVECs were ordered from ATCC. NIPAAm monomer and acrylic acid (AAc) were purchased from Acros Organics. 2,2'-azobisisobutyronitrile (AIBN), and N,N'-dicyclohexylcarbodiimide (DCC) were purchased from Sigma-Aldrich. EBM-2 and supplemental growth factors were purchased from Lonza. The Flexcell Tension System FX-4000 and BioFlex plates were purchased from Flexcell International. Trizol, SuperScript III First-Strand Synthesis System for RT-PCR, PCR Supermix, primers, and Alexa Fluor 488 and 568 phalloidin were purchased from Invitrogen. Full-range rainbow marker was purchased from GE. Mini PROTEAN 3, Ready Gel Tris-HCl Gel (4–15%, 10-well, 50 µl), Mini Trans-Blot Electrophoretic Transfer Cell, and nonfat milk were purchased from BioRad. Smooth muscle 22α (SM22α) antibody (NB600-507) was purchased from Novus Biologicals, and α-smooth muscle actin (α-SMA) (SC-32251) was purchased from Santa Cruz Biotechnology. GAPDH antibody (ab9484) and goat anti-

mouse IgG FITC (ab6787) were purchased from Abcam. All other reagents were purchased from Thermo Fisher.

Cell Culture

HUVECs were cultured at 37°C and 5% CO_2 in EBM-2 medium with growth factor supplementation plus 10% FBS. When growth reached 80% confluence, cells were washed with DPBS, detached using trypsin/EDTA solution, and sub-cultured in growth medium. All cells were used at passage 6–9.

P(NIPAAm-co-AAc)-modified Plates

BioFlex plates were modified as previously described.[21] Briefly, P(NIPAAm-co-acrylic acid) (P(NIPAAm-co-AAc)) was synthesized with NIPAAm monomer, AAc, and AIBN as an initiator in tetrahydrofuran (THF). The silicone membrane in the BioFlex plate was swollen to equilibrium in tert-butanol. P(NIPAAm-co-AAc) copolymer was dissolved in tert-butanol with DCC and added to each well of the BioFlex plate overnight. Excess reagents were removed by multiple washes in excess tert-butanol at 30°C for 20–40 min, then rinsed in excess room temperature water.

Cyclic Strain

HUVECs were seeded and grown to 80% confluence in EBM-2/10% FBS on both unmodified and modified BioFlex plates. Before being subjected to mechanical deformation, cells were serum starved for 16 hr. Flexcell FX-4000 Tension System was

used to mechanically condition cells at either 0% or 10% elongation strain, 1 Hz for 48 hr. The applied cyclic strains are within the range reported by Dobrin, where the magnitude of physiological strain ranges from 2% to 18% in large arteries during the normal cardiac cycle.[25] Culture dishes were placed in a humidified incubator (37°C, 5% CO_2) equipped with 25 mm diameter loading posts located beneath each well. The flexible elastic membrane bottom of each culture well was uniformly strained over the post by a vacuum source. Static control cultures were also plated and grown on unmodified and modified BioFlex plates.

Reverse-transcriptase Polymerase Chain Reaction (RT-PCR)

RT-PCR was used to determine mRNA expression. Total RNA was isolated from nonconditioned and conditioned cells using Trizol reagent according to the manufacturer's protocol. Reverse transcription for complementary DNA was synthesized using SuperScript III First-Strand Synthesis System for RT-PCR according to the manufacturer's protocol. PCR Supermix was used for RT-PCR according to the manufacturer's protocol. Primers and sequences are listed in Table 3.1 for human SM22-α, α-SMA, smooth muscle myosin heavy chain (SMMHC), human von Willebrand factor (vWF), vascular endothelial growth factor receptor-2 (VEGFR-2) and glyceraldehydes-3-phosphate-dehydrogenase (GAPDH).[19] PCR products were subjected to electrophoresis on 1% agarose gel and stained with ethidium bromide (10 μg/ml). Gels were photographed using Kodak Image Station 440CF, and images were densitometrically quantified with NIH ImageJ, version 1.44p.

Table 3.1. RT-PCR Primers for Smooth Muscle and Endothelial Cells[1]

Gene	Forward sequence	Reverse Sequence
SM22-α	GATCCAACTGGTTTATGAAGAAAGC	TCTAACTGATGATCTGCCGAGGTC
α-SMA	CCAGCAGATGTGGATCAGCA	AAGCATTTGCGGTGGACAAT
SMMHC	TCAACATGCAGGCGCTCA	CGTCTCATACTCGTGAAGCTGTCT
vWF	GCAGTGCCAGCTTCTGAAGAG	TCACACAAAGTCTTCTCACACAGG
VEGFR-2	GCAGGGGACAGAGGGACTTG	GAGGCCATCGCTGCACTCA
GAPDH	TGCCATGTAGACCCCTTGAA	GGTTGAGCACAGGGTACTTTA

1. Cevallos M, Riha GM, Wang X, Yang H, Yan S, Li M, Chai H, Yao Q, Chen C. Cyclic strain induces expression of specific smooth muscle cell markers in human endothelial cells. Differentiation 2006;74(9-10):552-61.

Western Blot Analysis

Protein was isolated from cell monolayers using RIPA buffer with Halt Protease Inhibitor Cocktail according to protocol. Protein concentration was measured using MicroBCA assay. GE Full-range Rainbow Marker was used as the molecular weight standards. Samples were denatured in Laemmeli buffer (4% SDS, 10% beta-mercaptoethanol, 20% glycerol, 0.004% bromophenol blue, 0.125 M Tris-HCl) at 99°C for 3 min, and run using Mini PROTEAN 3 Cell on Ready Gel Tris-HCl Gel, 4–15%, 10-well, 50 µl in 25 mM Tris, 190 mM glycine, 0.1% SDS running buffer at 100 V for 1 hr. Mini Trans-Blot Electrophoretic Transfer Cell was used for wet transfer of proteins to nitrocellulose membrane in 48 mM Tris, 39 mM glycine, 0.1% SDS, 20% methanol transfer buffer at

100 V for 1 hr. The membrane was blocked for 1 hr at room temperature in either 5% nonfat milk or 5% bovine serum albumin (BSA). Primary antibody was incubated at 4°C overnight with agitation (SM22α, 0.03 μg/ml; α-SMA, 1:200; GAPDH loading control, 1:5000 dilution), followed by three 10 min washes in Tris-buffered saline Tween-20 (TBST). Secondary antibody (HRP-conjugated goat anti-mouse or rabbit anti-goat, 1:2000 dilution) was incubated at room temperature for 1 hr, followed by three 10 min washes in TBST. Membranes were incubated with SuperSignal West Pico Chemiluminescent Substrate (Pierce) made according to the manufacturers' instructions for 5 min. Blots were exposed to film for 1 s to 5 min exposures.

Immunostaining of Cell Monolayers

Following mechanical conditioning, nonconditioned and conditioned cells were stained for SM22α and α-SMA. All solutions were pre-warmed to 37°C, and all incubations were performed at 37°C. Cells were fixed with 3.7% paraformaldehyde for 15 min. Following 3 rinses with PBS, cells were permeabilized with 0.1% TritonX-100 for 10 min. After 3 rinses with PBS, cells were blocked with 1% bovine serum albumin (BSA) for 1 hr. Blocked cells were incubated with SM22-α (2 μg/ml) or α-SMA (1:50 dilution) for 1 hr in a humidified chamber. After rinsing 3 times with PBS, secondary antibody was applied (SM22-α, rabbit anti-goat IgG FITC, 1:50 dilution; α-SMA, goat anti-mouse IgG Texas Red, 1:500 dilution) for 30 min in a humidified chamber. The samples were rinsed 3 times with PBS and mounted with VectaShield with DAPI.

Layering Cell Monolayers

To visualize separate monolayers, individual layers were stained with either Alexa Fluor 488 (fluorescin alternative) or 568 (Texas Red alternative) for phalloidin before layering. Cells were fixed, permeabilized, and blocked as above. Following blocking, cells were incubated with Alexa Fluor 488 or 568 for 20 min in a humidified chamber and then rinsed 3 times with 0.1% BSA in PBS. Samples were then incubated in Hoechst 33258 for 15 min in a humidified chamber and rinsed 3 times with PBS. The cell sheets were then layered and arranged as in Figure 3.1 by cutting out the silicone membrane from the Flexcell housing plate and orienting one membrane on tissue-culture treated polystyrene in a humidified chamber for 1 hr with a weight on top of the membrane. The sample was then incubated in 4°C for 1 hr with the weight before removal of the silicone membrane and repeating with the second membrane as oriented in Figure 3.1.

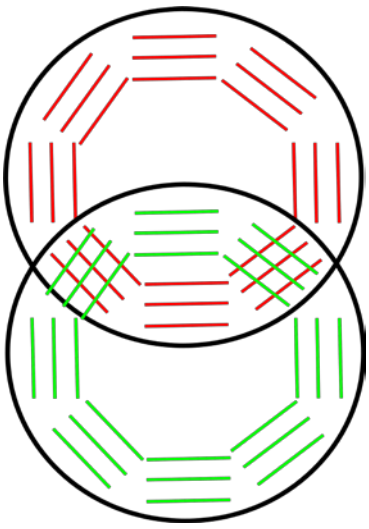

Figure 3.1. Orientation of cellular sheets.

Results

Effect of cyclic strain on cell morphology and F-actin organization in HUVECs

Cell shape is determined by actin filaments, which are also necessary in cell movements such as contraction.[19] Cells were stained for F-actin with phalloidin after 48 hrs of cyclic strain. Static HUVECs showed random organization and shape (Figure 3.2), which contrasts with cyclically strained HUVECs. These cells exhibited parallel fibrillar deposition and cellular elongation along the perpendicular axis of strain (Figure 3.3) on both unmodified and modified plates.

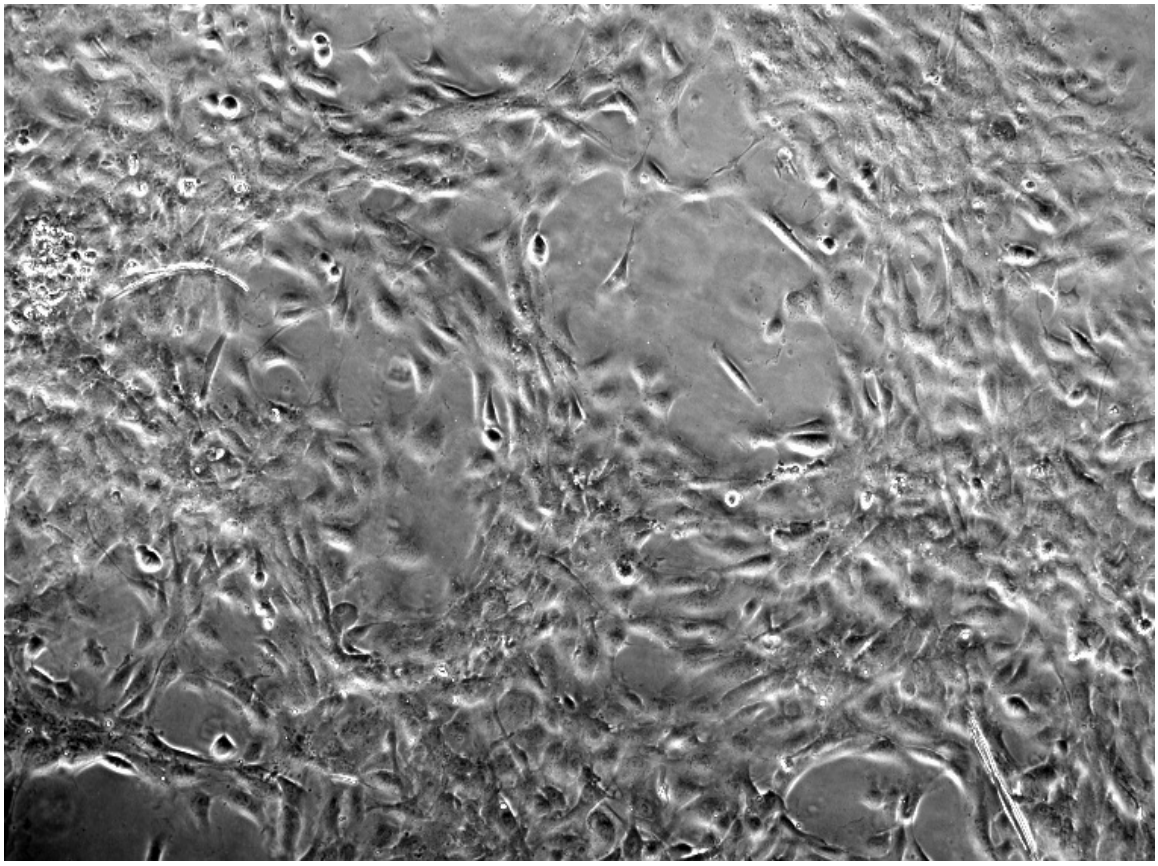

Figure 3.2. Static culture cells after 48 hrs.

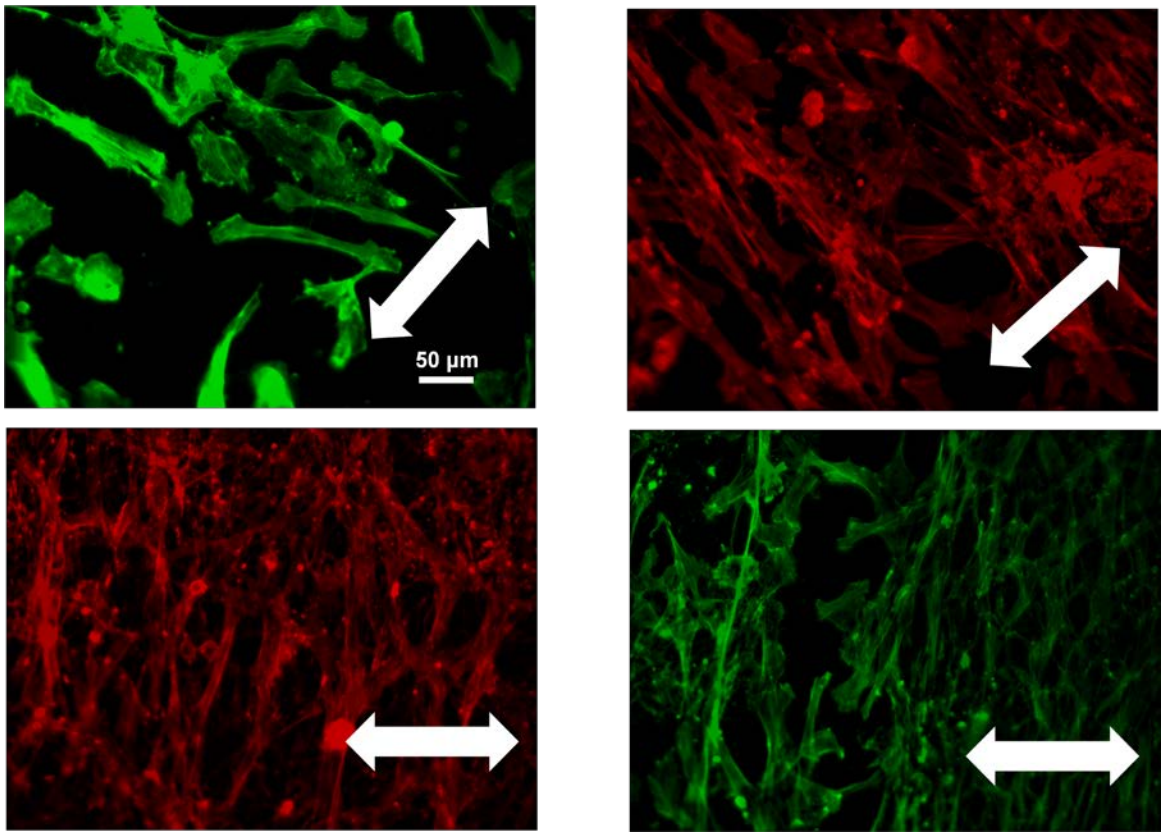

Figure 3.3. HUVECs cyclically conditioned at 10% strain show fibers oriented perpendicular to the direction of strain.

Effect of cyclic strain on mRNA levels of SMC markers in HUVECs

SM22-α and α-SMA are contractile proteins expressed in vascular SMCs. Our singular data point showed decreases in all contractile proteins (SM22-α, -24.4%; α-SMA, -5.0%; and SMMHC, -30.6%), a slight increase in vWF (6.7%), and a negligible decrease in VEGFR-2 (-2.3%) from static culture to 10% cyclic strain on unmodified surfaces (Figures 3.4 and 3.5). On the other hand, cells on modified surfaces showed an increase in contractile proteins SM22-α (28.6%) and SMMHC (19.6%) and an increase in

endothelial proteins vWF (31.0%) and VEGFR-2 (3.3%), with a dramatic decrease in expression of α-SMA (-65.5%) from static culture to 10% cyclic strain.

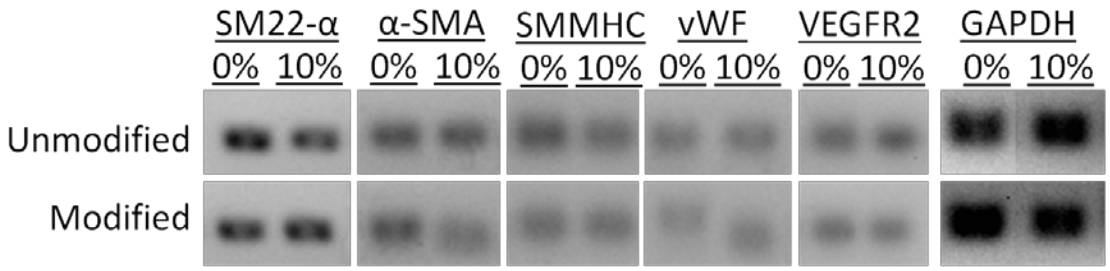

Figure 3.4. RT-PCR of smooth muscle cell and endothelial markers.

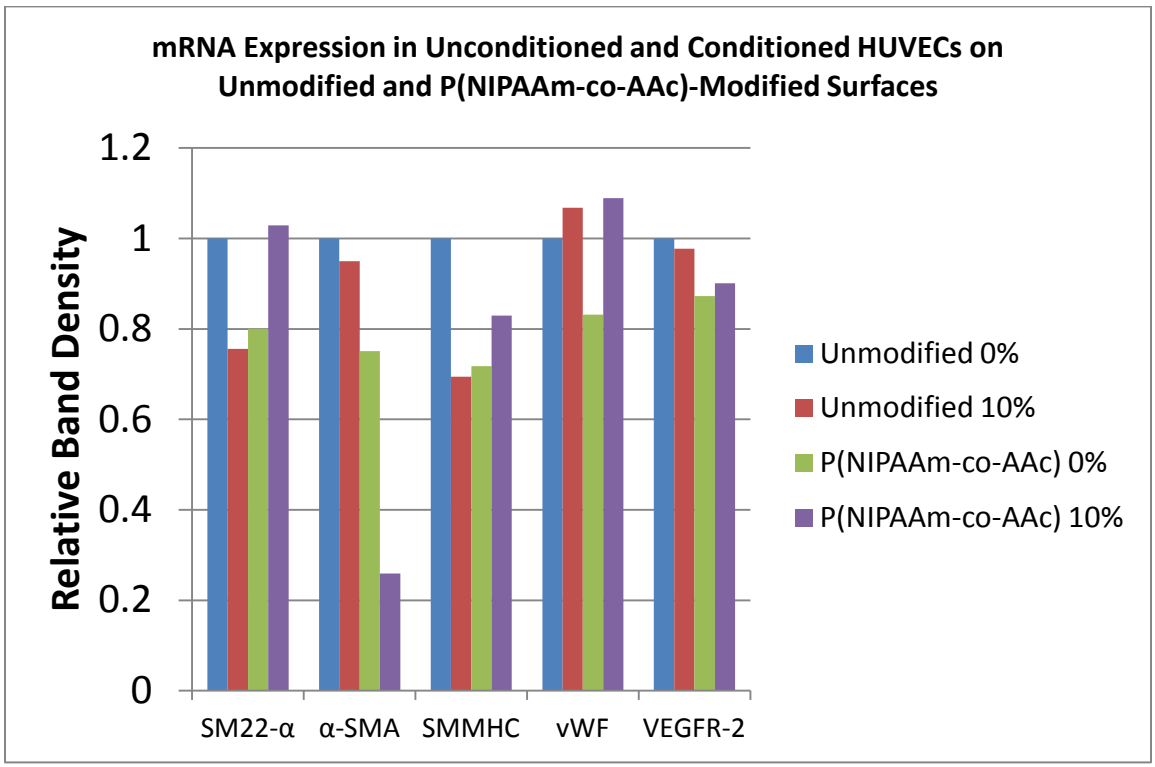

Figure 3.5. mRNA Expression in Nonconditioned and Conditioned HUVECs on Unmodified and P(NIPAAm-co-AAc)-Modified Surfaces**.**

Effect of cyclic strain on protein levels of SMC markers in HUVECs

Western blot analysis of proteins was attempted several times, but antibody dilutions and solutions have yet to be optimized. Qualitatively, the distribution of expression of SM22-α in static culture cells is random, and the morphology is globular (Figure 3.6). On the other hand, SM22-α expression in cells cyclically strained at 10% showed elongated morphology with parallel alignment of cells (Figure 3.7).

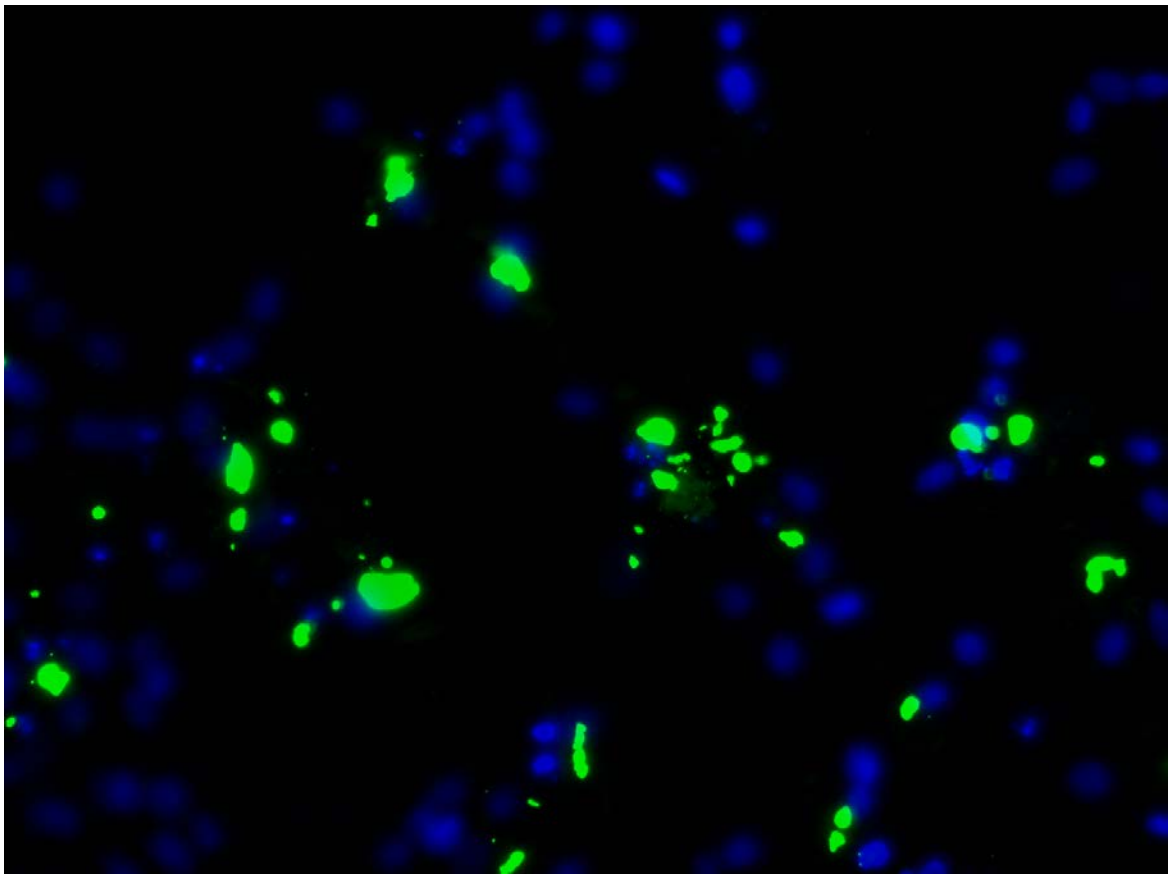

Figure 3.6. SM22-α expression in static culture cells after 48 hrs.

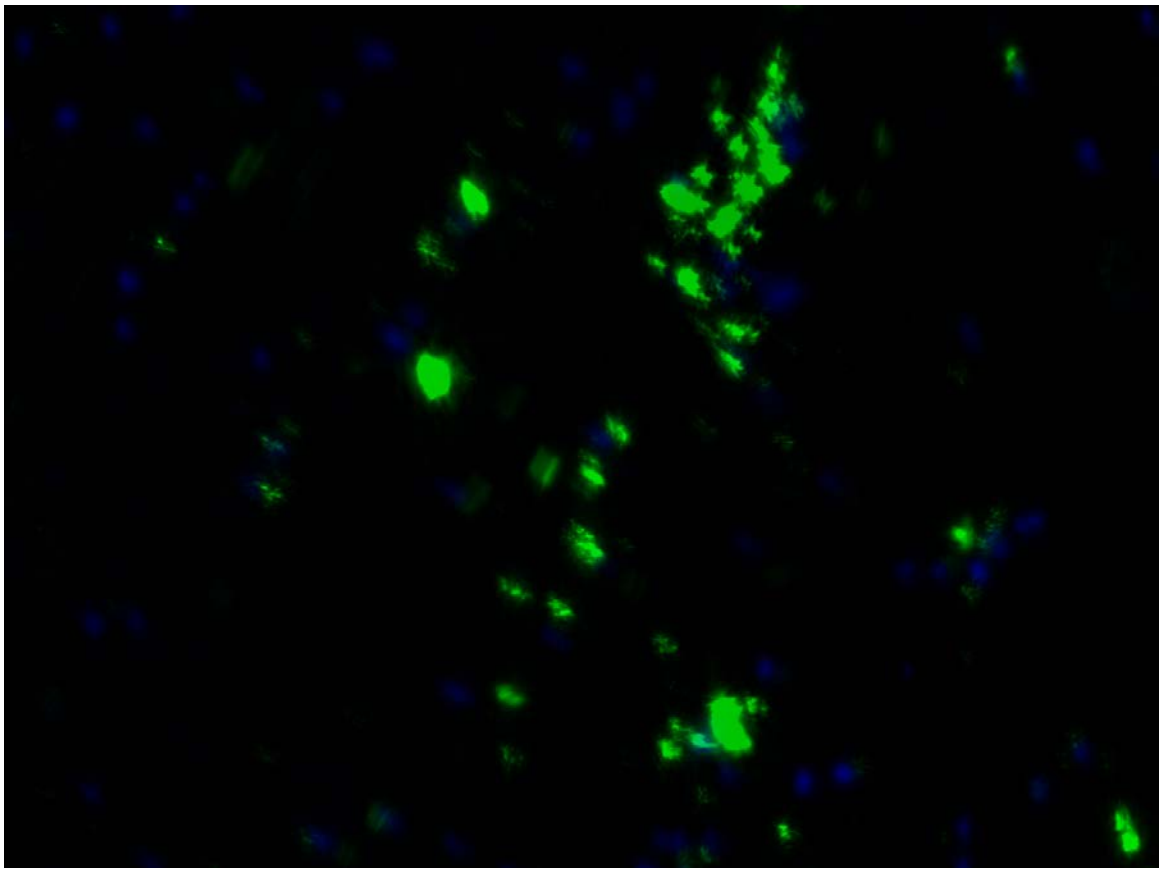

Figure 3.7. SM22-α expression in HUVECs conditioned at 10% strain after 48 hrs.

Stacking of cell sheets of HUVECs

Thermoresponsive copolymer P(NIPAAm-co-AAc) allows for the cell-to-cell and cell-to-membrane contacts to be retained (Figure 3.8). We demonstrated that we can configure the cell sheets such that they form a "herringbone" pattern, in which the alignment of one cell sheet is stacked at a different angle to another aligned cell sheet (Figure 3.9). The original cell orientations of the individual sheets were maintained after harvest and stacking.

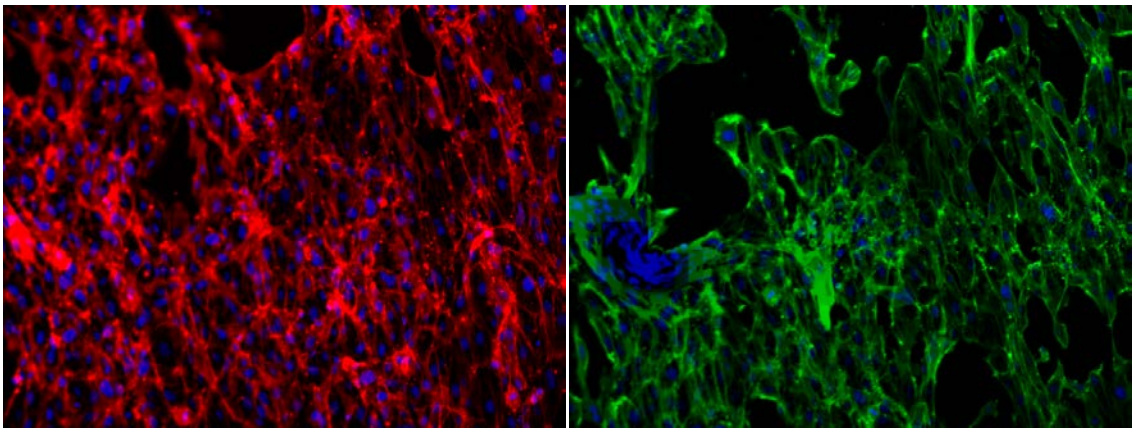

Figure 3.8. Cell sheets stretched at 10% strain, 1 Hz, 48 hrs and transferred for detachment to tissue culture polystyrene retain cell alignment.

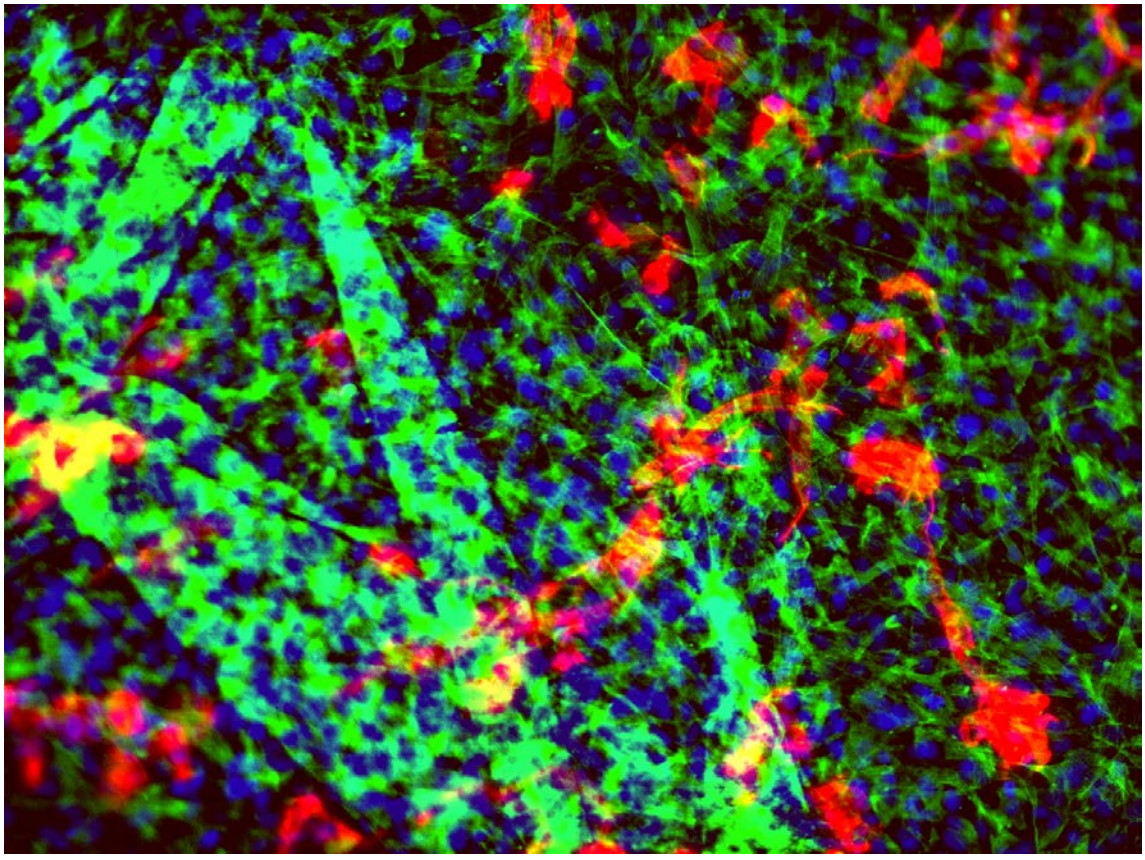

Figure 3.9. Layered and aligned construct of cell sheets stacked on top of each other.

Discussion

Cevallos and colleagues demonstrated previously that HUVECs mechanically stimulated by cyclic conditioning can induce transdifferentiation of the endothelial cell to a smooth muscle cell type.[19] The current study performed the same body of work with different results; however, we were able to demonstrate that we can successfully stretch cell sheets to allow for alignment and then manipulate those cells sheets to detach from their present surfaces and attach to another cell layer for a cell layer stacking construct.

Cell morphology and orientation of static and strained cells remained the same between both studies. HUVECs subjected to cyclic strain presented with a parallel distribution of F-actin that was oriented perpendicular to the direction of strain, which contradicts Cevallos and colleagues' study in which they find cells orient parallel to the direction of strain. Nevertheless, parallel F-actin organization seen in strained SMC cultures is suggestive of a SMC phenotype,[26,27] which suggests that HUVECs exposed to cyclic strain differentiate along a SMC lineage. Both unmodified and P(NIPAAm-co-AAc)-modified plates exhibited such organization.

In contrast to expected results, unmodified plates demonstrated a decrease in SMC contractile proteins between static culture and cells cyclically strained at 10%. Modified plates showed an increase of contractile proteins SM22-α and SMMHC, and a dramatic decrease in α-SMA expression. However, this is only a singular data point, and more data points are necessary to draw a definitive conclusion. The dramatic decrease in α-SMA expression may be due to error in loading.

The change in endothelial factors vWF and VEGFR-2 was negligible for both nonconditioned cells and cells conditioned at 10% strain on unmodified plates. Likewise, VEGFR-2 expression change was negligible, but unexpectedly, vWF expression in cells conditioned at 10% strain on modified plates increased when compared to nonconditioned cells. This is contradictory to the findings by Cevallos and colleagues, who found that endothelial factors decreased with cyclic strain, further indicating transdifferentiation of HUVECs to a SMC phenotype.

Western blot analysis is another technique that could support the hypothesis that cyclic strain induces endothelial cell type to express a SMC phenotype; however, ourantibody dilutions thus far do not produce any visible bands, so we need to perform antibody titer tests to find the titer that produces a signal. Additionally, we only tested our antibodies in milk and did not yet try BSA. We first need to arrange for the proper antibody dilutions and blocking solution to produce a signal before we can further support or negate our argument that HUVECs transdifferentiate, and that our modified plates can perform as unmodified plates do.

Expression of SM22-α was globular in nature for nonconditioned cells, while conditioned cells exhibited parallel arrangement with elongated morphology. Both unmodified and modified plates displayed the same results (data not shown), indicating that our P(NIPAAm-co-AAc)-modified plates can perform as well as unmodified plates.

Since artery structure is critical to function, tissue engineered constructs should mimic native tissue organization in an attempt to also mimic mechanical properties. The goals of this study were to demonstrate similarity in utility of both unmodified and

P(NIPAAm-co-AAc)-modified plates, and to control cell alignment of individual sheets such that a multi-layer construct could be made. Stacking of cell sheets into complex patterns was achieved, demonstrating the possibility of layered control of tissue structure.

In summary, we have demonstrated that the functionality of our P(NIPAAm-co-AAc)-modified plates is similar to that of unmodified plates, as well as showed the feasibility of layered control stacking of cell sheets. Although mRNA expression was different from previous reports, arrangement of F-actin and SM22-α alignment did show the same results for both unmodified and modified plates. Additionally, we were able to manipulate oriented cell sheets to stack on top of other cell sheets to create complex structures, like the artery wall.

Chapter IV: Increasing Contractile Protein and Extracellular Matrix Secretion of Cell Monolayers by Inducing Hypertrophy

Elaine L. Lee, Kelli C. Watson, and Horst A. von Recum

Case Western Reserve University, Cleveland, OH 44106

*This article was submitted to *Tissue Engineering, Part A.*

Abstract

Cell therapy treatment of post-myocardial infarction patients aims to regenerate tissue to improve function and prevent scarring. Although scaffold-free cell sheets offer an attractive solution, the monolayers are limited by their integrity as the layers cannot match the mechanical force transduction of the myocardium. In this study, we have explored stretching HL-1 mouse cardiomyocytes and mouse embryonic stem cells derived into cardiomyocytes cultured in monolayers to increase contractile protein and extracellular matrix (ECM) secretion for the purpose of reinforcing the baseline proteins and ECM. Cells were stretched at 3 conditions (5%, 10%, and 19%) along with static controls at 1 Hz for 24 hrs. Contractile proteins α-myosin heavy chain (αMHC) and sarcomeric α-actinin exhibited a significant increase in protein expression for all conditions. Although atrial natriuretic factor (ANF) and connexin43 (Cx43) mRNA expression did increase between static and 5% strain conditioned cells, the general trend was a decrease in expression as the percent of strain decreased. At 19% strain, mRNA and protein expression increased at a lesser rate than cyclically strained cells at 5% as a result of strain in the hypertrophic range. Effective engineering of cell

monolayers with improved mechanical integrity may require an optimal strain condition to achieve maximum expression.

Introduction

Cellular therapy for cardiac repair offers the option to improve systolic function or to prevent scarring during the remodeling process (1, 2). Preliminary clinical trials with this in mind are already underway (2-11). Acute myocardial infarction patients have been transplanted with a direct injection into the myocardium or an intracoronary infusion of autologous bone marrow or peripheral blood-derived progenitor cells in an effort to regenerate left ventricular contractility (2, 7). Both cell types have been demonstrated to improve left ventricular function after myocardial infarction (12), but have also shown potential for calcification (13) and intramyocardial tumor formation (14). Other cell types (e.g., myoblasts, cardiomyocytes, bone-marrow-derived cells) have shown improvement for cardiac performance, but direct injection still poses other problems, such as cell loss by leakage (15-18), cell death due to ischemia and apoptosis (19, 20), inappropriate integration and proliferation (21), and cardiac arrhythmia (22). One group has genetically engineered transplanted cells to overexpress connexin-43 to improve cell graft integration with limited success (23). True myocardial regeneration using embryonic stem cells or induced pluripotent stem cells is challenged by the introduction into the injured myocardium (24).

Despite these achievements in clinical trials, a better method of cell delivery to improve cardiac function is desired. To this end, tissue-engineered constructs that preserve the matrix may present a solution to the overall problems experienced by

direct injection (2). Multiple studies have shown greater improved cardiac function as a result of cell sheet implantations when compared to injection of cell suspensions, since cell sheets deter cell loss and inappropriate integration by using a targeted approach (2, 19, 25-28).

The end goal is a functional tissue that is capable of generating force during contraction (2–4 mN/mm^2) and propagating electrical signals (~25 cm/s) (26). The challenge to the cell sheet implantation approach remains the diffusion limitation for necrosis that limits the viable tissue thickness to ~200 μm (26, 29). As a result, groups have developed complex sheet structures to overcome this barrier. Scaffold-free development of engineered constructs is preferred since use of scaffolds can lead to abnormal tissue development, insufficient electrical communication due to lack of cell-to-cell connections, inflammatory responses, fibrous tissue formation, and an unnecessary use of the diffusion distance (2). Stevens and coworkers differentiated human embryonic stem cells into cardiomyocytes and then placed the cells into suspension on a rotating orbital shaker to create a myocardial patch (30). The first generation of patches, comprised of only cardiomyocytes, did not form significant grafts after implantation, as evidenced by rare, isolated human cardiomyocytes, indicating cell death for the majority of the tissue and therefore prevention of diffusion-based survival. Consequently, the second generation of patches consisted of cardiomyocytes, endothelial cells, and fibroblasts, forming patches without exogenous materials that were vascularized, actively contracted, could be electrically paced, and displayed mechanics more similar to native myocardium than patches with cardiomyocytes alone.

Scaffold-free cell sheets can preserve the cell morphology, orientation, cell-cell adhesion, and extracellular matrix (ECM), but requires technology that can allow cell detachment without needing proteolytic enzymes that would damage the preserved architecture. Accordingly, one technology that achieves such detachment is the temperature-responsive polymer poly(N-isopropylacrylamide) (P(NIPAAm)). Above 32°C, P(NIPAAm) is a hydrophobic polymer that allows cell adhesion; below 32°C, the polymer becomes hydrophilic and swollen, allowing cell detachment of intact sheets that retain their ECM. Not only are cell-to-cell and cell-to-ECM adhesions maintained, but cell viability and proliferation capability are also maintained. To construct a three-dimensional structure, several cell sheets can be layered. From approximately 34–46 minutes, Haraguchi and colleagues demonstrated that 2 cell sheets can electrically couple and allow for synchronous beating, and small molecule exchange through gap junctions between layering appears approximately 30 minutes after layering (27, 31).

The limited success of cell sheet patches can be improved upon with mechanical conditioning prior to implantation. The orientation and alignment of cardiomyocytes are stress-sensitive, making mechanical load an important regulator in the developing or remodeling heart tissue. Current studies of cell sheet implantations have shown disorganized fibers, which may lead to detrimental remodeling. However, we can improve upon the current patch by mechanically conditioning the cell sheet to allow for cell alignment to increase electrical pacing and integration and to allow for secretion of cardiac proteins for structural and functional support that more closely mimics that of the native environment. Previously, we reported a device in which we modified the

commercially available Flexcell product BioFlex plates to allow for both cell stretching and nondamaging cell detachment using thermoresponsive copolymer P(N-isopropylacrylamide-co-acrylic acid) (P(NIPAAm-co-AAc) (32). Here we show the capacity to use this bioreactor to induce the secretion of hypertrophic proteins to increase the cell monolayer's integrity in conditioned cell sheets as compared to nonconditioned cell sheets before detachment and layering into a patch. Cells on our P(NIPAAm-co-AAc)-modified surfaces performed comparably to cells on unmodified surfaces.

Materials and Methods

Materials

The immortalized cardiomyocyte line HL-1 was generously provided by Dr. William C. Claycomb from Louisiana State University. Gelatin, fibronectin, Claycomb media, defined fetal bovine serum (FBS), norepinephrine, L-glutamine, penicillin-streptomycin, and *N,N'*-dicyclohexylcarbodiimide (DCC) was purchased from Sigma Aldrich. , N-isopropylacrylamide (NIPAAm) and acrylic acid (AAc) were purchased from Acros Organics. Cor.At cardiomyocytes, Cor.At medium, and puromycin were purchased from Lonza. Flexcell Tension System FX-4000, unmodified BioFlex plates, and plates modified with ProNectin were purchased from Flexcell International. Trizol, SuperScript III First-Strand Synthesis System for RT-PCR, PCR Supermix, and primers were purchased from Invitrogen. Full-range rainbow marker was purchased from GE. Mini PROTEAN 3, Ready Gel Tris-HCl Gel (4–15%, 10-well, 50 µl), Mini Trans-Blot Electrophoretic Transfer Cell, and nonfat milk were purchased from BioRad. Heart lysate from 14-day-old mouse

(ab7194) and antibodies GAPDH (ab9484), cardiac myosin heavy chain (ab15), and sarcomeric α-actinin (ab9465) was purchased from Abcam. HRP-conjugated goat anti-mouse or anti-rabbit secondary antibody was purchased from Jackson ImmunoResearch. SuperSignal West Pico Chemiluminescent Substrate was purchased from Pierce. Weigert's iron hematoxylin solution (parts A and B), Biebrich scarlet-acid fuchsin, phosphomolybdic-phosphotungstic acid, aniline blue solution, Alcian Blue, periodic acid, Schiff's Reagent were purchased from Richard Allen Scientific. All other reagents were purchased from Thermo Fisher.

Cell Culture

The HL-1 cell line exhibits a differentiated atrial cardiomyocyte phenotype and was cultured on gelatin/fibronectin-coated flasks (1 mg fibronectin in 80 ml 0.02% gelatin) in Claycomb media supplemented with 10% defined FBS, 2 mM L-glutamine, penicillin-streptomycin, and 0.1 mM norepinephrine in a 5% CO_2 humidified incubator.

Cor.At cardiomyocytes are highly standardized, 99.9% pure murine pluripotent stem cell-derived cardiomyocytes that are puromycin-resistant and have the green fluorescent protein (GFP) reporter gene driven by a cardiac-specific promoter (αMHC). Cells were seeded 10^6 cells/well onto BioFlex plates with matrix-bonded growth surface ProNectin (RGD) and cultured in Cor.At medium with puromycin (10 µg/ml) for 48 hrs. Media was changed to Cor.At medium without puromycin for 24 hrs before cell conditioning at 10% elongation strain at 1 Hz for 24 hrs.

Cell Conditioning

HL-1 cells were seeded onto unmodified BioFlex silicone membrane surfaces or surfaces modified with a temperature-responsive copolymer that allows cell attachment at 37°C and cell detachment at room temperature as previously described (32). Briefly, NIPAAm and AAc were synthesized to formulate a copolymer (P(NIPAAm-co-AAc)). The silicone membrane of the BioFlex Culture Plate was proprietarily bonded with a low density of amines by the manufacturer, to which our copolymer was conjugated using DCC chemistry. Cells were seeded at a density of 1 million/well in a 6-well plate and stretched at 0%, 5%, 10%, or 19% strain at 1 Hz for 24 hrs. Stretch and control experiments were carried out simultaneously with cells from the same pool in each experiment.

RT-PCR

RT-PCR was used to determine mRNA expression in nonconditioned and conditioned cells. Total RNA was isolated from cells using Trizol reagent according to the manufacturer's protocol. Reverse transcription for complementary DNA was synthesized using SuperScript III First-Strand Synthesis System for RT-PCR according to the manufacturer's protocol. PCR Supermix was used for RT-PCR according to the manufacturer's protocol. Primers and sequences are listed in Table 4.1 for α-myosin heavy chain (Myh6), sarcomeric α-actinin (Actn2), atrial natriuretic factor (NPPA), Connexin 43 (Gja1), and glyceraldehydes-3-phosphate-dehydrogenase (GAPDH). Each primer set was designed using PrimerBLAST from the National Center for Biotechnology

Information (NCBI). Relative gene expression levels were normalized to GAPDH. PCR products were subjected to electrophoresis on 1% agarose gel and stained with ethidium bromide (10 µg/ml). Gels were photographed using Kodak Image Station 440CF, and images were densitometrically quantified with NIH ImageJ, version 1.44p.

Table 4.1. RT-PCR Primers for Cardiac Proteins

Gene	Forward sequence	Reverse Sequence
αMHC (Myh6)	CAACCCCTACAAGTGGCTGCCAG	GGCCAGTGCCCCGATGGAAT
Sarcomeric α-actinin (Actn2)	ACCCAGCGCCATGAATCAGATAGA	TGTGCGCCGAATCCACTCCAAC
Atrial natriuretic factor (ANF or NPPA)	CGCAGGCCCTGAGTGAGCAG	GAAGGCAGGAAGCCGCAGCT
Connexin43 (Cx43 or Gja1)	CTGGAGCGCCTTGGGGAAGC	CCGTCGGTCTGCGCCACTTT
GAPDH	ACCCCAGCAAGGACACTGAGCAAG	TGGGGGTCTGGGATGGAAATTGTG

Western Blot Analysis

Protein was isolated from cell monolayers using RIPA buffer with Halt Protease Inhibitor Cocktail according to protocol. Protein concentration was measured using MicroBCA assay. Full-range Rainbow Marker was used as the molecular weight

standards. Heart lysate from 14-day-old mouse was used as the positive control. Samples were denatured in Laemmeli buffer (4% SDS, 10% beta-mercaptoethanol, 20% glycerol, 0.004% bromophenol blue, 0.125 M Tris-HCl) at 99°C for 3 min, and run using Mini PROTEAN 3 Cell on Ready Gel Tris-HCl Gel, 4–15%, 10-well, 50 µl in 25 mM Tris, 190 mM glycine, 0.1% SDS running buffer at 100 V for 1 hr. Mini Trans-Blot Electrophoretic Transfer Cell was used for wet transfer of proteins to a nitrocellulose membrane in 48 mM Tris, 39 mM glycine, 0.1% SDS, 20% methanol transfer buffer at 100 V for 1 hr. The membrane was blocked for 1 hr at room temperature in either 5% nonfat milk or 5% bovine serum albumin (BSA). Primary antibody was incubated at 4°C overnight with agitation (GAPDH loading control, 1:5000 dilution; myosin heavy chain, 1:20,000; sarcomeric α-actinin, 1 µg/ml), followed by three 10 min washes in Tris-buffered saline Tween-20 (TBST). Secondary antibody (HRP-conjugated goat anti-mouse, 1:2000 dilution) was incubated at room temperature for 1 hr, followed by three 10 min washes in TBST. Membranes were incubated with SuperSignal West Pico Chemiluminescent Substrate made according to the manufacturers' instructions for 5 min. Blots were exposed to film for 1 s to 5 min exposures. Blots were analyzed using gel analysis in NIH ImageJ, version 1.44p.

Masson's Trichrome Stain for Collagen Fibers

Following cell nonconditioning or conditioning, the silicone membrane was cut from the BioFlex plate into 2 sections. Cells were fixed in 100% ice-cold acetone for 10 min, rehydrated through a graded series of ethanol (100%, 95%, 70%), and rinsed in

distilled water. Sections were stained in Weigert's iron hematoxylin working solution for 10 mins and then rinsed in running warm tap water for 10 mins. Following a wash in distilled water, sections were stained in Biebrich scarlet-acid fuchsin solution for 15 mins. After washing in distilled water, sections were differentiated in phosphomolybdic-phosphotungstic acid solution for 15 mins and transferred directly to aniline blue solution for 10 mins. A brief rinse in distilled water was followed by differentiation in 1% acetic acid solution for 5 mins. Following a wash in distilled water, sections were dehydrated quickly through 95% and 100% ethanol and cleared in xylene before mounting. Sections were imaged under a Leitz Laborlux S, and images were captured using Nikon CoolPix 995. Collagen and muscle fibers were counted by stereology by distinguishing color, counting if that color crossed one of 80 intersects, and normalizing against the total number of cells.

Alcian Blue/Periodic Acid-Schiff's Reagent Stain for Glycosaminoglycans

Following cell nonconditioning and conditioning, the silicone membrane was cut from the BioFlex plate into 2 sections. Cells were fixed in 100% ice-cold acetone for 10 min, rehydrated through a graded alcohol series (100%, 95%, 70%), and rinsed in distilled water. Sections were stained in Alcian Blue solution for 30 min at room temperature and rinsed in distilled water. Following staining in periodic acid solution for 5 min at room temperature, sections were rinsed in distilled water and stained in Schiff's Reagent for 15 min. Sections were rinsed in lukewarm running tap water for 10 min and rinsed in distilled water. Following dehydration through 95% and 100% ethanol

for 1 min each, sections were cleared twice in xylene and mounted in Cytoseal. Sections were imaged under a Leitz Laborlux S, and images were captured using Nikon CoolPix 995. GAGs and polysaccharides were counted as with the Alcian Blue stain.

Statistical Analysis

Data are presented as mean ± standard deviation, where N = 5. Experimental and control samples were compared using analysis of variance (ANOVA), where *p*-values <0.05 were considered significant.

Results

RT-PCR

We used RT-PCR to determine mRNA expression in nonconditioned and conditioned cells. When HL-1 cells were subjected to 5% cyclic strain, these cells expressed levels of αMHC and ANF higher than static controls (Figure 4.1). In comparison, αMHC expression was only slightly increased in 19% cyclically strained cells, and ANF was approximately the same as the static control. Although expression of Cx43 was approximately the same as static controls for 5% cyclically strained cells, it was dramatically decreased in 19% cyclically strained cells. Sarcomeric actinin mRNA expression was approximately the same as the respective static controls for both stretching conditions. GAPDH mRNA expression served as a control for both static and cyclically strained cells, and NIH3T3 cells served as a control for cardiac-specific protein expression, although NIH3T3 cells do express Cx43 naturally (33).

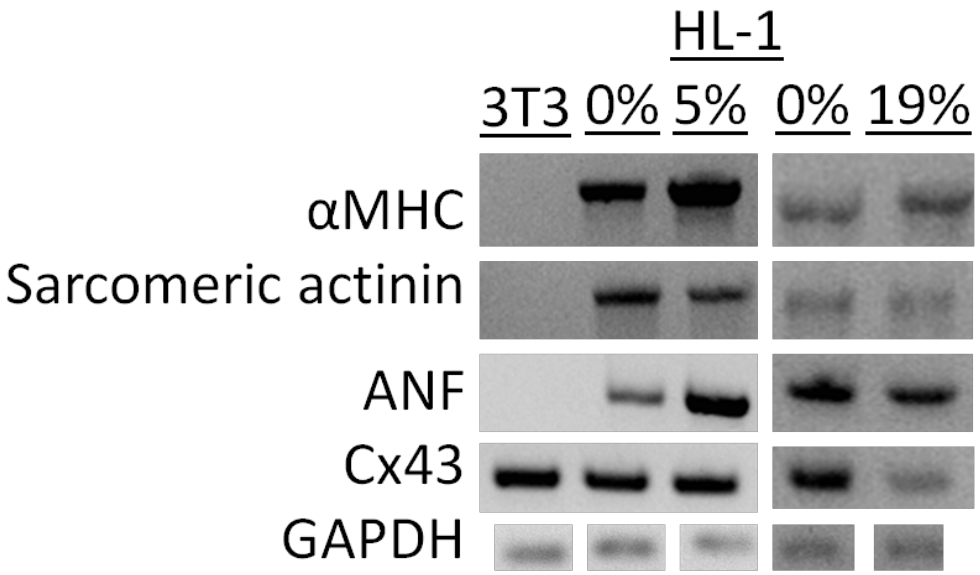

Figure 4.1. RT-PCR of contractile proteins and hypertrophic hormone for nonconditioned and conditioned cells.

Protein secretion increases with cell conditioning in HL-1 cells

To evaluate expression of cardiac contractile proteins in both static and strained HL-1 cells, Western blot analysis was performed as described above. MHC is characterized by two isoforms, alpha and beta. For αMHC (first band), protein levels increased 235.2 ± 37%, 256.4 ± 46%, and 17.6 ± 35% for 5%, 10%, and 19% strain, respectively, as compared with a static control, of which only 5% and 10% strain showed a significant increase in protein level (Figures 4.2 and 4.3). For βMHC (second band), protein levels increased 22.4 ± 27%, 99.8 ± 19%, and 89.4 ± 20% for 5%, 10%, and 19% strain, respectively, as compared with a static control, of which only 10% and 19% strain showed a significant increase in protein level. Sarcomeric actinin showed a significant

increase in protein level for all three strains, with increases of 194.4 ± 76%, 227.1 ± 61%, and 40.8 ± 19%, respectively.

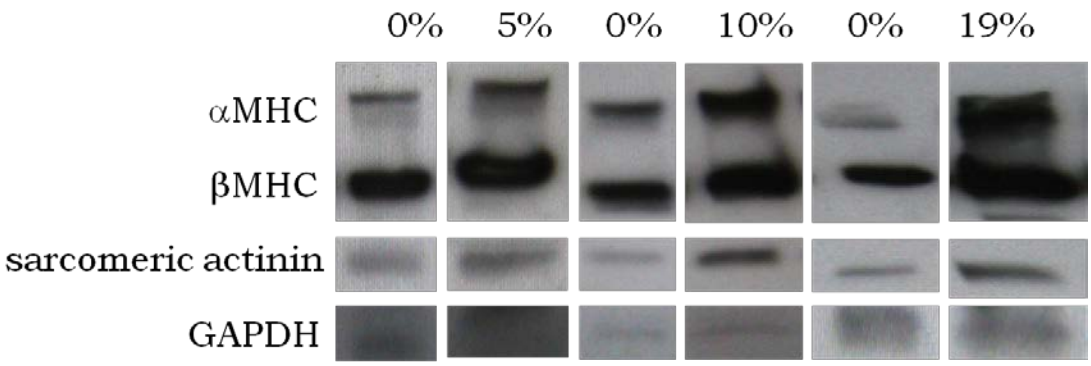

Figure 4.2. Representative Western blots for contractile proteins of nonconditioned and conditioned cells.

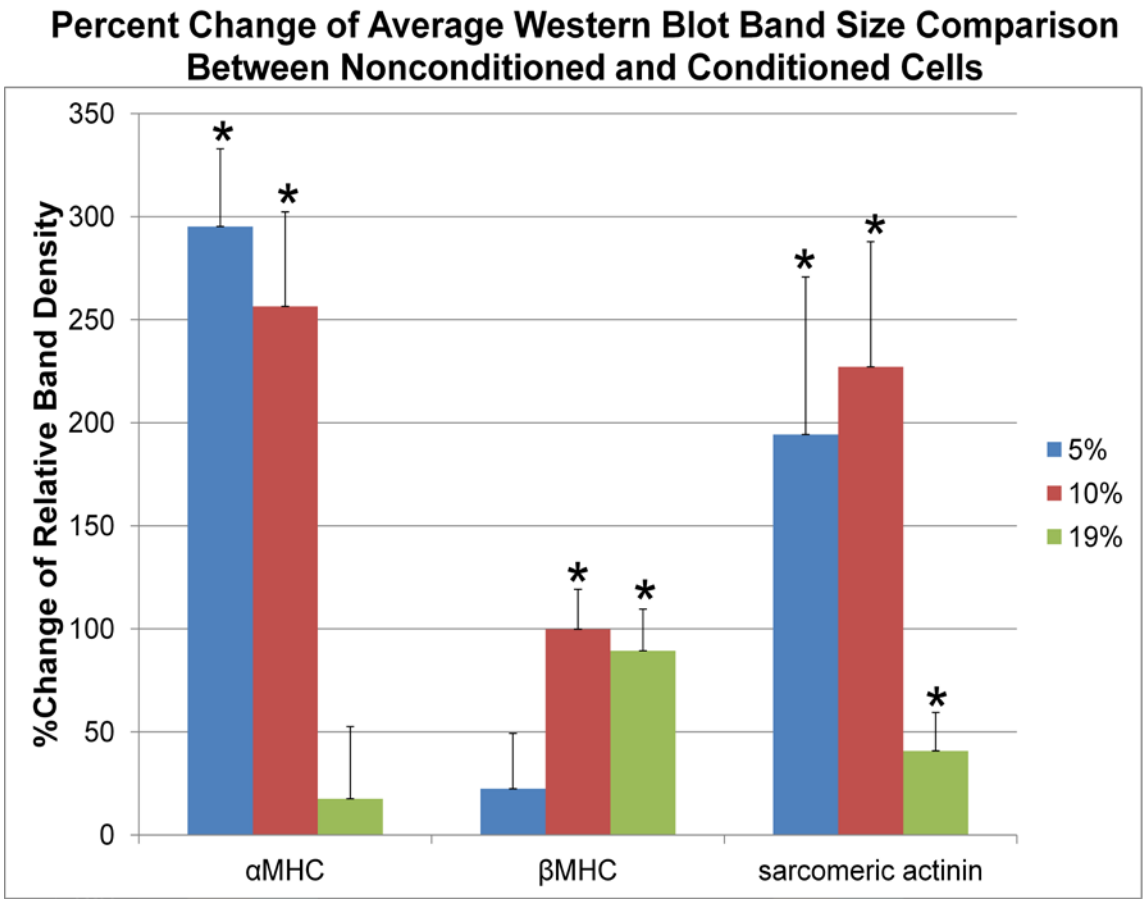

* Significant difference between nonconditioned and conditioned cells by ANOVA test.

Figure 4.3. Percent change of contractile proteins between nonconditioned and conditioned cells.

Cardiac contractile protein expression in embryonic stem cell-derived cardiomyocytes (Cor.At) showed an increase of 288.7% and 278.4% for αMHC and sarcomeric actinin, respectively (Figures 4.4 and 4.5).

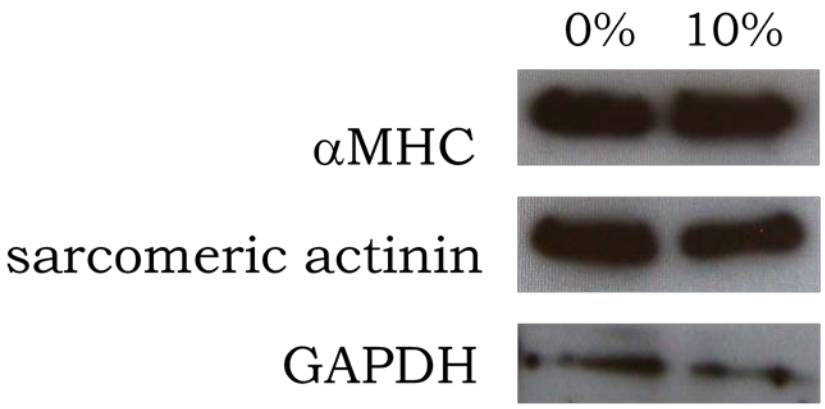

Figure 4.4. Western blot of contractile proteins for embryonic stem cell-derived cardiomyocytes.

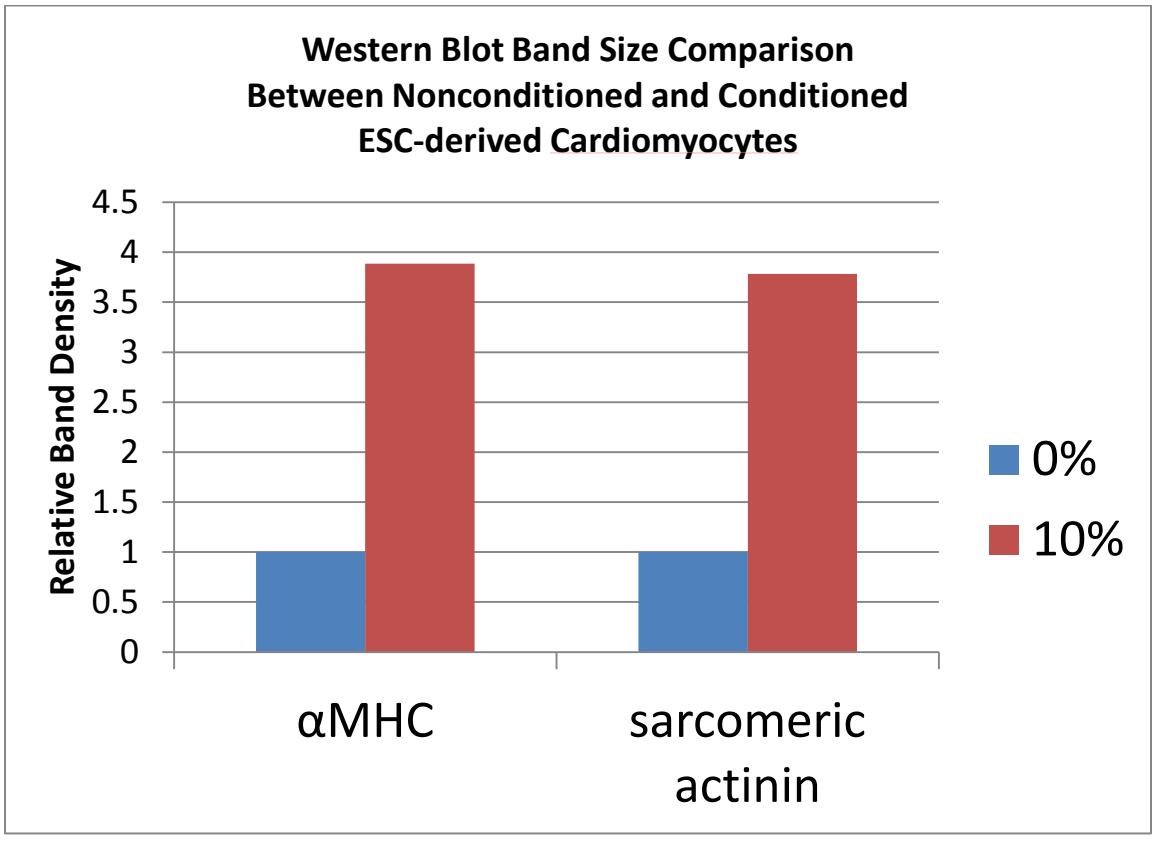

Figure 4.5. Band intensity of contractile proteins in embryonic stem cell-derived cardiomyocytes normalized to GAPDH.

Masson's Trichrome Stain for Collagen Fibers

From this stain, collagen was stained blue; nuclei were stained black; and muscle fibers, cytoplasm, and keratin were stained red. As part of the ECM, collagen provides support and structure, as well as gives strength to tissues. In HL-1 cells stretched at 10% as compared to a static control, collagen, muscle fibers, cytoplasm, and keratin protein expression were increased, but not significantly by analysis of variance (Figure 4.6).

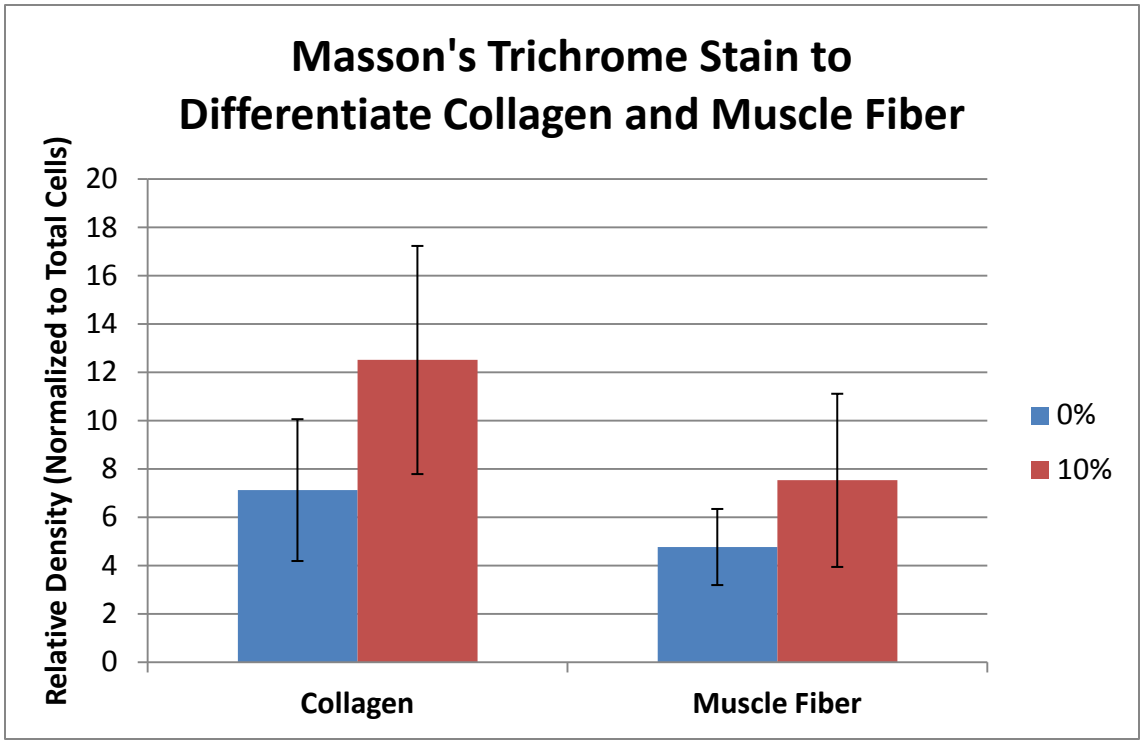

Figure 4.6. Collagen and muscle fiber content in nonconditioned and conditioned cardiomyocytes.

Alcian Blue/Periodic Acid-Schiff's Reagent Stain for Glycosaminoglycans

From this stain, glycosaminoglycans or acidic polysaccharides were stained blue, and basement membrane, glycogen, and neutral polysaccharides were stained magenta. Covalently linked to proteoglycans in the extracellular matrix, GAGs attract water to give resistance to externally applied pressure. In HL-1 cells stretched at 10% as compared to a static control, GAG, basement membrane, and glycogen expression were increased, but also not significantly by analysis of variance (Figure 4.7).

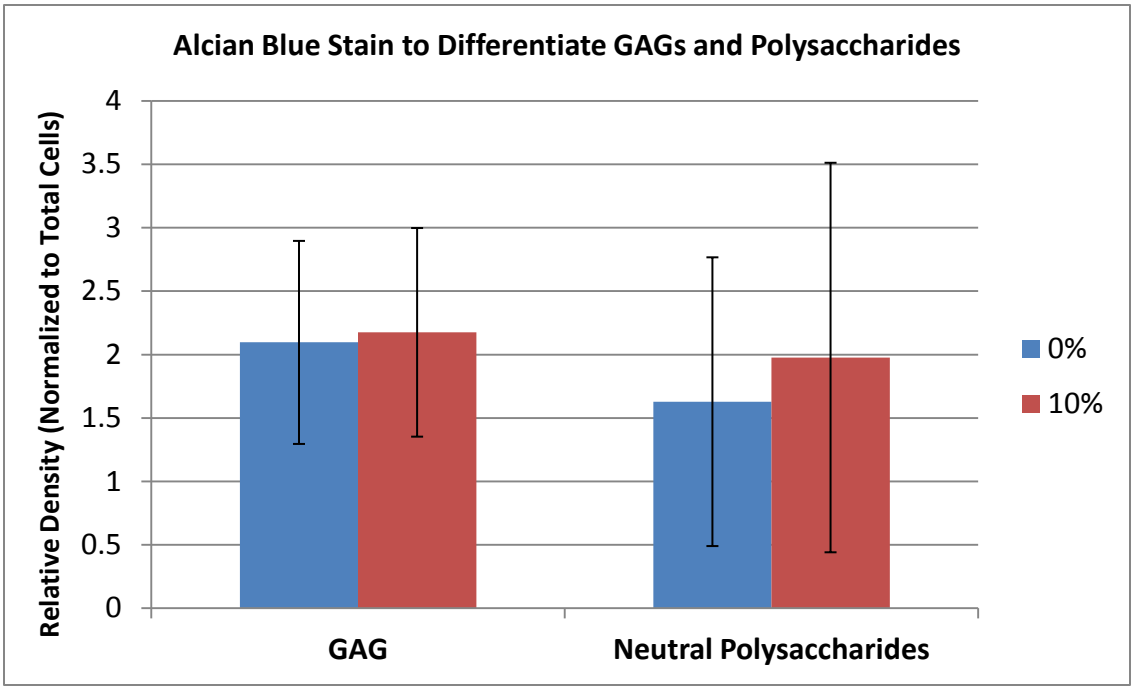

Figure 4.7. GAG content in nonconditioned and conditioned cardiomyocytes.

Discussion

The mechanical integrity of a single cellular monolayer sheet or a patch of layered sheets currently have a mechanical mismatch to the native environment. In this study, we explored improving the integrity by inducing hypertrophy on cardiomyocytes such that contractile protein secretion increases the mechanical properties of a single cell sheet. The results presented here demonstrate that such an endeavor requires an optimal straining condition before negating the effects produced from mechanical conditioning.

Atrial natriuretic factor (ANF) is a hypertrophic hormone released in response to atrial stretch. The significant increase in mRNA in 5% cyclic stretch compared to static controls indicates increase in ANF expression (Figure 4.1); on the other hand, ANF expression for cells stretched cyclically at 19% strain did not change and may have slightly decreased. Gardner and colleagues found that stretch-dependent release of ANF was suppressible by factors that impair enzymatic/metabolic activity, and no release was found in the medium, indicating that levels of ANF were only from secretion from the cell (34). However, although there was a 21% increment in cellular surface area, the study only stretched the cell twice in quick succession. To achieve in vivo hypertrophic strain, studies have applied 10–20% strain in short intervals (24 hrs) (35-39). The combination of the length of time of cyclic stretch with the high magnitude of strain may have caused cellular damage, which may have resulted in leakage of ANF into the medium.

αMHC, sarcomeric actinin, and ANF mRNA expression were not present in NIH3T3 cells (Figure 4.1), indicating that expression was exclusive to cardiac cells. Cx43 is not exclusive to cardiac tissues; it is also expressed in NIH3T3 cells. Indeed, Haraguchi and partners demonstrated that sheets of cardiomyocytes can form electrical interactions not only between cardiomyocyte sheets (31), but also between up to two layers of non-cardiomyocyte NIH3T3 cell sheets (33). Additionally, the significant decrease in Cx43 expression between nonconditioned cells and cells conditioned at 19% strain may signify that the increase in strain may be overstretching and breaking cell-to-cell interaction at the gap junctions.

For all proteins in all conditions, an increase in contractile proteins (α- and βMHC, sarcomeric actinin) was observed (Figures 4.2 and 4.3). This agrees with the embryonic stem cell-derived cardiomyocytes stretched at 10%, 1 Hz for 24 hrs, which showed an increase in αMHC and sarcomeric actinin (Figures 4.4 and 4.5). However, the percent change in band density of αMHC between nonconditioned cells and cells cyclically stretched at 5% strain was significantly greater than for 19% strain conditions, which is also reflected in the RT-PCR data. Additionally, the significant increase in βMHC in 10% and 19% stretch as compared to their static controls along with the respective concomitant percent change decrease in αMHC from 5% to 19% strain may indicate reversion to the fetal program. In mice, the fast contracting ventricles are characterized by the V_1 or αα isoform. Although αMHC transcripts decrease in ventricular myocytes shortly before birth in mice, a surge in thyroid hormones shortly after birth causes αMHC expression levels to rise, replacing βMHC by 7 days postnatally as the

predominant cardiac isoform. βMHC exerts greater efficiency in electromechanical force transduction than αMHC (40). Thus, like the native environment, this finding indicates that induced hypertrophy of cell sheets in tissue engineering myocardial patches also has an optimal amount of strain to induce secretion of desired cardiac isoforms.

Our Western blot analysis showed an increase in sarcomeric actinin expression in conditioned cells when compared to nonconditioned cells. However, densitometric analysis of RT-PCR showed that the mRNA expression level remained the same for both nonconditioned and conditioned cells for 5% strain and decreased by 16.5% for cells conditioned at 19% strain (data not shown). This discrepancy may indicate that increase in translation may occur independently from changes in mRNA levels.

Overall, the increase in protein expression in comparison to controls is not as high for cells cyclically stretched at 19% strain as it is for 5% and 10% strains. This further corroborates that cell monolayers engineered for cardiac patches have an optimal strain to induce secretion of proteins.

As expected, GAG and collagen content showed increased expression in cells conditioned at 10% when compared to static cells (Figures 4.6 and 4.7); however, the increase may not be significant. As a result of the qualitative nature of the assays performed, more quantitative methods of determining GAG and collagen content via fluorophore assisted carbohydrate electrophoresis (FACE) and hydroxyproline assay, respectively, may be necessary to be conclusive.

The goal of cellular therapy for post-myocardial infarction is to improve function and prevent scarring. Scaffold-free cell sheets for regenerative cardiac patches may be a

solution, but are limited by integrity for mechanical force transduction that is disparate from the myocardium. In this study, we have investigated stretching cardiomyocytes cultured in monolayers to increase contractile protein and ECM secretion. Overall, mRNA, proteins, and ECM components were found to increase with cell conditioning, but the effective secretion of these proteins may have an optimal strain condition to achieve maximum expression. Cell sheets grown on our bioreactor have previously been shown to be capable of cell sheet detachment.

Acknowledgements

This work was supported by a Predoctoral Fellowship from the American Heart Association for E. L. Lee and a pilot award from the National Center for Regenerative Medicine.

Chapter V: Scalable Production of Functional Cardiomyocytes Derived from Embryonic Stem Cells for Use in a Regenerative Myocardial Patch

Elaine L. Lee, Diana Ramirez, and Horst von Recum

Case Western Reserve University, Cleveland, OH 44106

*This article is written in preparation for submission to *Tissue Engineering, Part C.*

Abstract

The pluripotent and self-renewable capabilities of embryonic stem cells (ESCs) and their capacity to avoid immune system complications give ESCs the potential to revolutionize regenerative cell therapy by the possibility of scalable production of functional cardiomyocytes derived from these progenitors. Fabrication of a regenerative myocardial patch for post-myocardial infarction remodeling will depend on generating large numbers of cardiomyocytes. Various methods are available for generating functional cardiomyocytes: the hanging drop method, suspension culture using low-attachment plates, rotary suspension culture, and spinner flask suspension culture. This study examines these methods of differentiation and makes comparisons into the efficiency of each method to produce beating EBs for careful consideration in the future design of the scaffold-free myocardial patch.

Introduction

The severe reduction or complete lack of blood flow that brings oxygen to the heart is called a coronary attack or heart attack, and an estimated 785,000 Americans will experience a new coronary attack each year, while 470,000 will have a recurrent attack.[1] An additional 195,000 Americans will have their first myocardial infarction, which is the death or damage of heart muscle as a result of ischemia. Approximately every 25 seconds, an American will have a coronary event, and approximately every minute, someone will die of one.

During myocardial infarction, the heart may experience a significant loss of cardiomyocytes that is later replaced by non-contractile scar tissue. As a result, the remaining heart muscle may experience an increase in load that maladaptively affects the remodeling process. Because of this remodeling process, the decline may lead to ventricular dysfunction, which may ultimately lead to congestive heart failure and death.[2] Since cardiomyocytes do not regenerate, potential cell therapies to repair the infarct will require a renewable source of cells.

Many cell types have been considered for regenerating ischemic tissue, including embryonic stem cells (ESCs), induced pluripotent stem cells (iPSCs), neonatal cardiomyocytes, skeletal myoblasts (SKMs), endothelial progenitor cells (EPCs), bone marrow mononuclear cells (BMMNCs), mesenchymal stem cells (MSCs), and cardiac stem cells (CSCs).[3] SKMs were the first cells to be used clinically for heart regeneration since they are contractile, can be harvested for autologous transplantation, and are resistant to ischemia.[4-6] Despite the functional benefit, SKMs showed a high incidence of

ventricular arrhythmias in several small non-randomized phase I trials, as a result of the formation of myotubes that lack gap junctions.[7-10] Bone marrow-derived cells are easily accessible (e.g., MSCs), but an early study that reported the transdifferentiation of bone marrow-derived cells into cardiomyocytes has been contested, bringing the functional benefits into question.[11,12] Induced pluripotent stem cells have been demonstrated to retain epigenetic memory of their somatic cell of origin, which may possibly affect lineage-specific differentiation.[13,14] Additionally, although iPS cells may not have the ethical and immunologic issues associated with ESCs, protocols to reprogram iPS cells have low and inconsistent efficiency, and depend on research and understanding of ESCs.[15]

Embryonic stem cells have the potential to be derived into hundreds of cell types, but this also is the bane of using ESCs, namely that they typically do differentiate into many of these lineages at the same time and in the same dish. To promote differentiation of ESCs, three-dimensional aggregates known as embryoid bodies (EBs) are formed. We can monitor ESC differentiation to efficiently generate highly enriched differentiated cell populations by using lineage-restricted gene promoters in ESCs with reporters or selection markers (e.g., cardiac-restricted promoter with a green fluorescent protein reporter or an antibiotic resistance gene).[16] Additionally, deriving patient-specific ESC or iPSC equivalents would evade immune system complications. Although normal or injured tissues lack the signaling cues required to induce proper ESC differentiation, advanced differentiation of ESCs and their subsequent enrichment for the desired cell type, along with screening for the presence of undifferentiated cells, can

reduce the likelihood of teratomas, which are tumors derived from all three germ layers.[16,17]

Thus far, injection of cells directly into the myocardium or the coronary vasculature has been the typical method of stem cell delivery in clinical feasibility studies.[18] However, this method comes with its associated problems: cellular washout through channel leakage,[19-21] apoptosis due to extracellular matrix (ECM) disruption and anchorage loss (anoikis),[22] and arrhythmogenic issues.[8,9,18,23,24] Cell sheet engineering provides an alternative, with the main advantage of preservation of ECM and cell-cell contact typically lost upon trypsin treatment. Along with its targeted approach to prevent cellular washout,[25,26] cell sheet engraftment may be a better solution to arrhythmia than cellular suspension injections.[27] Attractive in its use, thermoresponsive-polymer technology via poly (N-isopropylacrylamide) offers the option for cells to be cultured at 37°C and detached spontaneously without enzymatic means at room temperature. Thus, cellular sheets of cells can be cultured, detached intact, and layered to form a scaffold-free myocardial patch.

Although appealing in potential for cellular replacement therapy, the use of cardiomyocytes derived from ESCs is plagued by the difficulty in differentiating cells into highly pure populations of cardiomyocytes and optimally amplifying differentiation. In this study, we examine the effects of culture conditions on cardiomyocyte generation, as well as methods to scale-up production of embryoid bodies to increase the yield of functional cardiomyocytes for the use of regenerative myocardial patches.

Materials and Methods

Cell Culture

E14TG2A α-myosin heavy chain with green fluorescent protein (E14 αMHC-GFP) embryonic stem (ES) cell line was generously provided by Dr. Marc Penn at Northeast Ohio Medical University and the Summa Cardiovascular Institute in Akron, OH. Cells were cultivated on mouse embryonic fibroblasts (MEFs) from thawing in DMEM (Hyclone) supplemented with 10% fetal bovine serum (FBS), 1% non-essential amino acids (NEAA), and 1% penicillin-streptomycin (PS) antibiotics. Cells were then cultivated on gelatin (0.1%)-coated dishes in ES culture media (DMEM supplemented with 10% fetal bovine serum (FBS, selected batches), 1% NEAA, 2-mercaptoethanol (Sigma, 100 mM), 1% PS, and leukemia inhibiting factor (LIF, 1000 units/ml)). The first differentiation media formula was the same as the ES culture media but with 15% FBS. The second differentiation media included DMEM supplemented with 15% FBS, 1% PS, and 1-thioglycerol (MTG, 450 µM). The third differentiation media included IMDM supplemented with 15% FBS (select batches), ascorbic acid (50 µg/ml), 1% L-glutamine, 1% PS, 1% insulin-transferrin-selenium (ITS), MTG (450 µM), and transferrin (167 nM).

Undifferentiated MB1 mouse ES cells generously donated by Paul Tesar from Case Western Reserve University were transfected via electroporation with a plasmid carrying an αMHC promoter in front of an enhanced green fluorescent protein fused with a puromycin resistance gene (EGFP-puro), with a neomycin resistance gene under a separate constitutive promoter. For transfection, the cells were suspended in 800 µl phosphate-buffered saline (PBS) at a density of 1×10^6 cells and electroporated with 50

μg linearized DNA (Sac I) using the Neon Transfection System (1400 V, pulse width 20 ms, 3 pulses; Invitrogen). Electroporated cells were cultivated and selected for 14 days in culture medium containing G418 (200 μg/ml) at 37°C in humidified air with 5% CO_2. MB1 αMHC-EGFP-puro cell line was generated by picking and expanding single clones in G418 (400 μg/ml) for an additional 3 weeks. Clones were selected for robust growth as undifferentiated cells. Insertion of αMHC-EGFP-puro into the genomic DNA was verified by polymerase chain reaction (PCR). MEFs were cultivated in DMEM with high glucose media (Gibco BRL, Life Technologies, Germany) supplemented with 10% ES-cell qualified FBS (Gibco), 1% L-glutamine (Gibco, 2 mM), and 1% NEAA. ES cells were cultivated on MEFs in knockout DMEM (Gibco) supplemented with 15% knockout serum replacement (KSR, Gibco, selected batches), 5% ES-cell qualified FBS, 1% L-glutamine, 1% NEAA, and 2-mercaptoethanol (100 nM final concentration) with LIF (1000 units/ml) added with every media change. Differentiation media did not include LIF.

Hanging Drop

Cells were differentiated into spontaneously beating cardiomyocytes as previously described[28,29] by two different methods (Figure 5.1). MB1 αMHC-EGFP-puro cells were MEF-depleted before making hanging drops by allowing the trypsinized cells to adhere to a 0.1% gelatin-coated plate for 45 mins; the remaining cells in suspension were used for hanging drops. For the first method, cells were cultivated in hanging drops as embryoid bodies (EBs) in differentiation media. A definite number of ES cells (2000 cells) were placed in 15 μl drops on the lids of Petri dishes filled with PBS. After 2

days in hanging drops, the EBs were resuspended in medium in bacteriological Petri dishes and cultivated for further 5 days in suspension. On day 7, the EBs were plated onto gelatin-coated 6-cm dishes. For the second method, cells were cultivated and resuspended at day 2 in 6-cm bacteriological dishes as in the first method, either in normoxia or hypoxia (5% O_2). After 2 days in suspension (day 4) in normoxia or hypoxia, respectively, the EBs were plated in a low volume of medium onto gelatin-coated 6-cm dishes (approximately 50–60 EBs/dish) and allowed to adhere for 3 hrs before bringing the volume up to normal. For both methods, approximately 60–80 drops were added to each 6-cm dish.

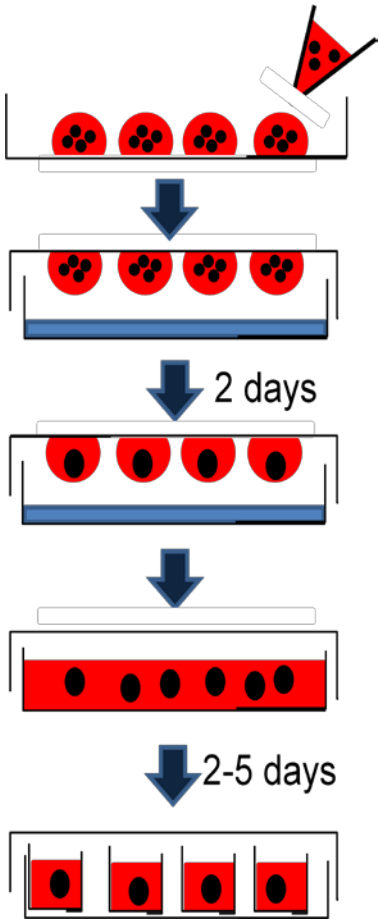

Figure 5.1. Schematic of the hanging drop method.

Suspension Using Ultra Low Attachment Plates

Ultra-low attachment plates (Corning, Lowell, MA) are modified with hydrophilic, neutrally-charged hydrogel surfaces that minimize cell attachment, protein absorption, and enzyme activation. Cells can remain in a suspended, unattached state to prevent stem cells from attachment-mediated differentiation. Cells were plated into each well and allowed to form EBs for 6 days (8.8×10^4 cells/well) (Figure 5.2). As with hanging drops, MB1 αMHC-EGFP-puro cells were MEF-depleted before being plated. EBs were then plated onto gelatin-coated 6-well plates, to promote specific cell attachment. Puromycin (0–3 µg/ml) was added to MB1 αMHC-EGFP-puro EBs on day 10. Media was changed every other day; for EBs in suspension, EBs were collected by settling the EBs gravitationally before changing media.

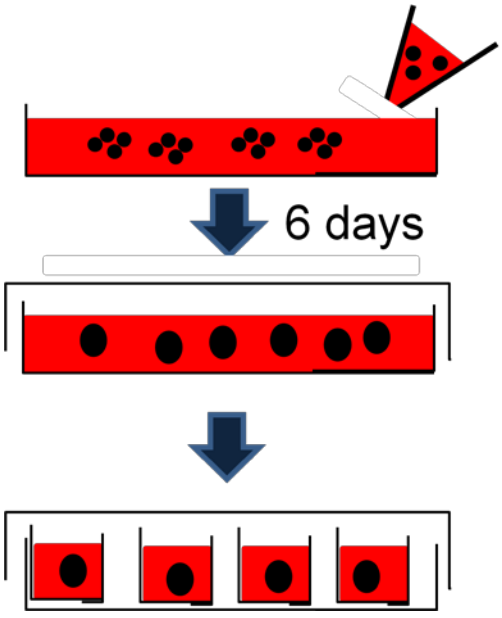

Figure 5.2. Schematic of suspension culture using ultra-low attachment plates.

Rotary Suspension Culture

Rotary suspension culture uses hydrodynamic conditions to aggregate ESCs into homogenous, uniformly sized EBs (Figure 5.3).[30-32] Briefly, suspension cultures of EBs were initiated by resuspending 4 x 10^5 cells/ml in differentiation medium (growth medium without LIF). Rotary suspension cultures were cultivated in sterile 10-cm bacteriological Petri dishes (Becton Dickinson Biosciences, San Jose, CA) with 10 ml differentiation medium. Rotary suspension culture EBs were initiated by placing dishes on an orbital rotary shaker (Lab-Line Lab Rotator; Barnstead International, Dubuque, IA) set at approximately 30 rpm. EBs were maintained for up to 7 days in suspension, with medium changed every 1–2 days by allowing EBs to sediment in 15-ml centrifuge tubes, aspirating the old medium, and resuspending in fresh medium.

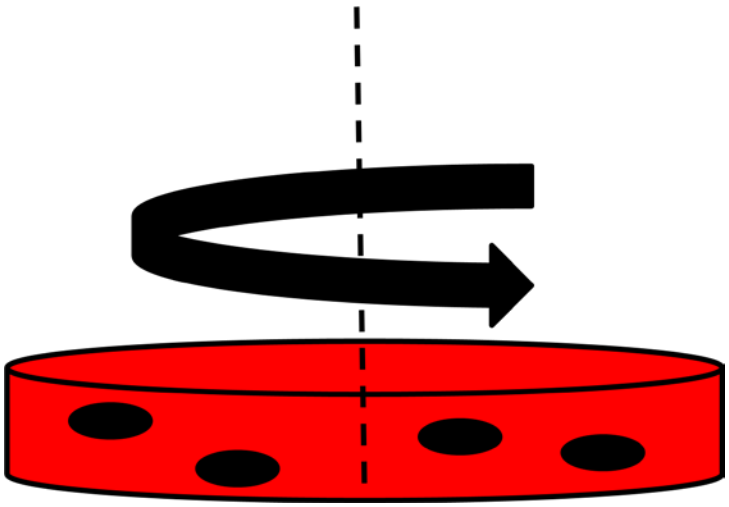

Figure 5.3. Schematic of rotary orbital shaker suspension culture.

Spinner Flask Cultures

For inoculation, E14 αMHC-GFP cells were washed with phosphate buffered saline (PBS) (Thermo Scientific) and dispersed into single cells using trypsin (Thermo Scientific). After resuspension in differentiation medium, a spinner flask equipped with an adjustable blade impeller with a dimpled bottom (Bellco Glass, Vineland, NJ) was separately inoculated with 125 ml of the differentiation medium (DMEM supplemented with 15% fetal bovine serum (FBS, selected batches), 1% NEAA, 2-mercaptoethanol (Sigma, 100 mM), 1% PS) containing $2x10^5$ cells/ml and stirred at 60–120 rpm (Figure 5.4).[33] Flasks were filled up to 250 ml after 48 h, followed by a daily half medium exchange. Cardiomyocyte selection was initiated by adding Geneticin (G418, 400 mg/ml) to eliminate non-cardiac cells following an 11-day long expansion and differentiation phase. All-trans retinoic acid was also supplemented at 10 nM final concentration beginning on day 9. One-ml samples for EB count were taken daily.

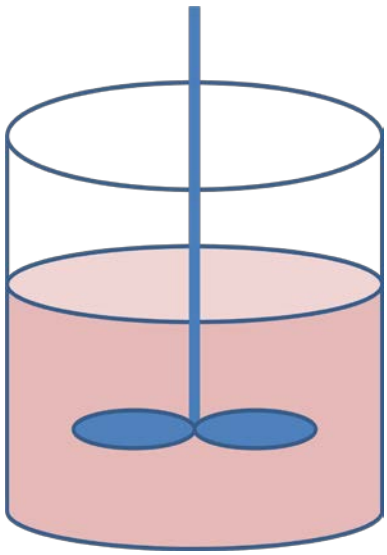

Figure 5.4. Spinner flask suspension culture vessel.

Results

Hanging Drop

E14 αMHC-GFP EBs differentiated by EBs in suspension for 5 days did not yield any beating or fluorescing EBs. E14 αMHC-GFP EBs differentiated by EBs in suspension for 2 days in the first (DMEM supplemented with 15% fetal bovine serum (FBS, selected batches), 1% NEAA, 2-mercaptoethanol (Sigma, 100 mM), 1% PS) and second (DMEM supplemented with 15% FBS, 1% PS, and MTG (450 µM)) differentiation media formulations began to fluoresce on day 3, where the EBs in the second differentiation medium were slightly larger. By day 13, G418 (400 µg/ml) was added to EBs in the second media formulation, and no significant cell death was observed. Beating was observed on day 13 of E14 αMHC-GFP EBs differentiated by EBs in suspension for 2 days in differentiation media (IMDM supplemented with 15% FBS (select batches), ascorbic acid (50 µg/ml), 1% L-glutamine, 1% PS, 1% insulin-transferrin-selenium (ITS), MTG (450 µM), and transferrin (167 nM)) in both normoxia and hypoxia conditions, where EBs in hypoxia were larger.

EBs under normoxia had an average area of 59.2 ± 19 x 10^3 µm^2, with a major axis of 302.5 ± 56 µm and a minor axis of 245.4 ± 42 µm (Figure 5.5) (Table 5.1). The circularity index of hanging drop EBs was 0.82 ± 0.1, where 1 indicates a perfect circle.

Table 5.1. Embryoid Body Comparison

	Hanging Drop (N = 28)	Rotary Culture (N = 12)	Spinner Flask (N = 107)
Area (x 10^3)	59.2 ± 19 μm^2	54.2 ± 38 μm^2	25.9 ± 20 μm^2
Major Axis	302.5 ± 56 µm	319.2 ± 109 µm	179.3 ± 74 µm
Minor Axis	245.4 ± 42 µm	205.0 ± 73 µm	156.5 ± 57 µm
Circularity (Circle = 1) $\frac{4\pi(Area)}{Perimeter^2}$	0.82 ± 0.1	0.59 ± 0.2	0.97 ± 0.1

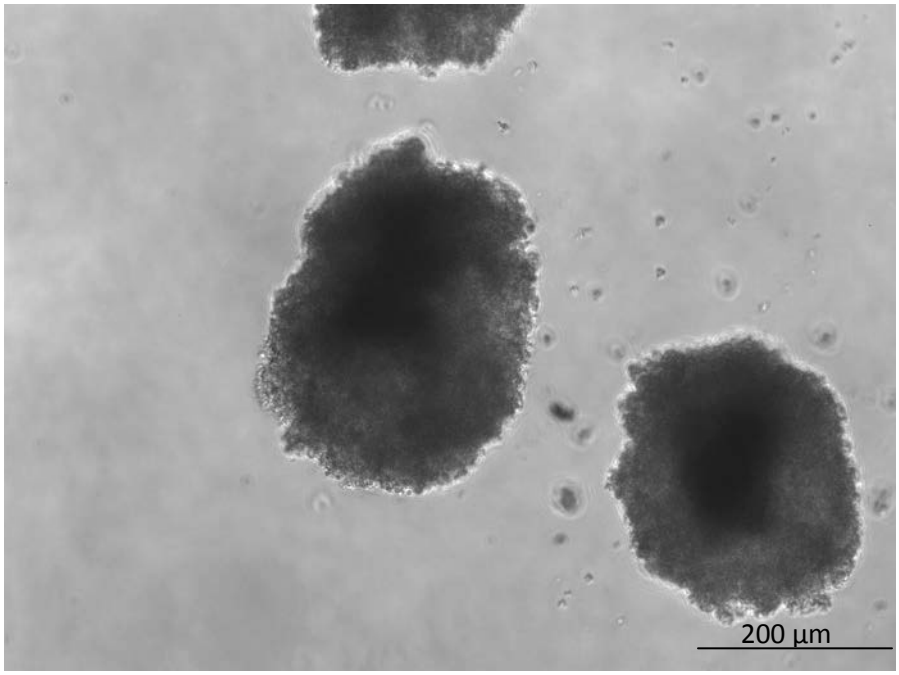

Figure 5.5. Representative hanging drop embryoid bodies.

Suspension Using Ultra-Low Attachment Plates

MB1 αMHC-EGFP-puro cells were transferred from ultra-low attachment plates after 6 days to a gelatin-coated 6-well tissue culture-treated plate. On day 10, no beating was observed, but EBs were fluorescent. Puromycin was added on day 10, and almost 100% cell death was observed in 1–3 µg/ml puromycin by day 14. Cells began to shear from the plate by day 15.

Rotary Suspension Culture

E14 αMHC-GFP EBs plated on gelatin-coated plates on day 7 did not beat or fluoresce. EBs had an average area of 54.2 ± 38 x 10^3 µm^2, with a major axis of 319.2 ± 109 µm and a minor axis of 205.0 ± 73 µm (Figure 5.6) (Table 5.1). The circularity index of rotary culture EBs was 0.59 ± 0.2.

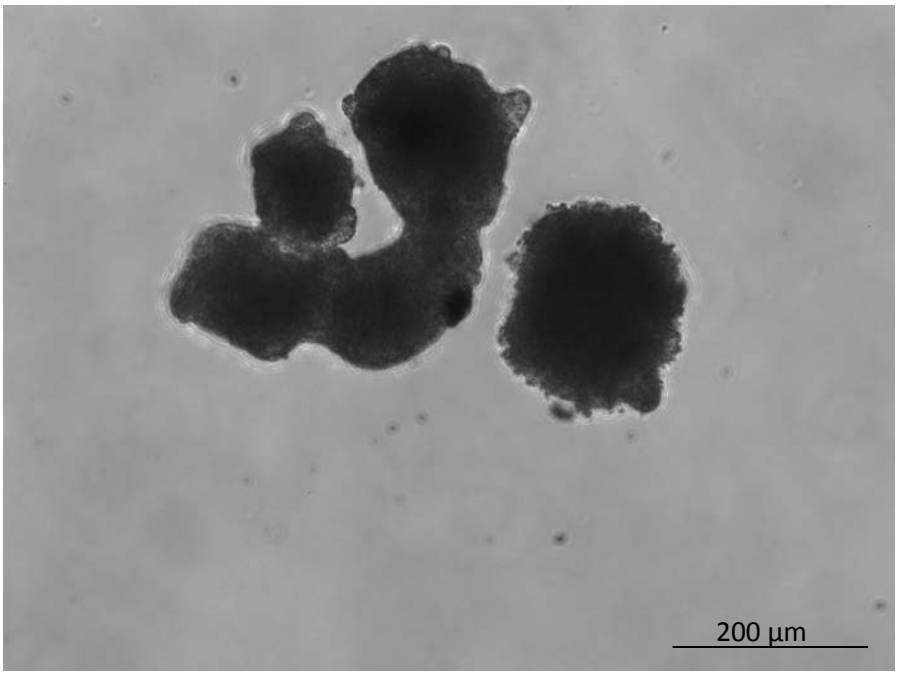

Figure 5.6. Representative rotary orbital shaker suspension culture embryoid bodies created from orbital speeds of 30 rpm.

Spinner Flask Cultures

For E14 αMHC-GFP cells, EBs had formed by day 3. On days 5 and 7, EBs were plated onto a gelatinized dish to check for beating EBs, but these did not beat. Following the addition of retinoic acid on day 9 and G418 on day 11 to the spinner flask and plated EBs, cells did not appear to be dying. No fluorescence was observed in any of the EBs.

EBs had an average area of 25.9 ± 20 x 10^3 μm^2, with a major axis of 179.3 ± 74 µm and a minor axis of 156.5 ± 57 µm (Figure 5.7) (Table 5.1). The circularity index of spinner flask EBs was 0.97 ± 0.1.

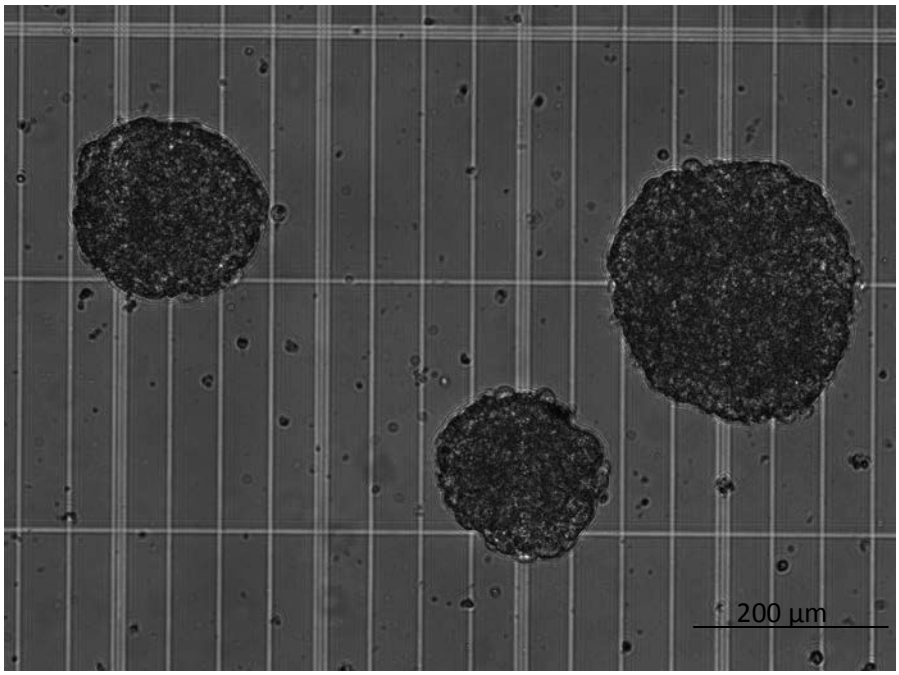

Figure 5.7. Representative spinner flask suspension culture embryoid bodies created by speed setting 60–120 rpm.

Discussion

Scale-up engineering of purified populations of functional cardiomyocytes derived from embryonic stem cells for myocardial regeneration is highly desirable. Such a feat could transform cardiomyocyte transplantation. Determining the most efficient method of generating large numbers of contractile EBs was the goal of this study.

Burridge and partners have developed a highly efficient method for cardiac differentiation from human embryonic stem cells and induced pluripotent stem cells that has eliminated variability across multiple stem cell lines that we have applied here in part.[34] Briefly, their method allowed for uniform growth of cells before forced aggregation on day 0 to allow mesoderm induction and EB formation, followed by

growth factor removal on day 2 to allow cardiac specification, followed by adhesion on day 4 while the cardiomyocytes developed further for contraction on day 7, with maximum percentage of contraction by day 9. We adopted some of their method (2 days in hanging drop, 2 days in suspension before attachment) to our murine E14 αMHC-GFP stem cell line that also increased our efficiency in differentiating cardiomyocytes.

Chemically defined medium affects contracting EB efficiency. The addition of insulin on days 0–2 and its subsequent removal on days 2–4 was a critical component of EB formation; insulin was found to completely inhibit cardiac specification by day 3 by Burridge and associates.[34] They also determined that the addition of 25 ng/ml BMP4 and 5 ng/ml FGF2 on days 2–4 increased differentiation efficiency.[34] It was also established that 400 µM MTG was optimal, but the addition of 2-mercaptoethanol resulted in nearly 0% of contracting EBs on day 9; this concurs with our results where EBs in our second media formulation (DMEM supplemented with 15% FBS, 1% PS, and MTG, 450 µM)) containing MTG not only yielded larger EBs, but also survived the adhesion phase. Although L-ascorbic acid was found to have a detrimental effect on human embryoid body (hEB) contraction by Burridge and collaborators, we used it in our media formulation (IMDM supplemented with 15% FBS, ascorbic acid, L-glutamine, ITS, MTG, and transferrin) since many other groups have found ascorbic acid to have an increase in differentiation efficiency.[35-38] Although high doses may have teratogenic effects,[39] many groups have also found that the time- and concentration-dependent addition of all-trans retinoic acid (RA) accelerates expression of cardiac-specific genes,

promoting cardiomyocyte differentiation, proliferation, and survival and prohibiting undifferentiated cell proliferation.[33,39-42] Zandstra and coworkers found that the addition of RA to large flasks of bulk stirred suspension cultures of cardiac promoter-driven differentiation of cells with antibiotic resistance yielded twice as many cardiomyocytes as those without RA treatment.[40]

Additionally, the mesoderm induction by aggregation of the cells may be accelerated by forced aggregation (e.g., centrifugation).[34] Another critical factor that may have affected our efficiency was the number of days following passage to initiation of EB formation. Burridge and colleagues determined that cells that were not grown to confluence made a crucial difference in efficient differentiation.[34] Specifically, cells passaged one day prior to forced aggregation had a 93.8 ± 3.3% success rate for contracting EBs, compared to passage at 2 days (46.9 ± 4.1%) or 3 days (26.0 ± 8.0%). Future studies should incorporate this information.

Although the least efficient and most tedious method, hanging drop formation did reproducibly yield beating cardiomyocytes under both normoxia and hypoxia. Cell culture is usually carried out at atmospheric conditions (20–21% O_2), but oxygen concentrations are considerably lower in vivo.[43] Hypoxic conditions may explain why the EBs generated were larger in size, where larger EBs are favored since it was more likely for the EBs to adhere and differentiate.

The other three methods of differentiation were far less tedious, ably generating large numbers of EBs initially to allow for larger populations of cardiomyocytes. However, these methods did not yield beating EBs in our hands, although EBs were

observed to fluoresce in suspension culture using ultra-low attachment plates, indicating the presence of MHC-positive cells. Nonbeating areas can have highly variable expression of cardiac specific genes,[44,45] and cells that do not beat spontaneously can be paced in vitro.[46] Thus, beating may not matter in the long term (i.e., beyond day 16), but is another indication of cardiomyocyte differentiation beyond fluorescence. Suspension culture using ultra-low attachment plates have more variability in EB size and in the yield of cardiomyocytes depending on the day of differentiation,[38,47,48] but are infinitely preferable, along with rotary suspension culture and spinner flask culture, when large amounts of cardiomyocytes are required, such as for transplantation.

We found that hanging drop formation produced the largest EBs, while the conditions of rotary speed we used generated smaller EBs of varying size for rotary orbital shaker and spinner flask cultures. However, Sargent and colleagues found that the hydrodynamic conditions set by the orbital shaker method can affect EB formation, structure, and differentiation, where greater rotation speeds yielded more EBs with lesser area.[31] The spinner flask created the most round EBs, with a circularity index of 0.97 ± 0.1, followed by hanging drop and rotary culture EBs. On the other hand, Sargent and colleagues were able to produce homogeneously sized, round EBs, depending on the orbital shaker rotary speed.[31] Likewise, the speed of the spinner flask vane controlled uniform EB size formation, and the improved mass transport created by the stirring easily makes this culture scalable.[49] Additionally, the number of days the EBs are cultivated in the spinner flask affect EB diameter size.[50]

Conclusion and Future Directions

The pluripotent and self-renewable capabilities of ESCs and their capacity to avoid immune system complications give ESCs the potential to revolutionize regenerative cell therapy by the possibility of scalable production of functional cardiomyocytes derived from ESCs. Fabrication of a regenerative myocardial patch for post-myocardial infarction remodeling will depend on generating large numbers of cardiomyocytes. Various methods are available for generating functional cardiomyocytes: hanging drop method, suspension culture using low-attachment plates, rotary suspension culture, and spinner flask suspension culture. Although the hanging drop method is the most reproducible, the labor involved in creating individual drops to make each individual EB is unrealistic in producing the numbers of cardiomyocytes necessary for a myocardial patch. Suspension culture using ultra-low attachment plates produces variably sized EBs, which may decrease yield of beating EBs. Rotary suspension and spinner flask suspension cultures are the most cost-effective and allow the least exertion while having the potential to generate large quantities of cardiomyocytes. Future studies should take the formulation and timing of the addition or removal of components in the differentiation medium into careful consideration with the environment in the design of the scaffold-free myocardial patch.

Chapter VI: Conclusions and Future Directions

The goals of this dissertation were 1) to design a cell culture platform that would allow cell monolayers to be mechanically conditioned and subsequently detached without damage, 2) to validate that the functional aspect of the modified platform performs comparably to the unmodified platform, 3) to perform preliminary analysis of the biochemical properties of cell monolayers that have been mechanically conditioned, and 4) to create scalable productions of pure populations of cardiomyocytes derived from embryonic stem cells. Additionally, future generations of cardiac patches may incorporate 1) suicidal cancer cells to recruit angiogenic growth factors and create self-propagating vascular networks and 2) chondroitinase expression to decrease scar formation.

Cell Culture Platform with Mechanical Conditioning and Nondamaging Cellular Detachment

Myocardial infarction (MI), more commonly known as a heart attack, is the blockage of blood supply to the heart, causing tissue damage or death. Current therapies trying to regenerate this tissue have performed direct injections or attached cellular patches. Improper stimulation to these cell suspension injections or patches may cause undesirable remodeling as the surrounding myocardium is mechanically challenged under the stress of MI. A targeted delivery of a cardiac patch to regenerate the myocardium without bulky polymeric scaffolding is desired to avoid issues of

inflammation. Mechanical conditioning to cells prior to implantation can induce protein and ECM secretion that more closely mimics the native tissue.

Devices capable of applying mechanical forces to cells (e.g. stretch) exist, but cellular removal from these devices often results in irreversible damage. Conversely, devices are available that can detach intact cells, but these are inelastic, non-stretchable substrates. We created a cell culture platform that allows for mechanical conditioning and then subsequent nondamaging detachment of those cells.

Modifying silicone culture surfaces of the commercially available BioFlex plate (Flexcell International, Hillsborough, NC), we incorporated thermally responsive copolymers of poly (N-isopropylacrylamide-co-acrylic acid) (P(NIPAAm-co-AAc)) to create an elastic substrate that can also change surface properties with temperature change. P(NIPAAm-co-AAc) is a dense, hydrophobic film that allows cell attachment at 37°C, but is a loose, hydrated network that allows spontaneous cell detachment below 34°C. A copolymer of NIPAAm and 10% w/w acrylic acid (AAc) was conjugated through carbodiimide chemistry to an amine-bonded silicone surface that was swollen with tert-butanol. Excess reagents were removed through several cycles of washing in tert-butanol heated to 30°C, followed by rinses in room temperature water.

Analysis of the copolymer and the surface of the elastic membrane demonstrated properties specific to P(NIPAAm-co-AAc). The lower critical solution temperature (LCST) was determined to be 34°C, which still falls below cell culturing temperature at 37°C. Surface analysis by ATR-FTIR showed peaks characteristic of P(NIPAAm) (1650 nm^{-1}, 3300 nm^{-1}) in greater ratios that that of peaks characteristic of

silicone (1000-1100 nm^{-1}) and polystyrene controls. ESCA analysis showed an increase in the atomic percentage of nitrogen when compared to the commercial amine-bonded silicone surface (0.5 ± 0.1 vs. 1.5 ± 0.4). The contact angle of the modified silicone membrane surface measured below and above LCST showed before washing demonstrated hydrophobic angles for both temperatures (61.87 ± 4.1 at 25°C vs. 62.08 ± 1.6 at 37°C). After washing, the contact angle was hydrophobic at 37°C (66.21 ± 2.8), but became hydrophilic at room temperature (33.45 ± 15.8). The change in contact angle present after washing but not before may have been the result of methyl groups in the tert-butanol used to swell the membrane shielding the hydrophilic groups in P(NIPAAm-co-AAc).

Cells were able to attach to the resulting surfaces at 37°C and showed detachment by rounded morphology at 25°C. Focal adhesions on the unmodified silicone surfaces remained and did not show a discernible change in cell shape with a change in temperature. Cells showed no discernible differences in morphology when comparing the unmodified and modified silicone surfaces. Following mechanical stretching, cells showed alignment in the direction perpendicular to the strain and were still able to spontaneously detach from the modified silicone surfaces with temperature change.

Functional Comparison of Unmodified and Thermoresponsive Copolymer Modified Bioreactor

Cellular replacement therapy for vascular tissue engineering depends on understanding the effects of the mechanical forces on the vascular system. If we can manipulate the differentiation of vascular cells, we can treat atherosclerotic vascular disease, and there is great potential in the future of tissue engineering.

Lining the inner lumen of the blood vessel, endothelial cells are subjected to cyclic strain due to wall distension and shear stress due to frictional force by blood flow. Vascular smooth muscle cells (SMCs) exhibit a more contractile, mature smooth muscle phenotype when exposed to cyclic strain. Interestingly, Cevallos and associates demonstrated that human umbilical vein endothelial cells (HUVECs) can be induced to express smooth muscle cell markers by applying cyclic strain.

Although we can use mechanical conditioning to engineer a vessel with the natural scaffolding of the native environment, fully implantable small diameter grafts without polymer scaffolding cannot be realized without the use of thermoresponsive copolymer P(NIPAAm-co-AAc). At 37°C, cells can attach to P(NIPAAm-co-AAc)-modified surfaces and spontaneously detach from them at room temperature. We modified a bioreactor to allow for cyclic strain to be applied to cell cultures for the fabrication of natural ECM, and then subsequently allow the conditioned monolayer culture to be detached without damage. The pattern formed by the monolayers can be kept with precise control and can then be rolled up to form a vascular graft. In this study, we

replicate the experiments performed by Cevallos and collaborators to demonstrate that our modified cell culture bioreactor can perform comparably to the unmodified bioreactor while also allowing complete cellular recovery without damage.

Human umbilical vascular endothelial cells (HUVECs) were cultured on unmodified and P(NIPAAm)-modified plates and subjected to 10% elongation strain at 1 Hz for 48 hrs. Total RNA was isolated using Trizol for RT-PCR, and total protein was isolated using RIPA buffer for Western blot analysis. Cells were immunostained for SM22-α. Cell sheets were stained with two different phallotoxins to demonstrate complex layering and maintenance of structure.

Cells on both unmodified and modified plates exhibited the same morphology for static cultures and cultures cyclically strained at 10%. Static HUVECs showed random organization and shape, while conditioned HUVECs were arranged in parallel perpendicular to the direction of strain. mRNA expression, however, was contradictory to the original study, but SM22-α expression exhibited the same morphology on both unmodified and modified plates, with globular patterned cells on static cultures and aligned, elongated cells on strained cultures. We also demonstrated that we can configure the cell sheets such that they form a "herringbone" pattern, in which the alignment of one cell sheet is stacked at a different angle to another aligned cell sheet. The original cell orientations of the individual sheets were maintained after harvest and stacking. The current study performed the same body of work with different results from the original study; however, we were able to demonstrate that we can successfully stretch cell sheets to allow for alignment and then manipulate those cells sheets to

detach from their present surfaces and attach to another cell layer for a cell layer stacking construct.

Future Directions

Although the results obtained in this study contradict the original study, the main goals of maintaining functionality after P(NIPAAm-co-AAc)-modification to the silicone surface and subsequent detachment from that surface with intact cell sheets were achieved. Further data points in RT-PCR experiments and Western blot analysis would help validate the former goal. Additionally, studies in cell viability and proliferation would elucidate the functionality of our product.

Biochemical Properties of Mechanically Conditioned Cell Monolayers

The goal of cell therapy treatment of post-myocardial infarction patients is to regenerate the myocardium to improve function and prevent scarring. Although scaffold-free cell sheets offer an attractive solution, the monolayers are limited by their integrity since the layers cannot match the mechanical force transduction of the myocardium. In this study, we have explored reinforcing the baseline proteins and ECM by stretching immortalized HL-1 mouse cardiomyocytes and embryonic stem cells derived into cardiomyocytes cultured in monolayers before cellular detachment from our bioreactor. Cells were stretched at 3 conditions (5%, 10%, and 19%) along with static controls at 1 Hz for 24 hrs. Total RNA was isolated for RT-PCR, and protein was isolated for Western blot analysis. Masson's Trichrome stain was performed to differentiate

collagen fibers, and Alcian blue/periodic acid-Schiff's reagent stain was used to search for glycosaminoglycans (GAGs).

When HL-1 cells were subjected to 5% cyclic strain, these cells expressed mRNA levels of αMHC and ANF higher than static controls. In comparison, αMHC expression was only slightly increased in 19% cyclically strained cells, and there was a 15.5% decrease in ANF expression from the static control. Connexin 43 expression was approximately the same as static controls for 5% cyclically strained cells, but had a 61.5% decrease in expression in 19% cyclically strained cells. The high magnitude of strain in the hypertrophic region may have overstrained the cells at 19% strain, causing leakage of ANF into the medium and Cx43 bonds to be broken. Sarcomeric actinin mRNA expression was approximately the same as the respective static controls for both stretching conditions.

MHC is characterized by two isoforms, alpha and beta. For the αMHC, protein levels increased 235.2 ± 37%, 256.4 ± 46%, and 17.6 ± 35% for 5%, 10%, and 19% strain, respectively, as compared with a static control, of which only 5% and 10% strain showed a significant increase in protein level. For the βMHC, protein levels increased 22.4 ± 27%, 99.8 ± 19%, and 89.4 ± 20% for 5%, 10%, and 19% strain, respectively, as compared with a static control, of which only 10% and 19% strain showed a significant increase in protein level. Likewise, cardiac contractile protein expression in embryonic stem cell-derived cardiomyocytes showed an increase of 288.7% and 278.4% for αMHC and sarcomeric actinin, respectively. The increase in βMHC with the concomitant decrease of αMHC expression as strain magnitude increased indicates that the cells may have

reverted back to a fetal program. Sarcomeric actinin showed a significant increase in protein level for all three strains, with increases of 194.4 ± 76%, 227.1 ± 61%, and 40.8 ± 19%, respectively. However, these levels differed from the mRNA expression, which remained the same for both 5% and 19% strain as compared to their static controls, indicating that translation may occur independently from transcription levels. Overall, the increase in protein expression in comparison to controls is not as high for cells cyclically stretched at 19% strain as it is for 5% and 10% strains, corroborating that cell monolayers engineered for cardiac patches have an optimal strain to induce secretion of proteins.

In HL-1 cells stretched at 10% as compared to a static control, collagen, muscle fibers, cytoplasm, and keratin protein expression were increased, but not significantly using Masson's Trichrome stain, and GAG, basement membrane, and glycogen expression were increased, but also not significantly using Alcian blue/periodic acid-Schiff's reagent stain. However, the qualitative nature of these stains may require more quantitative methods to verify these findings.

Scaffold-free cell sheets for cardiac patches may be a solution to regenerating myocardium after myocardial infarction, but are limited by integrity for mechanical force transduction that is disparate from the myocardium. In this study, we have investigated stretching cardiomyocytes cultured in monolayers to increase contractile protein and ECM secretion. Overall, mRNA, proteins, and ECM components were found to increase with cell conditioning, but the effective secretion of these proteins may have an optimal strain condition to achieve maximum expression.

Future Directions

We have demonstrated an increase in contractile protein and ECM secretion in cardiomyocytes with induced hypertrophy, and we have shown that there is an optimal strain to achieve maximum secretion of proteins. With this knowledge, we are one step closer to fabricating myocardial patches with natural scaffolding for post-myocardial infarction patients. However, further studies in hypertrophic markers, such as ANF, should be undertaken to further optimize strain parameters. In addition, this study only examined protein secretion after 24 hrs at 1 Hz; further understanding of biochemical secretion would require longer time studies or studies under different stretching frequencies.

Proper induction of mechanical properties via naturally produced proteins and ECM can only be useful if the structure is maintained intact. With the use of our bioreactor, we can condition cell monolayers to stimulate protein production and then detach the layers without enzymatic means. Precise control and attention to cell sheet orientation during layering can help to achieve a patch that is able to regenerate myocardium. The layered control of cell sheets allows for heterogeneous combinations of cell sheets, such as endothelial cells for vasculature. With our bioreactor, we only need a renewable cell source to provide the numbers of cells necessary for a patch.

Although we have demonstrated increase in contractile proteins and ECM with mechanical stimulation, we should also validate that these increases also increase the elasticity of a cell monolayer. Comparisons of nonconditioned and conditioned cell

sheets should be performed to determine the effect of mechanical conditioning on mechanical properties of cell sheets. Such a task is nontrivial, as a device to measure such fragile structures as a single monolayer cell sheet has yet to be conceived.

Additionally, nonconditioned and conditioned layered cell sheet cardiac patches should be implanted into mouse infarct models in a functional study to determine if conditioned patches enhance mechanical function in comparison to nonconditioned patches. Also, because of the alignment of cells, electrical pacing studies should be performed to determine if synchronous electrical conduction capabilities are increased with conditioned cell sheets.

Pure Population Scalable Production of Cardiomyocytes Derived from Embryonic Stem Cells

Cardiomyocytes post-myocardial infarction do not have the capacity to regenerate, leaving potential cell therapies in need of a renewable source of cells. Despite the numerous cell types that have been considered for use in repairing ischemic tissue (e.g., induced pluripotent stem cells, skeletal myoblasts, bone marrow mononuclear cells), embryonic stem cells still may be one of the best options, given the capability to self-renew and the potential in avoiding immune problems.

Cellular sheet engineering allows for fabrication of a patch such that a targeted approach to restoring infarct tissue can be taken. Thermoresponsive polymer poly (N-isopropylacrylamide) (P(NIPAAm)) makes cellular sheet engineering possible, with its ability to allow cell attachment at 37°C and cell detachment at room temperature.

P(NIPAAm) also permits cell-cell and cell-matrix junctions to remain intact, giving the added advantage of allowing for synchronous electrical conduction. Thus, cellular sheets of cells can be cultured, detached intact, and layered to form a scaffold-free myocardial patch. To make the myocardial patch feasible requires large quantities of pure populations of cardiomyocytes, since the presence of undifferentiated cells can cause teratomas. In this study, we examine the effects of culture conditions on cardiomyocyte generation, as well as methods to scale-up production of embryoid bodies to increase the yield of functional cardiomyocytes for the use of regenerative myocardial patches.

E14TG2A cells with the α-myosin heavy chain promoter and green fluorescent protein reporter (E14 αMHC-GFP) and MB1 cells with the αMHC promoter and green fluorescent protein and puromycin resistance fusion gene (MB1 αMHC-EGFP-puro) were differentiated by hanging drop, ultra-low attachment suspension, rotary orbital shaker suspension, or spinner flask suspension cultures. E14 αMHC-GFP embryoid bodies (EBs) began to fluoresce by day 3 and began to beat by day 13 using the hanging drop method under normoxia and hypoxia. MB1 αMHC-EGFP-puro differentiated in ultra-low attachment plates had fluorescent EBs by day 10, but no beating was observed. In my hands, E14 αMHC-GFP EBs differentiated by rotary suspension and spinner flask suspension cultures did not fluoresce or beat. Rotary speed can determine the circularity of formed EBs, where spinner flask culture produced the most reproducible and homogeneous EBs.

Future Directions

Multiple factors can be employed to improve differentiation of functional cardiomyocytes. The addition or removal of components in differentiation media at specific time points can enhance cardiomyocyte differentiation yield. Mesoderm induction during EB formation increases the cardiomyocyte yield, which can be achieved by forced aggregation. Additionally, the numbers of days between passage and EB formation can augment the efficiency in differentiation.

Hanging drop formation was the most reproducible method in making beating EBs under both normoxic and hypoxic conditions, with slightly larger EBs formed under hypoxic conditions. However, the other three methods of differentiation yielded larger initial numbers of EBs, which can increase the final yield of cardiomyocytes. Combining the aforementioned factors with one of these three methods can increase the numbers of cardiomyocytes in a cost-effective and time-efficient manner.

Using Suicidal Cancer Cells to Recruit Angiogenic Factors for Propagating Vascular Networks

The trifecta of tissue engineering is the combination of scaffolding with cells and growth factors to form functional, regenerative tissue. Our proposed cardiac patch may be improved upon with angiogenic and wound healing properties.

Tumors appear to ably recruit a complex network of vascularization to feed the high demand for nutrients. However, it is unknown if tumors recruit these networks through angiogenic factors secreted from the cancerous cells, native cells, or cancerous

cells mimicking native cells. Because the vessel must invaginate, the cell type recruiting the vessels for vascularization should presumably outline the vessel, where the mimicry cell theory would produce a mosaic of both cells.

To determine the mechanism, cancerous cells (A549 and Lewis lung carcinoma (LLC)) were transfected with a hygromycin-thymidine kinase (HyTK) construct, which incorporates positive drug selection resistance (hygromycin) to select for successfully transformed cells and a negative selection suicide gene (thymidine kinase) to kill the remaining cells with ganciclovir (GCV) (antiviral medication used to treat cytomegalovirus infections). Successfully transformed cells were transplanted into a mouse model and allowed to grow into a tumor.

A549 cells had too slow proliferation to form a tumor, so LLCs were transfected with HyTK and selected with hygromycin (400 µg/ml) for 2 weeks. Preliminary death curves with 100 µg/ml hygromycin and increasing concentrations of GCV (0, 0.1, 0.5, 1, 2, 3 µM) were performed. Significant cellular death was observed by visual inspection for concentrations greater than 0.5 µM GCV after 4 days. Successful clones were expanded and resuspended in PBS for injection (10^7 cells) into 2 female C57 and 2 male DR4 mice. On day 4, a tumor about 5 mm in diameter (~108 mm^3 volume) had formed in one of the female C57 mice; the tumor was allowed to grow to 250 mm^3 before starting GCV treatment. By day 12, all 4 mice exhibited tumors or malformations, but were inconsistently shaped and not treated with GCV. Cells were then excised and minced for culture for flow cytometry analysis to test for the surface endothelial marker CD31 (PECAM). FACS, however, yielded no significant results.

Future Directions

Because of the observed variances in tumor formation, a more aggressive cancer cell line may be more suitable for tumor formation. HeLa cells were transfected with HyTK, but the expression was found to be transient. Since broken tumors were observed in the C57 mouse injected with GCV, simultaneous injection of EGFP-positive cells observed under whole mouse cryotomy may reveal cell migration and determine tumor targets while still keeping tumors spatially intact. As a next step in this study, a more consistent tumor model must be found before performing histology on excised tumors treated with GCV.

The implication of using cancerous cells in tissue engineering to create a vascular network before killing the cells is the oxygen and nutrient diffusion between tissues and blood vessels need no longer be limited. In the case of a myocardial patch, the high demand of cardiomyocytes for oxygen and nutrients can be satisfied with a vascular network recruited by suicidal cancer cells.

Decreasing Scar Formation by Chondroitinase Expression

Myocardial infarction is characterized by death of cardiomyocytes and scar tissue formation; a cardiac patch that secretes factors to increase wound healing may be the answer to decreasing scar tissue.

Chondroitin sulfates are glycosaminoglycans found in brain, cartilage, and bone; are compressible; and help maintain cellular shapes. In the event of a central nervous

system injury, scar formation inhibits axonal growth, and chondroitin sulfates are upregulated in these glial scars around the lesion site. Digestion of these chondroitin sulfate chains with chondroitinase ABC (Chase) has successfully shown reinitiation of axonal growth. Produced in the bacterium Proteous vulgaris, Chase has a short half-life.

We inserted the Chase gene into the pSecTag2C vector (Invitrogen), which contains a CMV promoter, a secretion tag for c-myc for detection with the anti-myc antibody, and a gene for zeocin resistance in mammals. The construct was made from inserting the Chase gene into the pSecTag2C vector after cutting with EcoRI. Following ligation, electrocompetent bacteria cells were transformed via electroporation and selected with ampicillin resistance. Restriction enzyme digest analysis was used to check the final plasmid, which was subsequently linearized with AhdI and transfected into 3T3 cells by electroporation (low voltage, 500 V, pulse length 99 μs, 1 pulse). Drug selection with zeocin began 24 hrs after transfection, and colonies were picked on day 9. Media from the cells was sent to the Silver lab for detection of the myc secretion tag, but no indication of its secretion was found.[3] In summary, we have produced a construct that has yet to be proven to perform functionally in cells.

Future Directions

High performance liquid chromatography (HPLC) may be used preliminarily to detect chondroitinase activity. Expression of the full-length chondroitinase gene generates an enzyme that is mostly insoluble, but solubility can be improved by engineering the removal of the hydrophobic N-terminal signal sequence.[1] We speculate

that the enzyme may be present in the tissue medium in its insoluble form. HPLC should resolve non-sulfated and sulfated disaccharides, as well as mono-, di-, and tri-sulfated disaccharides at 210 (undigested CS resolution) and 229 nm (digested CS resolution).[2]

The next step is determining the functionality of the construct. A functional construct may be inserted into a myocardial patch to decrease scar tissue formation following myocardial infarction.

Appendices

Appendix A: *Permssions*

Elaine Lee <elainellee@gmail.com>

Written permission for reprinting in my dissertation
3 messages

Elaine Lee <elaine.lee@case.edu> **Thu, Oct 20, 2011 at 4:47 PM**

To: Tony Mikos <mikos@rice.edu>

Hello Dr Mikos,

I hope this finds you well. We missed seeing you at BMES this year.

I am writing to request permission to reprint the book chapter ("Mechanical Conditioning," chapter 15) in my dissertation. If I need to speak to someone else about this matter, please advise me of that person.

Thank you,
Elaine

--
Elaine Lee
PhD Candidate
Biomedical Engineering
Case Western Reserve University
Work 216-368-4195
Cell 774-234-7237
Email elaine.lee@case.edu
http://bme.case.edu/cdmc/

---

mikos@rice.edu <mikos@rice.edu> **Thu, Oct 20, 2011 at 5:16 PM**

Reply-To: mikos@rice.edu

To: Elaine Lee <elaine.lee@case.edu>

Hi Elaine,

I am not sure I understand your request. Is Chapter 15 the book chapter you wrote for the CRC book? If that's the case you do not need any permission. You may want to acknowledge the reference as a footnote on the first page of the chapter of your thesis.

I am glad to hear you are writing your Ph.D. thesis.

Best wishes,

Tony

Tony Mikos, Ph.D.
Rice University
http://www.ruf.rice.edu/~mikosgrp/

From: Elaine Lee <elaine.lee@case.edu>

Sender: elainellee@gmail.com

Date: Thu, 20 Oct 2011 16:47:19 -0400

To: Tony Mikos<mikos@rice.edu>

Subject: Written permission for reprinting in my dissertation

[Quoted text hidden]

!DSPAM:5181,4ea089ed48341275827253!

Elaine Lee <elaine.lee@case.edu> **Thu, Oct 20, 2011 at 6:01 PM**

To: mikos@rice.edu

Thank you!

--

Elaine Lee
PhD Candidate
Biomedical Engineering
Case Western Reserve University
Work 216-368-4195
Cell 774-234-7237
Email elaine.lee@case.edu
http://bme.case.edu/cdmc/

[Quoted text hidden]

Gmail by Google

Elaine Lee <elainellee@gmail.com>

Permission to include figures in the CRC Biomedical Engineering Handbook, 4th Ed.
3 messages

Elaine Lee <elaine.lee@case.edu> **Fri, Jul 30, 2010 at 4:27 PM**

To: donald.ingber@childrens.harvard.edu

Dear Dr. Ingber:

I am a graduate student writing the book chapter on mechanical conditioning in collaboration with Dr. Horst von Recum from Case Western Reserve University for the CRC's Biomedical Engineering Handbook, 4th Ed. We would like to include Figure 2 from your 2008 review in *Progress in Biophysics and Molecular Biology*, as well as a figure from a symposium given at Subtle Technologies in 2006. (Link to figure)

To fully understand the necessity of mechanical conditioning for tissue engineers, we felt it necessary to discuss cell response to tension with respect to your tensegrity model. Your figures elegantly describe the theory at a glance. We would greatly appreciate the opportunity to include your figures in our chapter.

If you have any questions about our request, please do not hesitate to call or e-mail either Horst (216-368-5513 or horst.vonrecum@case.edu) or myself (774-234-7237 or elaine.lee@case.edu). We look forward to hearing from you.

Warm regards,
Elaine

--
Elaine Lee
PhD Candidate
Biomedical Engineering
Case Western Reserve University

Work 216-368-4195
Cell 774-234-7237
Email elaine.lee@case.edu
http://bme.case.edu/cdmc/

Ingber, Donald Elliott <don.ingber@wyss.harvard.edu> **Sun, Aug 1, 2010 at 6:53 AM**

To: Elaine Lee <elaine.lee@case.edu>, "Nisbet, Jeanne Marie" <jeanne.nisbet@wyss.harvard.edu>

You have my permission, but you require permission from the publishers as well.

Best,
Don

On 7/30/10 4:27 PM, "Elaine Lee" <elaine.lee@case.edu> wrote:

Dear Dr. Ingber:

I am a graduate student writing the book chapter on mechanical conditioning in collaboration with Dr. Horst von Recum from Case Western Reserve University for the CRC's Biomedical Engineering Handbook, 4th Ed. We would like to include Figure 2 from your 2008 review in *Progress in Biophysics and Molecular Biology*, as well as a figure from a symposium given at Subtle Technologies in 2006. (Link to figure <http://www.subtletechnologies.com/2006/symposium/Ingber.html>)

To fully understand the necessity of mechanical conditioning for tissue engineers, we felt it necessary to discuss cell response to tension with respect to your tensegrity model. Your figures elegantly describe the theory at a glance. We would greatly appreciate the opportunity to include your figures in our chapter.

If you have any questions about our request, please do not hesitate to call or e-mail either Horst (216-368-5513 or horst.vonrecum@case.edu) or myself (774-234-7237 or elaine.lee@case.edu). We look forward to hearing from you.

Warm regards,
Elaine

--
Elaine Lee
PhD Candidate
Biomedical Engineering
Case Western Reserve University
Work 216-368-4195
Cell 774-234-7237
Email elaine.lee@case.edu
http://bme.case.edu/cdmc/

Donald E. Ingber, MD,PhD
Director, Wyss Institute for Biologically Inspired Engineering at Harvard University
Judah Folkman Professor of Vascular Biology, Harvard Medical School & Vascular Biology Program, Children's Hospital
Professor of Bioengineering, Harvard School of Engineering and Applied Sciences
Wyss Institute
3 Blackfan Circle, CLSB 5th Floor
Boston MA 02115
ph: 617-432-7044 fax: 617-432-7828
email: don.ingber@wyss.harvard.edu
donald.ingber@childrens.harvard.edu
websites: www.wyss.harvard.edu
www.childrenshospital.org/research/ingber/

Elaine Lee <elaine.lee@case.edu> **Sun, Aug 1, 2010 at 7:49 AM**

To: "Ingber, Donald Elliott" <don.ingber@wyss.harvard.edu>

Cc: "Nisbet, Jeanne Marie" <jeanne.nisbet@wyss.harvard.edu>

Dear Dr. Ingber,

Thank you so much! We wanted to make sure before we sent the necessary paperwork to all parties involved. We'll send it along once it has been prepared by the publisher.

Thank you again!

Warm regards,
Elaine

--
Elaine Lee
PhD Candidate
Biomedical Engineering
Case Western Reserve University
Work 216-368-4195
Cell 774-234-7237
Email elaine.lee@case.edu
http://bme.case.edu/cdmc/

[Quoted text hidden]

Gmail by Google

Elaine Lee <elainellee@gmail.com>

Thank you for your Rightslink / Elsevier order
2 messages

Copyright Clearance Center <rightslink@marketing.copyright.com> **Tue, Aug 3, 2010 at 5:25 PM**

Reply-To: Copyright Clearance Center <reply-fe601779756d067f7015-20206491_HTML-546246414-114453-21072@marketing.copyright.com>

To: elaine.lee@case.edu

To view this email as a web page, go here.

To ensure that you continue to receive our emails,
please add rightslink@marketing.copyright.com to your address book.

Thank You For Your Order!

Dear Elaine,

Thank you for placing your order through Copyright Clearance Center's Rightslink service. Elsevier has partnered with Rightslink to license its content.

Your order details and publisher terms and conditions are available by clicking the link below:
http://s100.copyright.com/CustomerAdmin/PLF.jsp?IID=2010080_1280870670115

Order Details
Licensee: Elaine L Lee
License Date: Aug 03, 2010
License Number: 2481551110115
Publication: Progress in Biophysics and Molecular Biology
Title: Tensegrity-based mechanosensing from macro to micro
Type Of Use: reuse in a book/textbook
Total: 0.00 USD

To access your account, please visit https://myaccount.copyright.com.

Invoices are issued daily and are payable immediately upon receipt.

To ensure we are continuously improving our services, please take a moment to complete our customer satisfaction survey.

B.1:v4.2

+1-877-622-5543 / Tel: +1-978-646-2777
customercare@copyright.com
http://www.copyright.com

This email was sent to: **elaine.lee@case.edu**

Please visit Copyright Clearance Center for more information.

This email was sent by Copyright Clearance Center
222 Rosewood Drive Danvers, MA 01923 USA

To view the privacy policy, please go here.

Elaine Lee <elaine.lee@case.edu> **Tue, Aug 3, 2010 at 5:57 PM**

To: John P Fisher <jpfisher@umd.edu>, Tony Mikos <mikos@rice.edu>

Cc: michael.slaughter@taylorandfrancis.com

Hello Drs. Fisher and Mikos,

Below you will find the permissions for Fig. 2B of our text. The figure from the article that we would like to use is Fig. 2.

Also, to obtain the permissions for the figure from Dr. Grande-Allen, I need to know the print run of the book. Could you please provide me with some assistance?

Last, I am in the process of obtaining the permissions for the 2nd figure from Dr. Ingber, and will keep you posted.

Sincerely,
Elaine

--
Elaine Lee
PhD Candidate
Biomedical Engineering
Case Western Reserve University
Work 216-368-4195

Cell 774-234-7237
Email elaine.lee@case.edu
http://bme.case.edu/cdmc/

[Quoted text hidden]

Gmail by Google

Elaine Lee <elainellee@gmail.com>

Picture permissions
2 messages

Elaine Lee <elaine.lee@case.edu> **Fri, Jul 30, 2010 at 3:58 PM**

To: Jane Grande-Allen <grande@rice.edu>

Hi Jane,

Hope things are going well. We had a couple weeks of hot, humid days -- it felt just like home, but without AC! Good thing that's finally broken, and we're back to nice 80 deg days :)

I wanted to ask you if it would be OK to use a picture of Vishal's culture loading system, either from the article in Tissue Engineering or Annals of Biomedical Engineering. I'm still waiting for the permissions form from the publisher, but it would be for the CRC Biomedical Engineering Handbook, 4th ed. Horst and I are writing the chapter on mechanical conditioning, and we'd really appreciate it! If you have any questions for me, you can either call me or email me back.

Tell everyone I said Hi!

Elaine

--
Elaine Lee
PhD Candidate
Biomedical Engineering
Case Western Reserve University
Work 216-368-4195
Cell 774-234-7237
Email elaine.lee@case.edu

http://bme.case.edu/cdmc/

Jane Grande-Allen <grande@rice.edu> **Fri, Jul 30, 2010 at 6:47 PM**

To: Elaine Lee <elaine.lee@case.edu>

Yes

Sent from my iPhone

[Quoted text hidden]

Gmail by Google

Elaine Lee <elainellee@gmail.com>

Written permission for reproduction in dissertation
3 messages

Elaine Lee <elaine.lee@case.edu> **Thu, Oct 20, 2011 at 4:44 PM**

To: jrnlprodjbma@cadmus.com

Dear Diane Grube:

I am writing to request permission to reprint the article "Cell culture platform with mechanical conditioning and nondamaging cellular detachment" from Journal of Biomedical Materials Research Part A from 2011, volume 93, issue 2, pages 411-8 in my dissertation. If you are the incorrect person to contact, please advise me to whom I should speak.

Thank you,
Elaine

--
Elaine Lee
PhD Candidate
Biomedical Engineering
Case Western Reserve University
Work 216-368-4195
Cell 774-234-7237
Email elaine.lee@case.edu
http://bme.case.edu/cdmc/

Elaine Lee <elaine.lee@case.edu> **Thu, Oct 27, 2011 at 2:40 PM**

To: James.Anderson@case.edu

Dear Dr. Anderson:

I am writing to request permission to reprint the article "Cell culture platform with mechanical conditioning and nondamaging cellular detachment" from Journal of Biomedical Materials Research Part A from 2010, volume 93, issue 2, pages 411-8, which won the Masters Student Award for Outstanding Research, in my dissertation. I contacted the email address given on the JBMR website last week, but haven't heard back yet. If you need any more information, please let me know.

Thank you,
Elaine

--
Elaine Lee
PhD Candidate
Biomedical Engineering
Case Western Reserve University
Work 216-368-4195
Cell 774-234-7237
Email elaine.lee@case.edu
http://bme.case.edu/cdmc/

[Quoted text hidden]

James Anderson <jma6@case.edu> **Thu, Oct 27, 2011 at 2:45 PM**

To: Elaine Lee <elaine.lee@case.edu>

Dear Ms. Lee:

There's no problem with reprinting the article for your dissertation, as long as you

appropriately cite the reference.

With kindest regards,

Bonnie Lou Berry

Assistant to Dr. Anderson

[Quoted text hidden]

Appendix B: *Chapter I References*

Alexander, D. E., K. L. Ratzlaff, R. J. Roggero, and J. S. Hsieh. 1999. Inexpensive, semi-automated system for measuring mechanical properties of soft tissues. J Exp Zoo 284: 374-8.

Alexander, R. S. 1976. Series elasticity of urinary bladder smooth muscle. Am J Physiol 231: 1337-42.

Aufderheide, A. C. and K. A. Athanasiou. 2006. A direct compression stimulator for articular cartilage and meniscal explants. *Ann Biomed Eng* 34**:** 1463-74.

Ayajiki, K., M. Kindermann, M. Hecker, I. Fleming, and R. Busse. 1996. Intracellular pH and tyrosine phosphorylation but not calcium determine shear stress-induced nitric oxide production in native endothelial cells. *Circ Res* 78**:** 750-8.

Bacabac, R. G., T. H. Smit, S. C. Cowin, et al. 2005. Dynamic shear stress in parallel-plate flow chambers. *J Biomech* 38**:** 159-67.

Banes, A., J. Gilbert, D. Taylor, and O. Monbureau. 1985. A new vacuum-operated stress-providing instrument that applies static or variable duration cyclic tension or compression to cells in vitro. *J Cell Sci* 42**:** 35-42.

Benbrahim, A., G. J. L'Italien, B. B. Milinazzo, et al. 1994. A compliant tubular device to study the influences of wall strain and fluid shear stress on cells of the vascular wall. *J Vasc Surg* 20**:** 184-94.

Bett, G. and F. Sachs. 2000. Whole-cell mechanosensitive currents in rat ventricular myocytes activated by direct stimulation. *J Membr Biol* 173**:** 255-263.

Bottlang, M., M. Simnacher, H. Schmitt, R. A. Brand, and L. Claes. 1997. A cell strain system for small homogeneous strain applications. *Biomed Tech (Berl)* 42**:** 305-9.

Brighton, C. T., B. Strafford, S. B. Gross, D. F. Leatherwood, J. L. Williams, and S. R. Pollack. 1991. The proliferative and synthetic response of isolated calvarial bone cells of rats to cyclic biaxial mechanical strain. *J Bone Joint Surg* 73**:** 320-31.

Brown, D. and R. Larson. 2001. Improvements to parallel plate flow chambers to reduce reagent and cellular requirements. *BMC Immunol* 2**:** 9.

Brown, T. D. 2000. Techniques for mechanical stimulation of cells in vitro: a review. *J Biomech* 33**:** 3-14.

Brown, T. D., M. Bottlang, D. R. Pedersen, and A. J. Banes. 1998. Loading paradigms--intentional and unintentional--for cell culture mechanostimulus. *Am J Med Sci* 316**:** 162-8.

Brown, T. D., M. Bottlang, D. R. Pedersen, and A. J. Banes. 2000. Development and experimental validation of a fluid/structure-interaction finite element model of a vacuum-driven cell culture mechanostimulus system. *Comput Methods Biomech Biomed Engin* 3**:** 65-78.

Burton-Wurster, N., M. Vernier-Singer, T. Farquhar, and G. Lust. 1993. Effect of compressive loading and unloading on the synthesis of total protein, proteoglycan, and fibronectin by canine cartilage explants. *J Orthop Res* 11**:** 717-29.

Carpenedo, R. L., C. Y. Sargent, and T. C. McDevitt. 2007. Rotary suspension culture enhances the efficiency, yield, and homogeneity of embryoid body differentiation. *Stem Cells* 25**:** 2224-34.

Carpenter, A. E., T. R. Jones, M. R. Lamprecht, et al. 2006. CellProfiler: image analysis software for identifying and quantifying cell phenotypes. *Genome Biol* 7: R100.

Chamson, A., F. Sudre, C. Le Guen, J. Le, A. Rattner, and J. Frey. 1997. Morphological alteration of fibroblasts mechanically stressed in a collagen lattice. *Arch Dermatol Res* 289**:** 596-9.

Chen, C. S., M. Mrksich, S. Huang, G. M. Whitesides, and D. E. Ingber. 1997. Geometric control of cell life and death. *Science* 276**:** 1425-8.

Chen, X., H. Xu, C. Wan, M. McCaigue, and G. Li. 2006. Bioreactor expansion of human adult bone marrow-derived mesenchymal stem cells. *Stem Cells* 24**:** 2052-9.

Chiquet, M., M. Matthisson, M. Koch, M. Tannheimer, and R. Chiquet-Ehrismann. 1996. Regulation of extracellular matrix synthesis by mechanical stress. *Biochem Cell Biol* 74**:** 737-44.

Chiquet, M., V. Tunc-Civelek, and A. Sarasa-Renedo. 2007. Gene regulation by mechanotransduction in fibroblasts. *Appl Physiol Nutr Metab* 32**:** 967-73.

Chokalingam, K., N. Juncosa-Melvin, S. A. Hunter, et al. 2009. Tensile stimulation of murine stem cell-collagen sponge constructs increases collagen type I gene expression and linear stiffness. *Tissue Eng Part A* 15: 2561-70.

Cormier, J. T., N. I. zur Nieden, D. E. Rancourt, and M. S. Kallos. 2006. Expansion of undifferentiated murine embryonic stem cells as aggregates in suspension culture bioreactors. *Tissue Eng* 12**:** 3233-45.

Coucouvanis, E. and G. R. Martin. 1995. Signals for death and survival: a two-step mechanism for cavitation in the vertebrate embryo. *Cell* 83**:** 279-87.

Dahlmann-Noor, A. H., B. Martin-Martin, M. Eastwood, P. T. Khaw, and M. Bailly. 2007. Dynamic protrusive cell behaviour generates force and drives early matrix contraction by fibroblasts. *Exp Cell Res* 313**:** 4158-69.

Dang, S. M., M. Kyba, R. Perlingeiro, G. Q. Daley, and P. W. Zandstra. 2002. Efficiency of embryoid body formation and hematopoietic development from embryonic stem cells in different culture systems. *Biotechnol Bioeng* 78**:** 442-53.

De Witt, M. T., C. J. Handley, B. W. Oakes, and D. A. Lowther. 1984. In vitro response of chondrocytes to mechanical loading. The effect of short term mechanical tension. *Connect Tissue Res* 12: 97-109.

Eastwood, M., D. A. McGrouther, and R. A. Brown. 1994. A culture force monitor for measurement of contraction forces generated in human dermal fibroblast cultures: evidence for cell-matrix mechanical signalling. *Biochim Biophys Acta* 1201**:** 186-92.

Egerbacher, M., S. P. Arnoczky, O. Caballero, M. Lavagnino, and K. L. Gardner. 2008. Loss of homeostatic tension induces apoptosis in tendon cells: an in vitro study. *Clin Orthop Relat Res* 466**:** 1562-8.

Einav, S., C. Dewey, and H. Hartenbaum. 1994. Cone-and-plate apparatus: a compact system for studying well-characterized turbulent flow fields. *Experiments in Fluids* 16**:** 196-202.

Ellis, E. F., J. S. McKinney, K. A. Willoughby, S. Liang, and J. T. Povlishock. 1995. A new model for rapid stretch-induced injury of cells in culture: characterization of the model using astrocytes*. J Neurotrauma* 12: 325-39.

Engelmayr Jr., G. C., L. Soletti, S. C. Vigmostad, et al. 2008. A novel flex-stretch-flow bioreactor for the study of engineered heart valve tissue mechanobiology. *Ann Biomed Eng* 36**:** 700-12.

Fan, J. and K. B. Walsh. 1999. Mechanical stimulation regulates voltage-gated potassium currents in cardiac microvascular endothelial cells. *Circ Res* 84**:** 451-7.

Felix, J. A., M. L. Woodruff, and E. R. Dirksen. 1996. Stretch increases inositol 1,4,5-trisphosphate concentration in airway epithelial cells. *Am J Respir Cell Mol Biol* 14**:** 296-301.

Fletcher, D. A. and R. D. Mullins. 2010. Cell mechanics and the cytoskeleton. *Nature* 463**:** 485-92.

Forth, K. E. and C. S. Layne. 2008. Neuromuscular responses to mechanical foot stimulation: the influence of loading and postural context. *Aviat Space Environ Med* 79: 844-51.

Gerecht-Nir, S., S. Cohen, and J. Itskovitz-Eldor. 2004. Bioreactor cultivation enhances the efficiency of human embryoid body (hEB) formation and differentiation. *Biotechnol Bioeng* 86**:** 493-502.

Gilbert, J. A., A. J. Banes, G. W. Link, and G. L. Jones. 1990. Video analysis of membrane strain: an application in cell stretching. *Experimental Techniques* 14**:** 43-5.

Gilbert, J. A., P. S. Weinhold, A. J. Banes, G. W. Link, and G. L. Jones. 1994. Strain profiles for circular cell culture plates containing flexible surfaces employed to mechanically deform cells in vitro. *J Biomech* 27**:** 1169-77.

Gooch, K. J. and C. J. Tennant. 1997. *Mechanical Forces: Their Effects on Cells and Tissues.* New York: Springer.

Gov, N. 2009. Traction forces during collective cell motion. *HFSP J* 3**:** 223-7.

Grande-Allen, K. J., A. Calabro, V. Gupta, T. N. Wight, V. C. Hascall, and I. Vesely. 2004. Glycosaminoglycans and proteoglycans in normal mitral valve leaflets and chordae: association with regions of tensile and compressive loading. *Glycobiology* 14: 621-33.

Guilak, F., D. M. Cohen, B. T. Estes, J. M. Gimble, W. Liedtke, and C. S. Chen. 2009. Control of stem cell fate by physical interactions with the extracellular matrix. *Cell stem cell* 5**:** 17-26.

Guilak, F., B. C. Meyer, A. Ratcliffe, and V. C. Mow. 1994. The effects of matrix compression on proteoglycan metabolism in articular cartilage explants. *Osteoarthritis Cartilage* 2**:** 91-101.

Gupta, V. and K. J. Grande-Allen. 2006. Effects of static and cyclic loading in regulating extracellular matrix synthesis by cardiovascular cells. *Cardiovasc Res* 72: 375-83.

Gupta, V., J. A. Werdenberg, T. L. Blevins, and K. J. Grande-Allen. 2007. Synthesis of glycosaminoglycans in differently loaded regions of collagen gels seeded with valvular interstitial cells. *Tissue Eng* 13**:** 41-9.

Gupta, V., J. A. Werdenberg, B. D. Lawrence, J. S. Mendez, E. H. Stephens, and K. J. Grande-Allen. 2008. Reversible secretion of glycosaminoglycans and proteoglycans by cyclically stretched valvular cells in 3D culture. *Ann Biomed Eng* 36**:** 1092-103.

Gustafson, K. J., J. D. Sweeney, J. Gibney, and L. A. Fiebig-Mathine. 2006. Performance of dynamic and isovolumetric trained skeletal muscle ventricles. *J Surg Res* 134: 198-204.

Hasegawa, S., S. Sato, S. Saito, Y. Suzuki, and D. Brunette. 1985. Mechanical stretching increases the number of cultured bone cells synthesizing DNA and alters their pattern of protein synthesis. *Calcif Tissue Int* 37**:** 431-6.

Hasel, C., S. Dürr, S. Brüderlein, I. Melzner, and P. Möller. 2002. A cell-culture system for long-term maintenance of elevated hydrostatic pressure with the option of additional tension. *J Biomech* 35**:** 579-84.

Heiner, A. and J. Martin. 2004. Cartilage responses to a novel triaxial mechanostimulatory culture system. *J Biomech* 37**:** 689-95.

Huang, S., C. S. Chen, and D. E. Ingber. 1998. Control of cyclin D1, p27(Kip1), and cell cycle progression in human capillary endothelial cells by cell shape and cytoskeletal tension. *Mol Biol Cell* 9**:** 3179-93.

Huang, S. and D. E. Ingber. 2000. Shape-dependent control of cell growth, differentiation, and apoptosis: switching between attractors in cell regulatory networks. *Experiment Cell Res* 261**:** 91-103.

Hung, C. T. and J. L. Williams. 1994. A method for inducing equi-biaxial and uniform strains in elastomeric membranes used as cell substrates. *J Biomech* 27**:** 227-32.

Ingber, D. E. 2008a. Tensegrity-based mechanosensing from macro to micro. *Prog Biophys Mol Biol* 97**:** 163-79.

Ingber, D. E. 2008b. Tensegrity and mechanotransduction. *J Bodyw Mov Ther* 12**:** 198-200.

Ingber, D. E. 2010. From cellular mechanotransduction to biologically inspired engineering. *Ann Biomed Eng* 38**:** 1148-61.

Ishibashi, Y., H. Tsutsui, S. Yamamoto, et al. 1996. Role of microtubules in myocyte contractile dysfunction during cardiac hypertrophy in the rat. *Am J Physiol* 271**:** H1978-87.

Ives, C. L., S. G. Eskin, and L. V. McIntire. 1986. Mechanical effects on endothelial cell morphology: in vitro assessment. *In Vitro Cell Dev Biol* 22: 500-7.

Jessop, H. L., S. C. F. Rawlinson, A. A. Pitsillides, and L. E. Lanyon. 2002. Mechanical strain and fluid movement both activate extracellular regulated kinase (ERK) in osteoblast-like cells but via different signaling pathways. *Bone* 31**:** 186-94.

Jones, D. B., H. Nolte, J. G. Scholübbers, E. Turner, and D. Veltel. 1991. Biochemical signal transduction of mechanical strain in osteoblast-like cells. *Biomaterials* 12**:** 101-10.

Kandlikar, S. G., S. Garimella, D. Li, S. Colin, and M. R. King. 2006. *Heat transfer and fluid flow in minichannels and microchannels.* Kidlington, Oxford: Elsevier.

Kappagoda, C. T. and K. Ravi. 2006. The rapidly adapting receptors in mammalian airways and their responses to changes in extravascular fluid volume. *Experiment Physiol* 91**:** 647-54.

Keller, G. M. 1995. In vitro differentiation of embryonic stem cells. *Curr Opin Cell Biol* 7**:** 862-9.

Kim, S. and H. A. von Recum. 2009. Endothelial progenitor populations in differentiating embryonic stem cells I: Identification and differentiation kinetics. *Tissue Eng Part A* 15**:** 3709-18.

Kim, S. and H. A. von Recum. 2010. Endothelial progenitor populations in differentiating embryonic stem cells. II. Drug selection and functional characterization. *Tissue Eng Part A* 16**:** 1065-74.

Komuro, I., T. Kaida, Y. Shibazaki, et al. 1990. Stretching cardiac myocytes stimulates protooncogene expression. *J Biol Chem* 265: 3595-8.

Lambert, C. A., E. P. Soudant, B. V. Nusgens, and C. M. Lapière. 1992. Pretranslational regulation of extracellular matrix macromolecules and collagenase expression in fibroblasts by mechanical forces. *Lab Invest* 66**:** 444-51.

Lammi, M. J., R. Inkinen, J. J. Parkkinen, et al. 1994. Expression of reduced amounts of structurally altered aggrecan in articular cartilage chondrocytes exposed to high hydrostatic pressure. *Biochem J* 304 723-30.

Lau, E., S. Al-Dujaili, A. Guenther, D. Liu, L. Wang, and L. You. 2010. Effect of low-magnitude, high-frequency vibration on osteocytes in the regulation of osteoclasts. *Bone* 46**:** 1508-15.

Lavagnino, M., S. P. Arnoczky, E. Kepich, O. Caballero, and R. C. Haut. 2008. A finite element model predicts the mechanotransduction response of tendon cells to cyclic tensile loading. *Biomech Model Mechanobiol* 7**:** 405-16.

Lee, E. L. and H. A. von Recum. 2010. Cell culture platform with mechanical conditioning and nondamaging cellular detachment. *J Biomed Mater Res A* 93**:** 411-8.

Leung, D. Y., S. Glagov, and M. B. Mathews. 1977. A new in vitro system for studying cell response to mechanical stimulation. Different effects of cyclic stretching and agitation on smooth muscle cell biosynthesis. *Experiment Cell Res* 109: 285-98.

Li, H., H.-S. Yang, T.-J. Wu, et al. 2010. Proteomic analysis of early-response to mechanical stress in neonatal rat mandibular condylar chondrocytes. *J Cell Physiol* 223**:** 610-22.

Maltsev, V. A., A. M. Wobus, J. Rohwedel, M. Bader, and J. Hescheler. 1994. Cardiomyocytes differentiated in vitro from embryonic stem cells developmentally express cardiac-specific genes and ionic currents. *Circ Res* 75**:** 233-44.

Martinac, B. 2004. Mechanosensitive ion channels: molecules of mechanotransduction. *J Cell Sci* 117**:** 2449-60.

Matsuo, T., H. Uchida, and N. Matsuo. 1996. Bovine and porcine trabecular cells produce prostaglandin F2 alpha in response to cyclic mechanical stretching. *Jpn J Ophthalmol.* 40**:** 289-96.

Maul, T. M., D. W. Hamilton, A. Nieponice, L. Soletti, and D. A. Vorp. 2007. A new experimental system for the extended application of cyclic hydrostatic pressure to cell culture. *J Biomech Eng* 129**:** 110-6.

Meikle, M. C., J. J. Reynolds, a. Sellers, and J. T. Dingle. 1979. Rabbit cranial sutures in vitro: a new experimental model for studying the response of fibrous joints to mechanical stress*. Calcif Tissue Int* 28: 137-44.

Moore, J. E., E. Bürki, a. Suciu, et al. 1994. A device for subjecting vascular endothelial cells to both fluid shear stress and circumferential cyclic stretch. *Ann Biomed Eng* 22**:** 416-22.

Murray, D. and N. Rushton. 1990. The effect of strain on bone cell prostaglandin E 2 release: a new experimental method. *Calcif Tissue Int* 47: 35-9.

Myers, K. A., J. B. Rattner, N. G. Shrive, and D. A. Hart. 2007. Hydrostatic pressure sensation in cells: integration into the tensegrity model. *Biochem Cell Biol* 85**:** 543-51.

Nagatomi, J., B. P. Arulanandam, D. W. Metzger, A. Meunier, and R. Bizios. 2002. Effects of cyclic pressure on bone marrow cell cultures. *J Biomech Eng* 124**:** 308-14.

Neidlinger-Wilke, C., A. Liedert, K. Wuertz, et al. 2009. Mechanical stimulation alters pleiotrophin and aggrecan expression by human intervertebral disc cells and influences their capacity to stimulate endothelial migration. *Spine* 34: 663-9.

Neidlinger-Wilke, C., H. J. Wilke, and L. Claes. 1994. Cyclic stretching of human osteoblasts affects proliferation and metabolism: a new experimental method and its application. *J Orthop Res* 12: 70-8.

Ng, E., R. Davis, L. Azzola, E. Stanley, and A. Elefanty. 2005. Forced aggregation of defined numbers of human embryonic stem cells into embryoid bodies fosters robust, reproducible hematopoietic differentiation. *Blood* 106**:** 1601-3.

Nishimura, S., S. Nagai, M. Katoh, et al. 2006. Microtubules modulate the stiffness of cardiomyocytes against shear stress. *Circ Res* 98**:** 81-7.

Nishimura, S., K. Seo, M. Nagasaki, et al. 2008. Responses of single-ventricular myocytes to dynamic axial stretching. *Prog Biophys Mol Biol* 97**:** 282-97.

Norton, L. A., K. L. Andersen, D. Arenholt-Bindslev, L. Andersen, and B. Melsen. 1995. A methodical study of shape changes in human oral cells perturbed by a simulated orthodontic strain in vitro. *Arch Oral Biol* 40**:** 863-72.

Okano, T., N. Yamada, H. Sakai, and Y. Sakurai. 1993. A novel recovery system for cultured cells using plasma-treated polystyrene dishes grafted with poly(N-isopropylacrylamide). *J Biomed Mater Res* 27**:** 1243-51.

Orr, D. E. and K. J. L. Burg. 2008. Design of a modular bioreactor to incorporate both perfusion flow and hydrostatic compression for tissue engineering applications. *Ann Biomed Eng* 36**:** 1228-41.

Ozawa, H., K. Imamura, E. Abe, et al. 1990. Effect of a continuously applied compressive pressure on mouse osteoblast-like cells (MC3T3-E1) in vitro. *J Cell Physiol* 142**:** 177-85.

Ozerdem, B. and A. Tözeren. 1995. Physical response of collagen gels to tensile strain. *J Biomech Eng* 117: 397-401.

Palatinus, J. A., J. M. Rhett, and R. G. Gourdie. 2010. Translational lessons from scarless healing of cutaneous wounds and regenerative repair of the myocardium. *J Mol Cell Cardiol* 48**:** 550-7.

Parker, K. K., A. L. Brock, C. Brangwynne, et al. 2002. Directional control of lamellipodia extension by constraining cell shape and orienting cell tractional forces. *FASEB J* 16**:** 1195-204.

Parkkinen, J. J., M. J. Lammi, R. Inkinen, et al. 1995. Influence of short-term hydrostatic pressure on organization of stress fibers in cultured chondrocytes. *J Orthop Res* 13**:** 495-502.

Pitsillides, A., S. Rawlinson, R. Suswillo, and S. Bourrin. 1995. Mechanical strain-induced NO production by bone cells: a possible role in adaptive bone (re) modeling? *FASEB J* 9**:** 1614-22.

Polte, T. R., G. S. Eichler, N. Wang, and D. E. Ingber. 2004. Extracellular matrix controls myosin light chain phosphorylation and cell contractility through modulation of cell shape and cytoskeletal prestress. *Am J Physiol Cell Physiol* 286**:** C518-28.

Potier, E., J. Noailly, and K. Ito. 2010. Directing bone marrow-derived stromal cell function with mechanics. *J Biomech* 43**:** 807-817.

Pugin, J., I. Dunn, P. Jolliet, et al. 1998. Activation of human macrophages by mechanical ventilation in vitro. *Am J Physiol* 275**:** L1040-50.

Rana, O. R., C. Zobel, E. Saygili, et al. 2008. A simple device to apply equibiaxial strain to cells cultured on flexible membranes. *Am J Physiol Heart Circ Physiol* 294**:** H532-40.

Robling, A. G., D. B. Burr, and C. H. Turner. 2001. Recovery periods restore mechanosensitivity to dynamically loaded bone. *J Experiment Biol* 204**:** 3389-99.

Russell, B., D. Motlagh, and W. W. Ashley. 2000. Form follows function: how muscle shape is regulated by work. *J App Physiol* 88**:** 1127-32.

Sarasa-Renedo, A. and M. Chiquet. 2005. Mechanical signals regulating extracellular matrix gene expression in fibroblasts. *Scand J Med Sci Sports* 15**:** 223-30.

Sargent, C. Y., G. Y. Berguig, M. A. Kinney, et al. 2010. Hydrodynamic modulation of embryonic stem cell differentiation by rotary orbital suspension culture. *Biotechnol Bioeng* 105**:** 611-26.

Schaffer, J. L., M. Rizen, G. J. L'Italien, et al. 1994. Device for the application of a dynamic biaxially uniform and isotropic strain to a flexible cell culture membrane. *J Orthop Res* 12**:** 709-19.

Shaikh, F. M., T. P. O'Brien, A. Callanan, et al. 2010. New pulsatile hydrostatic pressure bioreactor for vascular tissue-engineered constructs. *Artif Organs* 34**:** 153-8.

Shimizu, T., H. Sekine, Y. Isoi, M. Yamato, A. Kikuchi, and T. Okano. 2006. Long-term survival and growth of pulsatile myocardial tissue grafts engineered by the layering of cardiomyocyte sheets. *Tissue Eng* 12**:** 499-507.

Shimko, V. F. and W. C. Claycomb. 2008. Effect of mechanical loading on three-dimensional cultures of embryonic stem cell-derived cardiomyocytes. *Tissue Eng Part A* 14**:** 49-58.

Sims, J. R., S. Karp, and D. E. Ingber. 1992. Altering the cellular mechanical force balance results in integrated changes in cell, cytoskeletal and nuclear shape. *J Cell Sci* 103**:** 1215-22.

Singhvi, R., A. Kumar, G. P. Lopez, et al. 1994. Engineering cell shape and function. *Science* 264**:** 696-8.

Sumpio, B. E., M. D. Widmann, J. Ricotta, M. A. Awolesi, and M. Watase. 1994. Increased ambient pressure stimulates proliferation and morphologic changes in cultured endothelial cells. *J Cell Physiol* 158**:** 133-9.

Tagawa, H., M. Koide, H. Sato, M. R. Zile, B. A. Carabello, and G. Cooper IV. 1998. Cytoskeletal role in the transition from compensated to decompensated hypertrophy during adult canine left ventricular pressure overloading. *Circ Res* 82**:** 751-61.

Tanck, E., W. D. van Driel, J. W. Hagen, E. H. Burger, L. Blankevoort, and R. Huiskes. 1999. Why does intermittent hydrostatic pressure enhance the mineralization process in fetal cartilage? *J Biomech* 32**:** 153-61.

Tomasek, J. J., C. J. Haaksma, R. J. Eddy, and M. B. Vaughan. 1992. Fibroblast contraction occurs on release of tension in attached collagen lattices: dependency on an organized actin cytoskeleton and serum. *Anat Rec* 232**:** 359-68.

Torzilli, P. A., R. Grigiene, C. Huang, et al. 1997. Characterization of cartilage metabolic response to static and dynamic stress using a mechanical explant test system. *J Biomech* 30**:** 1-9.

Trepat, X., L. Deng, S. S. An, et al. 2007. Universal physical responses to stretch in the living cell. *Nature* 447**:** 592-5.

Tsutsui, H., K. Ishihara, and G. Cooper IV. 1993. Cytoskeletal role in the contractile dysfunction of hypertrophied myocardium. *Science* 260**:** 682-7.

van Wamel, J. E., C. Ruwhof, E. J. van der Valk-Kokshoorn, P. I. Schrier, and A. van der Laarse. 2000. Rapid gene transcription induced by stretch in cardiac myocytes and fibroblasts and their paracrine influence on stationary myocytes and fibroblasts. *Pflugers Arch* 439**:** 781-8.

Vandenburgh, H. H. and P. Karlisch. 1989. Longitudinal growth of skeletal myotubes in vitro in a new horizontal mechanical cell stimulator. *In Vitro Cell Dev Biol* 25**:** 607-16.

Villemure, I. and I. A. Stokes. 2009. Growth plate mechanics and mechanobiology. A survey of present understanding. *J Biomech* 42**:** 1793-803.

Wang, H., L. Huang, M. Qu, et al. 2006a. Shear stress protects against endothelial regulation of vascular smooth muscle cell migration in a coculture system. *Endothelium* 2**:** 171-80.

Wang, X., G. Wei, W. Yu, Y. Zhao, X. Yu, and X. Ma. 2006b. Scalable producing embryoid bodies by rotary cell culture system and constructing engineered cardiac tissue with ES-derived cardiomyocytes in vitro. *Biotechnol Prog* 22**:** 811-8.

Wang, Y., Z. Zhao, Y. Li, et al. 2010. Up-regulated alpha-actin expression is associated with cell adhesion ability in 3-D cultured myocytes subjected to mechanical stimulation. *Mol Cell Biochem* 338**:** 175-81.

Williams, J. L., J. H. Chen, and D. M. Belloli. 1992. Strain fields on cell stressing devices employing clamped circular elastic diaphragms as substrates. *J Biomech Eng* 114**:** 377-84.

Winston, F. K., E. J. Macarak, S. F. Gorfien, and L. E. Thibault. 1989. A system to reproduce and quantify the biomechanical environment of the cell. *J App Physiol* 67**:** 397-405.

Wright, M., P. Jobanputra, C. Bavington, D. M. Salter, and G. Nuki. 1996. Effects of intermittent pressure-induced strain on the electrophysiology of cultured human chondrocytes: evidence for the presence of stretch-activated membrane ion channels. *Clin Sci (London)* 90**:** 61-71.

Yeung, T., P. C. Georges, L. A. Flanagan, et al. 2005. Effects of substrate stiffness on cell morphology, cytoskeletal structure, and adhesion. *Cell Motil Cytoskeleton* 60**:** 24-34.

Zandstra, P. W., C. Bauwens, T. Yin, et al. 2003. Scalable production of embryonic stem cell-derived cardiomyocytes. *Tissue Eng* 9**:** 767-78.

Zile, M. R., M. Koide, H. Sato, et al. 1999. Role of microtubules in the contractile dysfunction of hypertrophied myocardium. *J Am Coll Cardiol* 33**:** 250-60.

Appendix C: ***Chapter II References***

1. Tam CS, Khouri I. The role of stem cell transplantation in the management of chronic lymphocytic leukaemia. Hematol Oncol 2009;27(2):53-60.
2. Shimizu T, Sekine H, Yamato M, Okano T. Cell sheet-based myocardial tissue engineering: new hope for damaged heart rescue. Curr Pharm Des 2009;15(24):2807-14.
3. Duncan AW, Dorrell C, Grompe M. Stem cells and liver regeneration. Gastroenterology 2009;137(2):466-81.
4. Borlongan CV. Cell therapy for stroke: remaining issues to address before embarking on clinical trials. Stroke 2009;40(3 Suppl):S146-8.
5. Siniscalco D, Sullo N, Maione S, Rossi F, D'Agostino B. Stem cell therapy: the great promise in lung disease. Ther Adv Respir Dis 2008;2(3):173-7.
6. Flores MG, Hasegawa M, Yamato M, Takagi R, Okano T, Ishikawa I. Cementum-periodontal ligament complex regeneration using the cell sheet technique. J Periodontal Res 2008;43(3):364-71.
7. Al Mheid I, Quyyumi AA. Cell therapy in peripheral arterial disease. Angiology 2008;59(6):705-16.
8. Yang J, Yamato M, Nishida K, Hayashida Y, Shimizu T, Kikuchi A, Tano Y, Okano T. Corneal epithelial stem cell delivery using cell sheet engineering: not lost in transplantation. J Drug Target 2006;14(7):471-82.

9. Chiquet M, Matthisson M, Koch M, Tannheimer M, Chiquet-Ehrismann R. Regulation of extracellular matrix synthesis by mechanical stress. Biochem Cell Biol 1996;74(6):737-44.

10. Chiquet M, Tunc-Civelek V, Sarasa-Renedo A. Gene regulation by mechanotransduction in fibroblasts. Appl Physiol Nutr Metab 2007;32(5):967-73.

11. Sarasa-Renedo A, Chiquet M. Mechanical signals regulating extracellular matrix gene expression in fibroblasts. Scand J Med Sci Sports 2005;15(4):223-30.

12. Chiquet M, Renedo AS, Huber F, Fluck M. How do fibroblasts translate mechanical signals into changes in extracellular matrix production? Matrix Biol 2003;22(1):73-80.

13. Chiquet M. Regulation of extracellular matrix gene expression by mechanical stress. Matrix Biol 1999;18(5):417-26.

14. Harada I, Akaike T. Extracellular matrices as elastic scaffold and mechanical interaction. Biol Sci Space 2004;18(3):120-1.

15. Ingber DE. Mechanical control of tissue morphogenesis during embryological development. Int J Dev Biol 2006;50(2-3):255-66.

16. Shimko VF, Claycomb WC. Effect of Mechanical Loading on Three-Dimensional Cultures of Embryonic Stem Cell-Derived Cardiomyocytes. Tissue Eng 2007.

17. Terraciano V, Hwang N, Moroni L, Park HB, Zhang Z, Mizrahi J, Seliktar D, Elisseeff J. Differential response of adult and embryonic mesenchymal progenitor cells to mechanical compression in hydrogels. Stem Cells 2007;25(11):2730-8.

18. Ward DF, Jr., Salasznyk RM, Klees RF, Backiel J, Agius P, Bennett K, Boskey A, Plopper GE. Mechanical strain enhances extracellular matrix-induced gene focusing and promotes osteogenic differentiation of human mesenchymal stem cells through an extracellular-related kinase-dependent pathway. Stem Cells Dev 2007;16(3):467-80.

19. Engelmayr GC, Jr., Sales VL, Mayer JE, Jr., Sacks MS. Cyclic flexure and laminar flow synergistically accelerate mesenchymal stem cell-mediated engineered tissue formation: Implications for engineered heart valve tissues. Biomaterials 2006;27(36):6083-95.

20. Kurpinski K, Li S. Mechanical stimulation of stem cells using cyclic uniaxial strain. J Vis Exp 2007(6):242.

21. Ritchie AC, Wijaya S, Ong WF, Zhong SP, Chian KS. Dependence of alignment direction on magnitude of strain in esophageal smooth muscle cells. Biotechnol Bioeng 2009;102(6):1703-11.

22. Barron V, Brougham C, Coghlan K, McLucas E, O'Mahoney D, Stenson-Cox C, McHugh PE. The effect of physiological cyclic stretch on the cell morphology, cell orientation and protein expression of endothelial cells. J Mater Sci Mater Med 2007;18(10):1973-81.

23. Balachandran K, Konduri S, Sucosky P, Jo H, Yoganathan AP. An ex vivo study of the biological properties of porcine aortic valves in response to circumferential cyclic stretch. Ann Biomed Eng 2006;34(11):1655-65.

24. Balachandran K, Sucosky P, Jo H, Yoganathan AP. Elevated cyclic stretch alters matrix remodeling in aortic valve cusps: implications for degenerative aortic valve disease. Am J Physiol Heart Circ Physiol 2009;296(3):H756-64.

25. Buck RC. Reorientation response of cells to repeated stretch and recoil of the substratum. Exp Cell Res 1980;127(2):470-4.

26. Kada K, Yasui K, Naruse K, Kamiya K, Kodama I, Toyama J. Orientation change of cardiocytes induced by cyclic stretch stimulation: time dependency and involvement of protein kinases. J Mol Cell Cardiol 1999;31(1):247-59.

27. Dartsch PC, Betz E. Response of cultured endothelial cells to mechanical stimulation. Basic Res Cardiol 1989;84(3):268-81.

28. Ives CL, Eskin SG, McIntire LV. Mechanical effects on endothelial cell morphology: in vitro assessment. In Vitro Cell Dev Biol 1986;22(9):500-7.

29. Badylak SF. The extracellular matrix as a scaffold for tissue reconstruction. Semin Cell Dev Biol 2002;13(5):377-83.

30. Eastwood M, McGrouther DA, Brown RA. A culture force monitor for measurement of contraction forces generated in human dermal fibroblast cultures: evidence for cell-matrix mechanical signalling. Biochim Biophys Acta 1994;1201(2):186-92.

31. Kulik TJ, Alvarado SP. Effect of stretch on growth and collagen synthesis in cultured rat and lamb pulmonary arterial smooth muscle cells. J Cell Physiol 1993;157(3):615-24.

32. Lee AA, Delhaas T, Waldman LK, MacKenna DA, Villarreal FJ, McCulloch AD. An equibiaxial strain system for cultured cells. Am J Physiol 1996;271(4 Pt 1):C1400-8.

33. Mitchell SB, Sanders JE, Garbini JL, Schuessler PK. A device to apply user-specified strains to biomaterials in culture. IEEE Trans Biomed Eng 2001;48(2):268-73.

34. von Recum HA, Okano T, Kim SW, Bernstein PS. Maintenance of retinoid metabolism in human retinal pigment epithelium cell culture. Exp Eye Res 1999;69(1):97-107.

35. Okano T, Yamada N, Sakai H, Sakurai Y. A novel recovery system for cultured cells using plasma-treated polystyrene dishes grafted with poly(N-isopropylacrylamide). J Biomed Mater Res 1993;27(10):1243-51.

36. Rollason G, Davies JE, Sefton MV. Preliminary report on cell culture on a thermally reversible copolymer. Biomaterials 1993;14(2):153-5.

37. von Recum HA, Kim SW, Kikuchi A, Okuhara M, Sakurai Y, Okano T. Novel thermally reversible hydrogel as detachable cell culture substrate. J Biomed Mater Res 1998;40(4):631-9.

38. Vernon B, Kim SW, Bae YH. Thermoreversible copolymer gels for extracellular matrix. J Biomed Mater Res 2000;51(1):69-79.

39. Kushida A, Yamato M, Konno C, Kikuchi A, Sakurai Y, Okano T. Decrease in culture temperature releases monolayer endothelial cell sheets together with

deposited fibronectin matrix from temperature-responsive culture surfaces. J Biomed Mater Res 1999;45(4):355-62.

40. Akiyama Y, Kushida A, Yamato M, Kikuchi A, Okano T. Surface characterization of poly(N-isopropylacrylamide) grafted tissue culture polystyrene by electron beam irradiation, using atomic force microscopy, and X-ray photoelectron spectroscopy. J Nanosci Nanotechnol 2007;7(3):796-802.

41. Liu L, Sheardown H. Glucose permeable poly (dimethyl siloxane) poly (N-isopropyl acrylamide) interpenetrating networks as ophthalmic biomaterials. Biomaterials 2005;26(3):233-44.

42. Reddy TT, Kano A, Maruyama A, Hadano M, Takahara A. Thermosensitive transparent semi-interpenetrating polymer networks for wound dressing and cell adhesion control. Biomacromolecules 2008;9(4):1313-21.

43. Ma D, Chen H, Shi D, Li Z, Wang J. Preparation and characterization of thermo-responsive PDMS surfaces grafted with poly(N-isopropylacrylamide) by benzophenone-initiated photopolymerization. J Colloid Interface Sci 2009;332(1):85-90.

44. Carpenter AE, Jones TR, Lamprecht MR, Clarke C, Kang IH, Friman O, Guertin DA, Chang JH, Lindquist RA, Moffat J and others. CellProfiler: image analysis software for identifying and quantifying cell phenotypes. Genome Biol 2006;7(10):R100.

Appendix D: ***Chapter III References***

1. Wang JH, Thampatty BP. An introductory review of cell mechanobiology. Biomech Model Mechanobiol 2006;5(1):1-16.
2. Chiquet M. Regulation of extracellular matrix gene expression by mechanical stress. Matrix Biol 1999;18(5):417-26.
3. Chiquet M, Matthisson M, Koch M, Tannheimer M, Chiquet-Ehrismann R. Regulation of extracellular matrix synthesis by mechanical stress. Biochem Cell Biol 1996;74(6):737-44.
4. Ingber DE. Tensegrity and mechanotransduction. J Bodyw Mov Ther 2008;12(3):198-200.
5. Ingber DE. Tensegrity-based mechanosensing from macro to micro. Prog Biophys Mol Biol 2008;97(2-3):163-79.
6. Ingber DE. Cellular mechanotransduction: putting all the pieces together again. Faseb J 2006;20(7):811-27.
7. Shyu KG. Cellular and molecular effects of mechanical stretch on vascular cells and cardiac myocytes. Clin Sci (Lond) 2009;116(5):377-89.
8. Riha GM, Lin PH, Lumsden AB, Yao Q, Chen C. Roles of hemodynamic forces in vascular cell differentiation. Ann Biomed Eng 2005;33(6):772-9.
9. Parizek M, Novotna K, Bacakova L. The role of smooth muscle cells in vessel wall pathophysiology and reconstruction using bioactive synthetic polymers. Physiol Res 2011;60(3):419-37.

10. Huang AH, Niklason LE. Engineering biological-based vascular grafts using a pulsatile bioreactor. J Vis Exp 2011(52).

11. Sharifpoor S, Simmons CA, Labow RS, Santerre JP. A study of vascular smooth muscle cell function under cyclic mechanical loading in a polyurethane scaffold with optimized porosity. Acta Biomater 2010;6(11):4218-28.

12. Birukov KG, Shirinsky VP, Stepanova OV, Tkachuk VA, Hahn AW, Resink TJ, Smirnov VN. Stretch affects phenotype and proliferation of vascular smooth muscle cells. Mol Cell Biochem 1995;144(2):131-9.

13. Reusch P, Wagdy H, Reusch R, Wilson E, Ives HE. Mechanical strain increases smooth muscle and decreases nonmuscle myosin expression in rat vascular smooth muscle cells. Circ Res 1996;79(5):1046-53.

14. Smith PG, Garcia R, Kogerman L. Strain reorganizes focal adhesions and cytoskeleton in cultured airway smooth muscle cells. Exp Cell Res 1997;232(1):127-36.

15. Tock J, Van Putten V, Stenmark KR, Nemenoff RA. Induction of SM-alpha-actin expression by mechanical strain in adult vascular smooth muscle cells is mediated through activation of JNK and p38 MAP kinase. Biochem Biophys Res Commun 2003;301(4):1116-21.

16. Cheung C, Sinha S. Human embryonic stem cell-derived vascular smooth muscle cells in therapeutic neovascularisation. J Mol Cell Cardiol 2011.

17. Shimizu N, Yamamoto K, Obi S, Kumagaya S, Masumura T, Shimano Y, Naruse K, Yamashita JK, Igarashi T, Ando J. Cyclic strain induces mouse embryonic stem cell

differentiation into vascular smooth muscle cells by activating PDGF receptor beta. J Appl Physiol 2008;104(3):766-72.

18. Riha GM, Wang X, Wang H, Chai H, Mu H, Lin PH, Lumsden AB, Yao Q, Chen C. Cyclic strain induces vascular smooth muscle cell differentiation from murine embryonic mesenchymal progenitor cells. Surgery 2007;141(3):394-402.

19. Cevallos M, Riha GM, Wang X, Yang H, Yan S, Li M, Chai H, Yao Q, Chen C. Cyclic strain induces expression of specific smooth muscle cell markers in human endothelial cells. Differentiation 2006;74(9-10):552-61.

20. Wang H, Yan S, Chai H, Riha GM, Li M, Yao Q, Chen C. Shear stress induces endothelial transdifferentiation from mouse smooth muscle cells. Biochem Biophys Res Commun 2006;346(3):860-5.

21. Lee EL, von Recum HA. Cell culture platform with mechanical conditioning and nondamaging cellular detachment. J Biomed Mater Res A 2010;93(2):411-8.

22. Athanasiou KA, Niederauer GG, Agrawal CM. Sterilization, toxicity, biocompatibility and clinical applications of polylactic acid/polyglycolic acid copolymers. Biomaterials 1996;17(2):93-102.

23. Bostman OM, Pihlajamaki HK. Adverse tissue reactions to bioabsorbable fixation devices. Clin Orthop Relat Res 2000(371):216-27.

24. Norotte C, Marga FS, Niklason LE, Forgacs G. Scaffold-free vascular tissue engineering using bioprinting. Biomaterials 2009;30(30):5910-7.

25. Dobrin PB. Mechanical properties of arterises. Physiol Rev 1978;58(2):397-460.

26. Albinsson S, Nordstrom I, Hellstrand P. Stretch of the vascular wall induces smooth muscle differentiation by promoting actin polymerization. J Biol Chem 2004;279(33):34849-55.

27. Zeidan A, Nordstrom I, Albinsson S, Malmqvist U, Sward K, Hellstrand P. Stretch-induced contractile differentiation of vascular smooth muscle: sensitivity to actin polymerization inhibitors. Am J Physiol Cell Physiol 2003;284(6):C1387-96.

Appendix E: ***Chapter IV References***

1. Orlic, D., Kajstura, J., Chimenti, S., Jakoniuk, I., Anderson, S.M., Li, B., Pickel, J., McKay, R., Nadal-Ginard, B., Bodine, D.M., Leri, A., and Anversa, P. Bone marrow cells regenerate infarcted myocardium. Nature 410, 701, 2001.
2. Villet, O.M., Siltanen, A., Patila, T., Mahar, M.A., Vento, A., Kankuri, E., and Harjula, A. Advances in cell transplantation therapy for diseased myocardium. Stem cells international 2011, 679171, 2011.
3. Assmus, B., Rolf, A., Erbs, S., Elsasser, A., Haberbosch, W., Hambrecht, R., Tillmanns, H., Yu, J., Corti, R., Mathey, D.G., Hamm, C.W., Suselbeck, T., Tonn, T., Dimmeler, S., Dill, T., Zeiher, A.M., and Schachinger, V. Clinical outcome 2 years after intracoronary administration of bone marrow-derived progenitor cells in acute myocardial infarction. Circ Heart Fail 3, 89, 2010.
4. Assmus, B., Schachinger, V., Teupe, C., Britten, M., Lehmann, R., Dobert, N., Grunwald, F., Aicher, A., Urbich, C., Martin, H., Hoelzer, D., Dimmeler, S., and Zeiher, A.M. Transplantation of Progenitor Cells and Regeneration Enhancement in Acute Myocardial Infarction (TOPCARE-AMI). Circulation 106, 3009, 2002.
5. Britten, M.B., Abolmaali, N.D., Assmus, B., Lehmann, R., Honold, J., Schmitt, J., Vogl, T.J., Martin, H., Schachinger, V., Dimmeler, S., and Zeiher, A.M. Infarct remodeling after intracoronary progenitor cell treatment in patients with acute myocardial infarction (TOPCARE-AMI): mechanistic insights from serial contrast-enhanced magnetic resonance imaging. Circulation 108, 2212, 2003.

6. Dill, T., Schachinger, V., Rolf, A., Mollmann, S., Thiele, H., Tillmanns, H., Assmus, B., Dimmeler, S., Zeiher, A.M., and Hamm, C. Intracoronary administration of bone marrow- derived progenitor cells improves left ventricular function in patients at risk for adverse remodeling after acute ST-segment elevation myocardial infarction: results of the Reinfusion of Enriched Progenitor cells And Infarct Remodeling in Acute Myocardial Infarction study (REPAIR-AMI) cardiac magnetic resonance imaging substudy. American heart journal 157, 541, 2009.

7. Leistner, D.M., Fischer-Rasokat, U., Honold, J., Seeger, F.H., Schachinger, V., Lehmann, R., Martin, H., Burck, I., Urbich, C., Dimmeler, S., Zeiher, A.M., and Assmus, B. Transplantation of progenitor cells and regeneration enhancement in acute myocardial infarction (TOPCARE-AMI): final 5-year results suggest long-term safety and efficacy. Clin Res Cardiol, 2011.

8. Meyer, G.P., Wollert, K.C., Lotz, J., Steffens, J., Lippolt, P., Fichtner, S., Hecker, H., Schaefer, A., Arseniev, L., Hertenstein, B., Ganser, A., and Drexler, H. Intracoronary bone marrow cell transfer after myocardial infarction: eighteen months' follow-up data from the randomized, controlled BOOST (BOne marrOw transfer to enhance ST-elevation infarct regeneration) trial. Circulation 113, 1287, 2006.

9. Nyolczas, N., Gyongyosi, M., Beran, G., Dettke, M., Graf, S., Sochor, H., Christ, G., Edes, I., Balogh, L., Krause, K.T., Jaquet, K., Kuck, K.H., Benedek, I., Hintea, T., Kiss, R., Preda, I., Kotevski, V., Pejkov, H., Dudek, D., Heba, G., Sylven, C., Charwat, S., Jacob, R., Maurer, G., Lang, I., and Glogar, D. Design and rationale

for the Myocardial Stem Cell Administration After Acute Myocardial Infarction (MYSTAR) Study: a multicenter, prospective, randomized, single-blind trial comparing early and late intracoronary or combined (percutaneous intramyocardial and intracoronary) administration of nonselected autologous bone marrow cells to patients after acute myocardial infarction. American heart journal 153, 212 e1, 2007.

10. Schachinger, V., Assmus, B., Britten, M.B., Honold, J., Lehmann, R., Teupe, C., Abolmaali, N.D., Vogl, T.J., Hofmann, W.K., Martin, H., Dimmeler, S., and Zeiher, A.M. Transplantation of progenitor cells and regeneration enhancement in acute myocardial infarction: final one-year results of the TOPCARE-AMI Trial. Journal of the American College of Cardiology 44, 1690, 2004.

11. Yousef, M., Schannwell, C.M., Kostering, M., Zeus, T., Brehm, M., and Strauer, B.E. The BALANCE Study: clinical benefit and long-term outcome after intracoronary autologous bone marrow cell transplantation in patients with acute myocardial infarction. Journal of the American College of Cardiology 53, 2262, 2009.

12. Dimmeler, S., Zeiher, A.M., and Schneider, M.D. Unchain my heart: the scientific foundations of cardiac repair. The Journal of clinical investigation 115, 572, 2005.

13. Yoon, Y.S., Park, J.S., Tkebuchava, T., Luedeman, C., and Losordo, D.W. Unexpected severe calcification after transplantation of bone marrow cells in acute myocardial infarction. Circulation 109, 3154, 2004.

14. Wolf, D., Reinhard, A., Seckinger, A., Gross, L., Katus, H.A., and Hansen, A. Regenerative capacity of intravenous autologous, allogeneic and human mesenchymal stem cells in the infarcted pig myocardium-complicated by myocardial tumor formation. Scand Cardiovasc J 43, 39, 2009.

15. Dow, J., Simkhovich, B.Z., Kedes, L., and Kloner, R.A. Washout of transplanted cells from the heart: a potential new hurdle for cell transplantation therapy. Cardiovascular research 67, 301, 2005.

16. Hudson, W., Collins, M.C., deFreitas, D., Sun, Y.S., Muller-Borer, B., and Kypson, A.P. Beating and arrested intramyocardial injections are associated with significant mechanical loss: implications for cardiac cell transplantation. The Journal of surgical research 142, 263, 2007.

17. Zhang, H., Song, P., Tang, Y., Zhang, X.L., Zhao, S.H., Wei, Y.J., and Hu, S.S. Injection of bone marrow mesenchymal stem cells in the borderline area of infarcted myocardium: heart status and cell distribution. The Journal of thoracic and cardiovascular surgery 134, 1234, 2007.

18. Smets, F.N., Chen, Y., Wang, L.J., and Soriano, H.E. Loss of cell anchorage triggers apoptosis (anoikis) in primary mouse hepatocytes. Molecular genetics and metabolism 75, 344, 2002.

19. Bel, A., Planat-Bernard, V., Saito, A., Bonnevie, L., Bellamy, V., Sabbah, L., Bellabas, L., Brinon, B., Vanneaux, V., Pradeau, P., Peyrard, S., Larghero, J., Pouly, J., Binder, P., Garcia, S., Shimizu, T., Sawa, Y., Okano, T., Bruneval, P., Desnos, M., Hagege, A.A., Casteilla, L., Puceat, M., and Menasche, P. Composite cell sheets:

a further step toward safe and effective myocardial regeneration by cardiac progenitors derived from embryonic stem cells. Circulation 122, S118, 2010.

20. Zhang, M., Methot, D., Poppa, V., Fujio, Y., Walsh, K., and Murry, C.E. Cardiomyocyte grafting for cardiac repair: graft cell death and anti-death strategies. Journal of molecular and cellular cardiology 33, 907, 2001.

21. Malliaras, K., and Marban, E. Cardiac cell therapy: where we've been, where we are, and where we should be headed. British medical bulletin 98, 161, 2011.

22. Menasche, P., Alfieri, O., Janssens, S., McKenna, W., Reichenspurner, H., Trinquart, L., Vilquin, J.T., Marolleau, J.P., Seymour, B., Larghero, J., Lake, S., Chatellier, G., Solomon, S., Desnos, M., and Hagege, A.A. The Myoblast Autologous Grafting in Ischemic Cardiomyopathy (MAGIC) trial: first randomized placebo-controlled study of myoblast transplantation. Circulation 117, 1189, 2008.

23. Coppen, S.R., Fukushima, S., Shintani, Y., Takahashi, K., Varela-Carver, A., Salem, H., Yashiro, K., Yacoub, M.H., and Suzuki, K. A factor underlying late-phase arrhythmogenicity after cell therapy to the heart: global downregulation of connexin43 in the host myocardium after skeletal myoblast transplantation. Circulation 118, S138, 2008.

24. Penn, M.S., and von Recum, H.A. A tale of two biologies: Stem cell patch: Myocardial interactions are criticial for myocardial regeneration. Journal of the American College of Cardiology In Press, 2011.

25. Sekine, H., Shimizu, T., Dobashi, I., Matsuura, K., Hagiwara, N., Takahashi, M., Kobayashi, E., Yamato, M., and Okano, T. Cardiac Cell Sheet Transplantation Improves Damaged Heart Function via Superior Cell Survival in Comparison with Dissociated Cell Injection. Tissue engineering, 2011.

26. Iyer, R.K., Chiu, L.L., Reis, L.A., and Radisic, M. Engineered cardiac tissues. Current opinion in biotechnology, 2011.

27. Miyagawa, S., Saito, A., Sakaguchi, T., Yoshikawa, Y., Yamauchi, T., Imanishi, Y., Kawaguchi, N., Teramoto, N., Matsuura, N., Iida, H., Shimizu, T., Okano, T., and Sawa, Y. Impaired myocardium regeneration with skeletal cell sheets--a preclinical trial for tissue-engineered regeneration therapy. Transplantation 90, 364, 2010.

28. Zakharova, L., Mastroeni, D., Mutlu, N., Molina, M., Goldman, S., Diethrich, E., and Gaballa, M.A. Transplantation of cardiac progenitor cell sheet onto infarcted heart promotes cardiogenesis and improves function. Cardiovascular research 87, 40, 2010.

29. Radisic, M., Malda, J., Epping, E., Geng, W., Langer, R., and Vunjak-Novakovic, G. Oxygen gradients correlate with cell density and cell viability in engineered cardiac tissue. Biotechnology and bioengineering 93, 332, 2006.

30. Stevens, K.R., Kreutziger, K.L., Dupras, S.K., Korte, F.S., Regnier, M., Muskheli, V., Nourse, M.B., Bendixen, K., Reinecke, H., and Murry, C.E. Physiological function and transplantation of scaffold-free and vascularized human cardiac muscle

tissue. Proceedings of the National Academy of Sciences of the United States of America 106, 16568, 2009.

31. Haraguchi, Y., Shimizu, T., Yamato, M., Kikuchi, A., and Okano, T. Electrical coupling of cardiomyocyte sheets occurs rapidly via functional gap junction formation. Biomaterials 27, 4765, 2006.

32. Lee, E.L., and von Recum, H.A. Cell culture platform with mechanical conditioning and nondamaging cellular detachment. Journal of biomedical materials research 93, 411, 2010.

33. Haraguchi, Y., Shimizu, T., Yamato, M., and Okano, T. Electrical interaction between cardiomyocyte sheets separated by non-cardiomyocyte sheets in heterogeneous tissues. Journal of tissue engineering and regenerative medicine 4, 291, 2010.

34. Gardner, D.G., Wirtz, H., and Dobbs, L.G. Stretch-dependent regulation of atrial peptide synthesis and secretion in cultured atrial cardiocytes. The American journal of physiology 263, E239, 1992.

35. Komuro, I., Kudo, S., Yamazaki, T., Zou, Y., Shiojima, I., and Yazaki, Y. Mechanical stretch activates the stress-activated protein kinases in cardiac myocytes. Faseb J 10, 631, 1996.

36. Raskin, A.M., Hoshijima, M., Swanson, E., McCulloch, A.D., and Omens, J.H. Hypertrophic gene expression induced by chronic stretch of excised mouse heart muscle. Mol Cell Biomech 6, 145, 2009.

37. Sadoshima, J., Jahn, L., Takahashi, T., Kulik, T.J., and Izumo, S. Molecular characterization of the stretch-induced adaptation of cultured cardiac cells. An in vitro model of load-induced cardiac hypertrophy. The Journal of biological chemistry 267, 10551, 1992.

38. Yamazaki, T., Komuro, I., Kudoh, S., Zou, Y., Shiojima, I., Mizuno, T., Takano, H., Hiroi, Y., Ueki, K., Tobe, K., and et al. Mechanical stress activates protein kinase cascade of phosphorylation in neonatal rat cardiac myocytes. The Journal of clinical investigation 96, 438, 1995.

39. van Wamel, A.J., Ruwhof, C., van der Valk-Kokshoorn, L.J., Schrier, P.I., and van der Laarse, A. Rapid effects of stretched myocardial and vascular cells on gene expression of neonatal rat cardiomyocytes with emphasis on autocrine and paracrine mechanisms. Archives of biochemistry and biophysics 381, 67, 2000.

40. Alpert, N.R., and Mulieri, L.A. Functional consequences of altered cardiac myosin isoenzymes. Medicine and science in sports and exercise 18, 309, 1986.

Appendix F: ***Chapter V References***

1. Roger VL, Go AS, Lloyd-Jones DM, Adams RJ, Berry JD, Brown TM, Carnethon MR, Dai S, de Simone G, Ford ES and others. Heart disease and stroke statistics--2011 update: a report from the American Heart Association. Circulation 2011;123(4):e18-e209.
2. Pfeffer MA, Braunwald E. Ventricular remodeling after myocardial infarction. Experimental observations and clinical implications. Circulation 1990;81(4):1161-72.
3. Malliaras K, Marban E. Cardiac cell therapy: where we've been, where we are, and where we should be headed. Br Med Bull 2011;98:161-85.
4. He KL, Yi GH, Sherman W, Zhou H, Zhang GP, Gu A, Kao R, Haimes HB, Harvey J, Roos E and others. Autologous skeletal myoblast transplantation improved hemodynamics and left ventricular function in chronic heart failure dogs. J Heart Lung Transplant 2005;24(11):1940-9.
5. Jain M, DerSimonian H, Brenner DA, Ngoy S, Teller P, Edge AS, Zawadzka A, Wetzel K, Sawyer DB, Colucci WS and others. Cell therapy attenuates deleterious ventricular remodeling and improves cardiac performance after myocardial infarction. Circulation 2001;103(14):1920-7.
6. Leobon B, Garcin I, Menasche P, Vilquin JT, Audinat E, Charpak S. Myoblasts transplanted into rat infarcted myocardium are functionally isolated from their host. Proc Natl Acad Sci U S A 2003;100(13):7808-11.

7. Hagege AA, Marolleau JP, Vilquin JT, Alheritiere A, Peyrard S, Duboc D, Abergel E, Messas E, Mousseaux E, Schwartz K and others. Skeletal myoblast transplantation in ischemic heart failure: long-term follow-up of the first phase I cohort of patients. Circulation 2006;114(1 Suppl):I108-13.

8. Menasche P, Alfieri O, Janssens S, McKenna W, Reichenspurner H, Trinquart L, Vilquin JT, Marolleau JP, Seymour B, Larghero J and others. The Myoblast Autologous Grafting in Ischemic Cardiomyopathy (MAGIC) trial: first randomized placebo-controlled study of myoblast transplantation. Circulation 2008;117(9):1189-200.

9. Menasche P, Hagege AA, Vilquin JT, Desnos M, Abergel E, Pouzet B, Bel A, Sarateanu S, Scorsin M, Schwartz K and others. Autologous skeletal myoblast transplantation for severe postinfarction left ventricular dysfunction. J Am Coll Cardiol 2003;41(7):1078-83.

10. Siminiak T, Kalawski R, Fiszer D, Jerzykowska O, Rzezniczak J, Rozwadowska N, Kurpisz M. Autologous skeletal myoblast transplantation for the treatment of postinfarction myocardial injury: phase I clinical study with 12 months of follow-up. Am Heart J 2004;148(3):531-7.

11. Balsam LB, Wagers AJ, Christensen JL, Kofidis T, Weissman IL, Robbins RC. Haematopoietic stem cells adopt mature haematopoietic fates in ischaemic myocardium. Nature 2004;428(6983):668-73.

12. Murry CE, Soonpaa MH, Reinecke H, Nakajima H, Nakajima HO, Rubart M, Pasumarthi KB, Virag JI, Bartelmez SH, Poppa V and others. Haematopoietic stem

cells do not transdifferentiate into cardiac myocytes in myocardial infarcts. Nature 2004;428(6983):664-8.

13. Kim K, Doi A, Wen B, Ng K, Zhao R, Cahan P, Kim J, Aryee MJ, Ji H, Ehrlich LI and others. Epigenetic memory in induced pluripotent stem cells. Nature 2010;467(7313):285-90.

14. Polo JM, Liu S, Figueroa ME, Kulalert W, Eminli S, Tan KY, Apostolou E, Stadtfeld M, Li Y, Shioda T and others. Cell type of origin influences the molecular and functional properties of mouse induced pluripotent stem cells. Nat Biotechnol 2010;28(8):848-55.

15. Bel A, Planat-Bernard V, Saito A, Bonnevie L, Bellamy V, Sabbah L, Bellabas L, Brinon B, Vanneaux V, Pradeau P and others. Composite cell sheets: a further step toward safe and effective myocardial regeneration by cardiac progenitors derived from embryonic stem cells. Circulation 2010;122(11 Suppl):S118-23.

16. Murry CE, Keller G. Differentiation of embryonic stem cells to clinically relevant populations: lessons from embryonic development. Cell 2008;132(4):661-80.

17. Nussbaum J, Minami E, Laflamme MA, Virag JA, Ware CB, Masino A, Muskheli V, Pabon L, Reinecke H, Murry CE. Transplantation of undifferentiated murine embryonic stem cells in the heart: teratoma formation and immune response. Faseb J 2007;21(7):1345-57.

18. Villet OM, Siltanen A, Patila T, Mahar MA, Vento A, Kankuri E, Harjula A. Advances in cell transplantation therapy for diseased myocardium. Stem Cells Int 2011;2011:679171.

19. Dow J, Simkhovich BZ, Kedes L, Kloner RA. Washout of transplanted cells from the heart: a potential new hurdle for cell transplantation therapy. Cardiovasc Res 2005;67(2):301-7.

20. Hudson W, Collins MC, deFreitas D, Sun YS, Muller-Borer B, Kypson AP. Beating and arrested intramyocardial injections are associated with significant mechanical loss: implications for cardiac cell transplantation. J Surg Res 2007;142(2):263-7.

21. Zhang H, Song P, Tang Y, Zhang XL, Zhao SH, Wei YJ, Hu SS. Injection of bone marrow mesenchymal stem cells in the borderline area of infarcted myocardium: heart status and cell distribution. J Thorac Cardiovasc Surg 2007;134(5):1234-40.

22. Smets FN, Chen Y, Wang LJ, Soriano HE. Loss of cell anchorage triggers apoptosis (anoikis) in primary mouse hepatocytes. Mol Genet Metab 2002;75(4):344-52.

23. Smits PC, Nienaber C, Colombo A, Ince H, Carlino M, Theuns DA, Biagini E, Valgimigli M, Onderwater EE, Steendijk P and others. Myocardial repair by percutaneous cell transplantation of autologous skeletal myoblast as a stand alone procedure in post myocardial infarction chronic heart failure patients. EuroIntervention 2006;1(4):417-24.

24. Veltman CE, Soliman OI, Geleijnse ML, Vletter WB, Smits PC, ten Cate FJ, Jordaens LJ, Balk AH, Serruys PW, Boersma E and others. Four-year follow-up of treatment with intramyocardial skeletal myoblasts injection in patients with ischaemic cardiomyopathy. Eur Heart J 2008;29(11):1386-96.

25. Furuta A, Miyoshi S, Itabashi Y, Shimizu T, Kira S, Hayakawa K, Nishiyama N, Tanimoto K, Hagiwara Y, Satoh T and others. Pulsatile cardiac tissue grafts using a novel three-dimensional cell sheet manipulation technique functionally integrates with the host heart, in vivo. Circ Res 2006;98(5):705-12.

26. Miyoshi S, Ikegami Y, Itabashi Y, Furuta A, Umezawa A, Ogawa S. Cardiac cell therapy and arrhythmias. Circ J 2007;71 Suppl A:A45-9.

27. Memon IA, Sawa Y, Fukushima N, Matsumiya G, Miyagawa S, Taketani S, Sakakida SK, Kondoh H, Aleshin AN, Shimizu T and others. Repair of impaired myocardium by means of implantation of engineered autologous myoblast sheets. J Thorac Cardiovasc Surg 2005;130(5):1333-41.

28. Maltsev VA, Rohwedel J, Hescheler J, Wobus AM. Embryonic stem cells differentiate in vitro into cardiomyocytes representing sinusnodal, atrial and ventricular cell types. Mech Dev 1993;44(1):41-50.

29. Wobus AM, Wallukat G, Hescheler J. Pluripotent mouse embryonic stem cells are able to differentiate into cardiomyocytes expressing chronotropic responses to adrenergic and cholinergic agents and Ca2+ channel blockers. Differentiation 1991;48(3):173-82.

30. Carpenedo RL, Sargent CY, McDevitt TC. Rotary suspension culture enhances the efficiency, yield, and homogeneity of embryoid body differentiation. Stem Cells 2007;25(9):2224-34.

31. Sargent CY, Berguig GY, Kinney MA, Hiatt LA, Carpenedo RL, Berson RE, McDevitt TC. Hydrodynamic modulation of embryonic stem cell differentiation by rotary orbital suspension culture. Biotechnol Bioeng 2010;105(3):611-26.

32. Sargent CY, Berguig GY, McDevitt TC. Cardiomyogenic differentiation of embryoid bodies is promoted by rotary orbital suspension culture. Tissue Eng Part A 2009;15(2):331-42.

33. Niebruegge S, Nehring A, Bar H, Schroeder M, Zweigerdt R, Lehmann J. Cardiomyocyte production in mass suspension culture: embryonic stem cells as a source for great amounts of functional cardiomyocytes. Tissue Eng Part A 2008;14(10):1591-601.

34. Burridge PW, Thompson S, Millrod MA, Weinberg S, Yuan X, Peters A, Mahairaki V, Koliatsos VE, Tung L, Zambidis ET. A universal system for highly efficient cardiac differentiation of human induced pluripotent stem cells that eliminates interline variability. PLoS One 2011;6(4):e18293.

35. E LL, Zhao YS, Guo XM, Wang CY, Jiang H, Li J, Duan CM, Song Y. Enrichment of cardiomyocytes derived from mouse embryonic stem cells. J Heart Lung Transplant 2006;25(6):664-74.

36. Riebeling C, Schlechter K, Buesen R, Spielmann H, Luch A, Seiler A. Defined culture medium for stem cell differentiation: applicability of serum-free conditions in the mouse embryonic stem cell test. Toxicol In Vitro 2011;25(4):914-21.

37. Takahashi T, Lord B, Schulze PC, Fryer RM, Sarang SS, Gullans SR, Lee RT. Ascorbic acid enhances differentiation of embryonic stem cells into cardiac myocytes. Circulation 2003;107(14):1912-6.

38. Wang Y, Chen G, Song T, Mao G, Bai H. Enhancement of cardiomyocyte differentiation from human embryonic stem cells. Sci China Life Sci 2010;53(5):581-9.

39. Pan J, Baker KM. Retinoic acid and the heart. Vitam Horm 2007;75:257-83.

40. Zandstra PW, Bauwens C, Yin T, Liu Q, Schiller H, Zweigerdt R, Pasumarthi KB, Field LJ. Scalable production of embryonic stem cell-derived cardiomyocytes. Tissue Eng 2003;9(4):767-78.

41. Stuckmann I, Evans S, Lassar AB. Erythropoietin and retinoic acid, secreted from the epicardium, are required for cardiac myocyte proliferation. Dev Biol 2003;255(2):334-49.

42. Wobus AM, Kaomei G, Shan J, Wellner MC, Rohwedel J, Ji G, Fleischmann B, Katus HA, Hescheler J, Franz WM. Retinoic acid accelerates embryonic stem cell-derived cardiac differentiation and enhances development of ventricular cardiomyocytes. J Mol Cell Cardiol 1997;29(6):1525-39.

43. Ivanovic Z. Hypoxia or in situ normoxia: The stem cell paradigm. J Cell Physiol 2009;219(2):271-5.

44. Zhou X, Quann E, Gallicano GI. Differentiation of nonbeating embryonic stem cells into beating cardiomyocytes is dependent on downregulation of PKC beta

and zeta in concert with upregulation of PKC epsilon. Dev Biol 2003;255(2):407-22.

45. Foshay K, Rodriguez G, Hoel B, Narayan J, Gallicano GI. JAK2/STAT3 directs cardiomyogenesis within murine embryonic stem cells in vitro. Stem Cells 2005;23(4):530-43.

46. Smits AM, van Vliet P, Metz CH, Korfage T, Sluijter JP, Doevendans PA, Goumans MJ. Human cardiomyocyte progenitor cells differentiate into functional mature cardiomyocytes: an in vitro model for studying human cardiac physiology and pathophysiology. Nat Protoc 2009;4(2):232-43.

47. Fuegemann CJ, Samraj AK, Walsh S, Fleischmann BK, Jovinge S, Breitbach M. Differentiation of mouse embryonic stem cells into cardiomyocytes via the hanging-drop and mass culture methods. Curr Protoc Stem Cell Biol 2010;Chapter 1:Unit 1F 11.

48. Rajala K, Pekkanen-Mattila M, Aalto-Setala K. Cardiac differentiation of pluripotent stem cells. Stem Cells Int 2011;2011:383709.

49. Rungarunlert S, Techakumphu M, Pirity MK, Dinnyes A. Embryoid body formation from embryonic and induced pluripotent stem cells: Benefits of bioreactors. World J Stem Cells 2009;1(1):11-21.

50. Hescheler J, Wartenberg M, Fleischmann BK, Banach K, Acker H, Sauer H. Embryonic stem cells as a model for the physiological analysis of the cardiovascular system. Methods Mol Biol 2002;185:169-87.

Appendix G: ***Chapter VI References***

1. Prabhakar V, Capila I, Bosques CJ, Pojasek K, Sasisekharan R. Chondroitinase ABC I from Proteus vulgaris: cloning, recombinant expression and active site identification. Biochem J 2005;386(Pt 1):103-12.
2. Zebrower M, Kieras FJ, Heaney-Kieras J. High pressure liquid chromatographic identification of hyaluronic acid and chondroitin sulphate disaccharides. Glycobiology 1991;1(3):271-6.
3. Prabhakar V, Raman R, Capila I, Bosques CJ, Pojasek K, Sasisekharan R. Biochemical characterization of the chondroitinase ABC I active site. Biochem J 2005;390:395-405.